Development and Testing of Highway Storm-Sewer Flow Measurement and Recording System

By F.A. Kilpatrick, W.R. Kaehrle, Jack Hardee, E.H. Cordes, and M.N. Landers

Prepared for

U.S. Department
of Transportation
Federal Highway Administration
Offices of Research & Development
Washington, D.C. 20590

By

U.S. Geological Survey
Water Resources Division
Reston, Virginia 22092

U.S. GEOLOGICAL SURVEY
Water-Resources Investigations Report 85-4111

UNITED STATES DEPARTMENT OF THE INTERIOR

DONALD PAUL HODEL, Secretary

GEOLOGICAL SURVEY

Dallas L. Peck, Director

For additional information
write to:

U.S. Geological Survey, WRD
415 National Center
Reston, Virginia 22092

Copies of this report can
be purchased from:

Open-File Services Section
Western Distribution Branch
U.S. Geological Survey
Box 25425, Federal Center
Denver, Colorado 80225

DISCLAIMER

This document is disseminated under the sponsorship of the Department of Transportation in the interest of information exchange. The United States Government assumes no liability for its contents or use thereof.

The contents of this report reflect the views of the authors who are responsible for the facts and the accuracy of the data presented herein. The contents do not necessarily reflect the official views or policy of the Department of Transportation.

This report does not constitute a standard, specification, or regulation.

The United State Government does not endorse products or manufacturers. Trade or manufacturers' names appear herein only because they are considered essential to the object of this document.

FOREWORD

This report presents the results of laboratory and field tests of various flow measuring and recording instruments for use in storm-sewer systems. The report should be of interest to engineers and others concerned with instrumenting storm-sewer systems for the improved hydraulic design of such systems and as a means of acquiring hydrologic design data.

This study was conducted at or near two U.S. Geological Survey facilities: the Hydrologic Instrumentation Facility located at the National Space Technology Laboratories, Bay St. Louis, Mississippi, and near the U.S. Geological Survey District Office in Jackson, Mississippi. The authors wish to acknowledge the extensive help received from numerous personnel in these two offices without which this study would have been impossible. In particular, thanks are given to Billy E. Colson, James W. Hudson, Vito J. Latkovich, Donald H. Rapp, and Lawrence C. Morey.

This study was performed by personnel of the Water Resources Division of the U.S. Geological Survey. The bulk of the funding for the work was provided by the Federal Highway Administration; equipment, instruments, and supplies, as well as numerous man-hours, were provided by the U.S. Geological Survey because of the mutual interest both agencies have in the advancement of flow measurement in storm-sewer systems.

TABLE OF CONTENTS

TABLE OF CONTENTS (Continued)

LIST OF FIGURES

LIST OF FIGURES (Continued)

LIST OF FIGURES (Continued)

LIST OF FIGURES (Continued)

LIST OF TABLES

LIST OF ABBREVIATIONS AND SYMBOLS

(All dimensional terms are in feet.)

a, b, and c	Constants in regression equations
A_c	Cross-section area at the critical depth section in a Palmer-Bowlus (P-B) flume.
α	Energy coefficient
B	Width of broad-crested weir at right angles to flow
B_e	Effective width of broad-crested weir
B_t	Top width at any given flow over broad-crested weir
$\overline{c}$	Average concentration
C_b	Broad-crested weir discharge coefficient
d	Depth of water
d_c	Critical depth
d_t	Distance from floor in throat of Palmer-Bowlus flume to crown of pipe
D	Diameter of pipe
D_I	Diameter of insert pipe comprising Pipe Insert Contraction (PIC) meter
g	Acceleration of gravity; taken as 32.16 ft/s^2 at sea level
h_a	Depth of water in approach to Palmer-Bowlus flume, one D distance upstream of entrance to flume throat
H	Fluid head above a zero flow datum such as the bottom of a "V" notch weir or the floor of a flume
H_a	Head in approach to Palmer-Bowlus flume, one D distance upstream of entrance to flume throat, referenced to flume floor
H_b	Head on a broad-crested weir

H_c	Head in unaltered catchment
H_{cw}	Head on curb weir referenced to lowest point
H_e	Effective head on broad-crested curb weir
H_I	Head on insert or PIC meter
H_t	Head measured in throat of Palmer-Bowlus flume, D distance downstream from entrance
H_T	Tailwater head
ΔH_{at}	Difference between head in the approach and throat of Palmer-Bowlus flume
ΔH_{cT}	Difference between head in unaltered catchment and tailwater head
ΔH_{IT}	Difference between head on insert in catchment and tailwater head
Q	Discharge in cubic feet per second
Q_c	Critical discharge in cubic feet per second
r^2	Coefficient of determination for a given regression equation
s	Slope of regression equation line
t	Thickness or height of Palmer-Bowlus flume floor measured from the pipe invert
V	Mean velocity in Palmer-Bowlus flume in feet per second; subscripts a, c, and t refer to the approach, critical depth, and throat sections, respectively
y	Elevations in a Palmer-Bowlus flume or pipe above an arbitary datum; subscripts, a, c, and t refer to approach, critical depth, and throat sections respectively
Z	Critical-section factor

EVM	Electromagnetic velocity meter
GCHC	Gulf Coast Hydroscience Center
NSTL	National Space Technology Laboratories
P-B flume	Palmer-Bowlus flume
PIC meter	Pipe insert contraction meter
PBT system	Pneumatic bubbler transducer system
USGS	U.S. Geological Survey

UNIT CONVERSION

Multiply inch-pound unit	by	To obtain SI unit
inch (in)	25.4	millimeter (mm)
foot (ft)	3.048	meter (m)
cubic foot (ft^3)	28.320	cubic meter (m^3)
foot per second (ft/s)	0.305	meter per second (m/s)
cubic foot per second (ft^3/s)	0.028	cubic meter per second (m^3/s)
degrees Fahrenheit (°F)	0.556	after subtracting 32.0° Celsius (°C)

DEVELOPMENT AND TESTING OF HIGHWAY STORM-SEWER FLOW MEASUREMENT AND RECORDING SYSTEM

By Frederick A. Kilpatrick, William R. Kaehrle, Jack Hardee, Edwin H. Cordes, and Mark N. Landers

ABSTRACT

A comprehensive study and development of measuring instruments and techniques for measuring all components of flow in a storm-sewer drainage system was undertaken by the U.S. Geological Survey under the sponsorship of the Federal Highway Administration. The study involved laboratory and field calibration and testing of measuring flumes, pipe insert meters, weirs, electromagnetic velocity meters as well as the development and calibration of pneumatic-bubbler pressure transducer head measuring systems. Tracer-dilution and acoustic flow-meter measurments were used in field verification tests. A single micrologger was used to record data from all the above instruments as well as from a tipping-bucket rain gage and also to activate on command the electromagnetic velocity meter and tracer-dilution systems.

INTRODUCTION

In recent years with advances in watershed rainfall-runoff modeling techniques, there has been emphasis on the modeling approach to storm-sewer design. A reveiw of this type of literature is replete with statements as to the need for more and better data bases to aid model development.[1,2,3] The study performed in 1969 by the American Society of Civil Engineers (ASCE) recommended a minimum program of urban drainage research at $10 million over several years which amounted to about 0.33 percent of the expected annual national investment in the construction of storm drainage. A major conclusion of a conference on urban hydrologic research conducted in 1965 by the Urban Hydrology Research Council of ASCE was that a major technological hiatus exists largely because of an absence of suitable measuring devices. Progress has been made in these ensuing years in developing devices and methods of measuring and recording data in storm-drainage systems, largely in instrumentation. It is little wonder, though, that the problem still exists, as the hydraulics of flow in storm-sewer systems may be extremely complex.

STORM-DRAINAGE HYDRAULICS

From the inception of rainfall, flow in roadways and gutters, collection via curb inlets and drop structures or catchments, and final conveyance from the area via lateral and trunkline pipes, the whole gamut of flow hydraulics can occur.

Flows in streets and gutters may be sheet flow (supercritical) depending on roughness and slopes; hydraulic jumps may form at transitions in grade or at inlets. Varying amounts of street runoff may bypass one inlet only to be collected at an adjoining one or by a series of downstream inlets.

The efficiency of flows into curb and street inlets is highly variable and largely a function of approach and entry slopes, effective opening areas where grates exist, and the capacity of the receiving catchments and associated outlet drainpipes. In most cases, especially on major highway systems, the catchment outlet pipes are over-designed compared with the hydraulic capacity and efficiency of the curb inlets; this is to ensure passage of debris and to facilitate maintenance.

Catchments may be simple or complex. A simple one receives the flow through a single curb inlet and discharges it through a single outlet pipe. A complex catchment is one receiving flow from several curb inlets and (or) from other pipes junctioning and flowing through the catchment: a combined catchment and junction box. The flow from the catchment through the outlet pipe may be quite complex depending on pipe area, roughness, and slope. Figure 1 depicts the possible

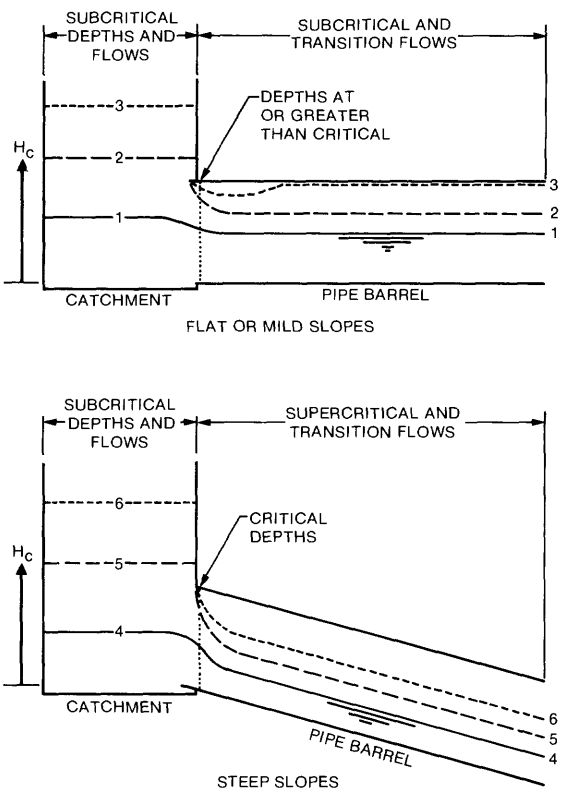

Figure 1. Catchment and outflow pipe hydraulics.

hydraulic conditions which may exist. Very common is case 1 where the outlet pipe is on a mild slope, and its area is small enough that control is at the entrance to the pipe where depths are at or greater than critical. As discharge increases and head in the catchment, H_c, increases to greater than the crown of the pipe, separation takes place with partially full flow existing in the barrel of the pipe (case 2). As discharge and head increase, the pipe barrel may fill despite some separation at the entrance (case 3). Between case 2 and case 3 a transition zone commonly exists where barrel roughness and slope determine if control is in the pipe barrel or still at the pipe entrance. This is an area where erratic and oscillating flow may occur made worse by the fact that as the pipe starts to flow full, it becomes more efficient causing the catchment head to drop. This in turn may cause pipe flow to momentarily return to open-channel flow. This transition flow region is hard to predict; for measurement purposes it is best avoided if possible.

When the slope of the pipe barrel is steep, control will almost always be at the entrance to this pipe where flow goes through critical depth. For cases 4, 5, and 6, supercritical flow will almost always exist in the barrel.

The exception will be if the barrel is rough, such as might be the case with a corrugated pipe or medium slopes exist causing the pipe to fill and thus to control. As before, there is a transition range where flow prediction is difficult.

Flows in larger trunklines may be any of the above but most commonly such sewer lines are placed on mild slopes of less than 1 percent. This and normal pipe roughness are more apt to cause trunklines to flow full at high flows and the transition zone to narrow. The presence of constrictive flow measurement devices such as flumes will almost invariably cause subcritical flow to occur upstream, if it isn't subcritical already, and rapid transition to pipe full flow when discharge and heads become large enough. Surcharge conditions occur when piezometric heads are above the pipe crown elevations and the system is experiencing pipe-full, pressure flow.

Backwater conditions, such as when trunklines discharge into nearby streams, may further complicate the hydraulic picture. Typically, trunkline pipes become submerged as the receiving stream reaches flood stage thus causing the trunklines to fill as free flow in the pipes cease to exist.[3,4] In extreme cases, negative flows may exist with flow coming from the stream. More commonly a lessened positive flow continues as trunklines adjacent to their receiving streams fill due to backwater. Flow-measuring devices in these trunklines which depend only on head measurements and free flow are no longer valid under such conditions.

OBJECTIVE

The objective of this study was to develop a complete data-collection package for the collection of field expressway runoff data in the evauluation of expressway drainage system modeling. This was to be accomplished by evaluating existing devices and techniques, both in the laboratory and field, that have been used in measuring storm-sewer flows as well as to consider new approaches and instruments. Finally to suggest an instrumentation package that would accurately measure all of the flow components which comprise a storm-sewer drainage system. The primary criteria in developing such a storm-sewer measuring package follows:

1. The instrumentation should be retrofittable to existing storm-sewer systems, through existing manholes and grate openings.

2. Instruments would restrict or alter existing flow capacities to the minimum.

3. Measuring structures and instruments should be reasonably self-cleaning and capable of operating in the hostile environment of a storm sewer.

4. A full range of flows from open channel to pressurized would be measurable as well as reversible flows.

5. Instrumentation would operate on battery power.

6. Measuring devices could be precalibrated or rated in the field.

7. Equipment should be affordable both to acquire and install; readily available items should be used to the extent possible.

SCOPE OF WORK

The data-collection package consists of two parts: the gaging instrumentation and the data recording and reduction system. The gaging instrumentation has two components: continuous measurement of storm-water flow into and past an inlet; and continuous measurement of flow in the underground storm sewer, including flows during surcharge conditions.

Following and guided by a literature review (1) the study will concentrate on the utilization of the best current technology and (or) the development of new technology and techniques to evaluate, (2) continuous measurement of drop structure outflows using commercially available pipe inserts, (3) indirect evaluation of flow bypassing the

street inlets by in-situ calibration of inlet and drop structures to establish hydraulic performance and efficiencies of each as a function of sewer-outlet discharge, (4) direct and continuous measurement of inlet bypass flows, (5) continuous measurement of trunkline flows, both base and runoff, for open-channel and pipe-full conditions, (6) development of compatible data recording and reduction systems for the above inputs, (7) all or part of instrumentation and data acquisition and recording systems would be field tested for 3 months, and (8) a final report on the entire effort would recommend the system to be used.

DEVELOPMENT OF A MEASUREMENT SYSTEM

LABORATORY AND FIELD TESTS

This study consisted of laboratory testing and calibration of the various instruments and equipment selected for consideration in measuring storm-sewer flows. This was followed by field testing, verification of the instruments selected, and in some instances, in-situ rating of instruments and structures. While in some instances, more sophisticated instruments might have been considered and tested, emphasis was on the practical application of techniques and instruments with the most proven reliability and applicability with the ultimate objective of presenting the best operational system.

PIPE-FLOW MEASUREMENT

A review of the literature indicates that most storm-sewer measurement devices and techniques have evolved from surface-water measurement techniques.[5] Something of a dilemma exists as to how to accurately measure flow in pipes which may experience the gamut of flow conditions previously described. Various types of flumes and constrictions have been the primary approach to the measurement of flows in pipes. The most common type of flume used for such measurements is the Palmer-Bowlus (P-B) flume which was originally proposed for this purpose by Messrs. Harold Palmer and Fred Bowlus in 1936.[6] Subsequent studies were performed which added to our understanding of this and other flumes.[7,8,9,10,11,12,13]

Initial studies of the P-B flume limited its use to open-channel flow. Wenzel suggested a flume design which might be titled a side-arc flume.[14] This design was one of the first to use the concept of a constrictive device to act as a free-surface flume during open-channel flow and as a venturi meter under full- and surcharged-flow conditions. Furthermore, Wenzel showed that the energy equation in conjunction with critical flow relations could be used to compute theoretical calibrations.

As mentioned earlier, one of the primary problems with measurement of flow in storm-sewer pipes is the necessity of measuring under both free surface and pipe full, pressurized flow. This problem would not be so severe except that the transition zone may be quite large and difficult to predict. To lessen this problem, the U.S. Geological Survey (USGS) designed and tested a U-shaped flume designed to operate as a conventional flume with open-channel flow and as a venturi with pipe-full flow.[15] The design was an attempt to lessen the extent of the transition range and to provide means of both predicting the flow state and the applicable calibration.[13]

The decision in this study was to rate a modified P-B type flume for open-channel flow and as a venturi meter for pipe-full flow. The problem with transition flows would be handled by measuring head upstream of the flume and in the throat; and thus by knowing the type of flow, the applicable calibration could be chosen. An 18-inch P-B flume would be fully calibrated in the laboratory, and 30-inch and 48-inch flumes tested and rated in the field if possible.

ELECTROMAGNETIC VELOCITY METER

It was recognized that measuring the flows in pipes with meters such as the P-B flume would apt to be poor in the transition range between free-surface and pipe-full flows. The decision was made to install an electromagnetic point velocity meter (EVM) in the approach to the P-B flume.[16] The use of a point velocity meter for this purpose has been advanced by several investigators recognizing the problem of measurements in the transition zone.[17,18] This point velocity meter would be activated when the pipe was approaching full and operated throughout the transition, with the pipe full, and deactivated when fully developed free-surface flow returned on the recession of runoff.

The decision to use an electromagnetic velocity meter as the point velocity meter was based on cost, reliability, and compatibility with the micrologger data system to be discussed later. Index velocity coefficients for the EVM would be obtained in the laboratory in conjunction with the 18-inch P-B flume tests.

BYPASS GUTTER FLOWS

Methodology and instrumentation for measuring street gutter flows bypassing inlets is virtually nonexistent; probably because of the great difficulty of making such measurements. The approach taken in this study is to rate in situ each curb inlet and catchment as an entity. The concept being that for a given curb inlet, the flow into the inlet and that bypassing it would be uniquely a function of the slope and roughness of the street and gutter approaching the inlet as

well as the design of the inlet. Thus if each inlet was rated in situ, the total approaching flow would have to be the sum of the bypass flow and that entering and leaving the catchment. A rating of bypass flow versus catchment outflow would be possible and a unique function for each catchment; measurement of catchment outflow by other means would then provide a means of predicting the flow bypassing each inlet. The rating of each inlet would be different and a separate in-situ calibration would be performed on each.

The need for a source of water such as from fire hydrants or nearby streams or lakes to accomplish an in-situ rating of each inlet structure was recognized as a severe restriction. As an alternative, a broad-crested weir installation would be tested and rated in situ in the street gutter.

CATCHMENT OUTFLOWS

It was found that most pipes draining catchments were from 12 to 18 in in diameter, seldom larger or smaller. This size precluded the ready placement of measuring flumes or other devices down in the pipes. The literature search revealed few approaches to measuring flows out of catchments. Those that were designed to measure catchment outflows usually involved weirs that required extensive modification of existing structures or would create their own backwater.[19,20]

One of the few is the Wallingford or gully meter developed at the Institute of Hydrology, Wallingford, England.[21] This meter is designed to fit down inside catchments* which have a 1- to 3-ft deep sediment trap below the invert of the outflow pipe. The meter is a deflection vane or gate positioned horizontally in a vertical pipe. Flow rises vertically through the pipe, deflects the gate and passes horizontally out the outflow pipe. This meter has a maximum capacity of 4 L/S (0.14 ft^3/s) and utilizes filters to keep the apparatus clear of silt and debris. Most inlets and catchments in the United States are designed to handle 0.5 to 5 ft^3/s discharges. The device seems to be limited to simple catchments as it might cause excessive backwater in other inflow pipes entering the catchment. The limited capacity and the potential for clogging and restricting the catchment were reasons to no longer consider this meter.

From examination of figure 1 for a simple catchment, it becomes apparent that unless the outlet pipe is on a very flat slope or is very rough, most flows will have their control at the entrance to this pipe. Even with the entrance to the outlet pipe submerged, hydraulic control is usually at the entrance. If stage measurements

---

*Referred to as gulleys in England.

could be made in the catchment box, a simple rating that would cover most flows experienced would be attainable. Unfortunately the pipe entrances to catchments may vary drastically due to both design and construction differences. Furthermore, approach conditions to the pipe may vary considerably due to how the flow enters from the street inlet. In addition, the flow in the catchment is quite turbulent.

Nevertheless, it was decided to design a meter which could be inserted into the entrance of the outlet pipe. This insert would have a rounded entrance and would contract the flow. It was expected that little if any capacity would be lost due to the improved efficiency derived from the rounding. The objective was to produce a pipe entrance that could be precalibrated. Head would be measured in a stilling well in the catchment and also in the barrel of the insert to provide a means of rating the Pipe Insert Contraction (PIC) meter as a venturi for those rare instances when the catchment outlet pipe would flow full.

STAGE AND HEAD MEASUREMENT SYSTEMS

In the normal storm-sewer system, it is impractical, if not impossible, in most instances to employ fluid intake systems with stilling wells and floats or other such direct means of measuring water stage or pressure heads in connection with flow-measurement devices. It was elected in this study to use the gas purge or bubbler and orifice system because of the flexibility and reliability offered. With this sytem a 3/8-in diameter plastic pneumatic line is positioned with its discharge orifice at locations where head or stage is to be measured.

This method involves balancing dynamic gas pressure (a bubble release) against the static potential exerted by a fluid column overlying a fixed submerged orifice (datum for stage or head measurement). The height of the column of fluid above the orifice opening is proportional to the pressure of the escaping gas. The system has been successfully used by the USGS since 1956 to measure water-level changes at over 2,000 sites on rivers, reservoirs, and wells in the United States.[22] In addition, the Rittmeyer Company in Switzerland as of 1974 had produced over 1,000 pneumatic bubbler units for the measurement of fluid levels in irrigation and waste-water systems.[23]

A direct conversion is made between inches or feet of water and pressure in pounds per square inch (psi) using the following equality: 2.31 ft of water equal 1 psi when the fluid density is 1 gram per milliliter (gm/mL). Any changes in the density of the fluid above the orifice, due to temperature or the amount of suspended or dissolved material, will affect the conversion relationship. Generally, these problems have proven negligible.

The standard gas-bubbler system in use by the USGS uses a liquid-mercury servo manometer system to convert pressure to feet of water. While refinement over the years has produced a reliable instrument, it is rather cumbersome and has the added disadvantage that it uses mercury which can be a health hazard if spilled or misused.[24]

Mechanical balancing systems have also been used to convert pneumatic pressure to feet of water, but these have proven to be extremely temperature sensitive.[23] Other types of mechanical and electrical manometers have been designed to convert pneumatic pressure to head in depth of water but have not been widely used.[25,26]

The substitution of a pressure transducer for the mercury manometer eliminates the mercury problem and provides a voltage signal compatible for direct input to the micrologger recorder. In addition, several transducer-bubbler orifice systems could be operated from one gas supply system, recording multiple data sources on one micrologger; all in less space than a single mercury manometer bubbler system.

DATA RECORDING SYSTEM

In recent years, numerous solid-state digital recorders have become available. Certain of the data loggers or microloggers have been tailored for the collection, storage, and processing of hydrologic data.[16,27] The USGS has tested a number of these units and is preparing to convert much of its hydrologic data collection to an Adaptable Hydrologic Data Acquisition System (AHDAS) which will be of microprocessor design and have solid-state memory.[28] In the mid-1970's, the USGS initiated studies in the Rocky Mountain and northern Great Plains States to model small coal mining basins which involved the collection of large amounts of climatic and streamflow data.[29] This program prompted Campbell Scientific, Inc., of Logan, Utah, to modify their CR-21 micrologger operating system to store and process hydrologic data. The CR-21 is an extremely low-powered, battery-operated, temperature-stable data logging and system control device. The unit uses a 12-volt power supply and has seven analog and two digital input channels and four output control ports.* This micrologger is a portable computer that can be programmed to sense and process data and emit control signals to other equipment based on time or parameter changes. Input channel readings are monitored every 10 seconds and are recorded when a user specified input exceeds

---

*At the time of this study this equipment was the most suitable for the purposes of the study. The Campbell CR21X micrologger in conjunction with their AM32-Input Multiplexer has 32 differential input capacity. This is not an endorsement of this equipment by the USGS over any other which may be available.

a given value. Activation of various instruments may be controlled in the same manner through the output control channels. This latter feature was important as the power consumption of an electromagnetic velocity meter would be excessive for prolonged battery operation unless it could be turned on only when needed. Furthermore, the CR-21 can be programmed to store data, only if a significant event occurs. The unit stores data in a buffer memory and unloads it automatically to cassette or solid-state storage.

More recently 35 of the CR-21 microloggers were put into use in watershed modeling studies in the Eastern States.[30] The favorable experience with this micrologger led to its selection for this study.

SYSTEM CHOSEN

Figure 2 shows conceptually the total system chosen for the measurement of storm-water drainage. Head measurements would be made

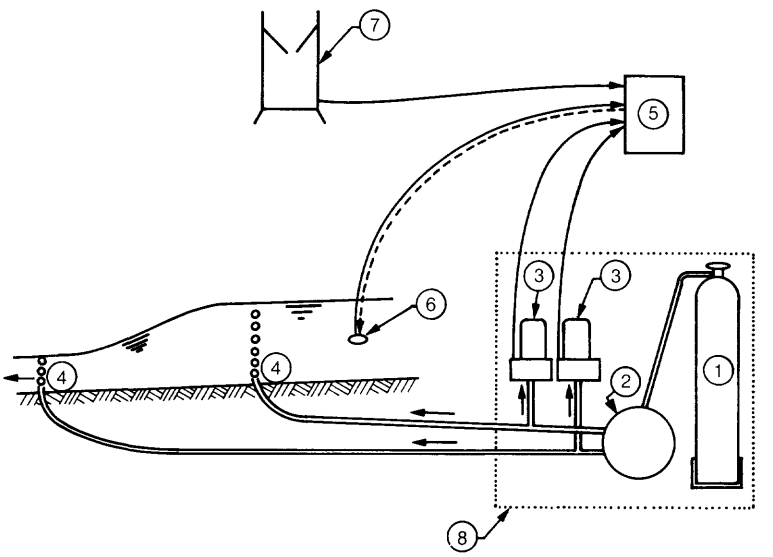

NOMENCLATURE

1 GAS SUPPLY
2 GAS FLOW REGULATOR
3 PRESSURE TRANSDUCERS
4 ORIFICES POSITIONED IN FLOW MEASURING DEVICES TO MEASURE HEADS
5 MICROLOGGER TO INTERROGATE, COMMAND RECEIVE AND STORE DATA FROM MULTIPLE SENSORS
6 ELECTROMAGNETIC VELOCITY METER, SENSES AND TRANSMITS ON COMMAND
7 RAIN GAGE
8 PNEUMATIC BUBBLER TRANSDUCER SYSTEM

Figure 2. Conceptual diagram of storm-sewer flow measurement system.

using a pneumatic bubbler approach with pressure transducers to convert sensed pressure to feet of water. As many orifices and their respective pressure transducers would serve as many measuring devices as required. Output from the transducers would be sensed by the micrologger and stored if flow or change in head was indicated. Above a given threshold of stage in any of the measuring devices, such as the trunkline, an electromagnetic velocity meter (or any other device) would be activated and then deactivated with falling stage. Data from other measuring devices, such as rain gages, would be stored by the micrologger.

TESTING PROCEDURES

LABORATORY TESTS

Laboratory tests on the 18-inch P-B flume and on a 10-inch and 15-inch PIC meter were performed at the Geological Survey's Gulf Coast Hydroscience Center (GCHC) located at the National Space Technology Laboratories (NSTL), Mississippi. Pressure transducers were also calibrated at the GCHC laboratory. Figure 3 is a sketch of the test flume used in the tests, and figure 4 is a photograph of the 18-inch concrete pipe used in the P-B flume tests.

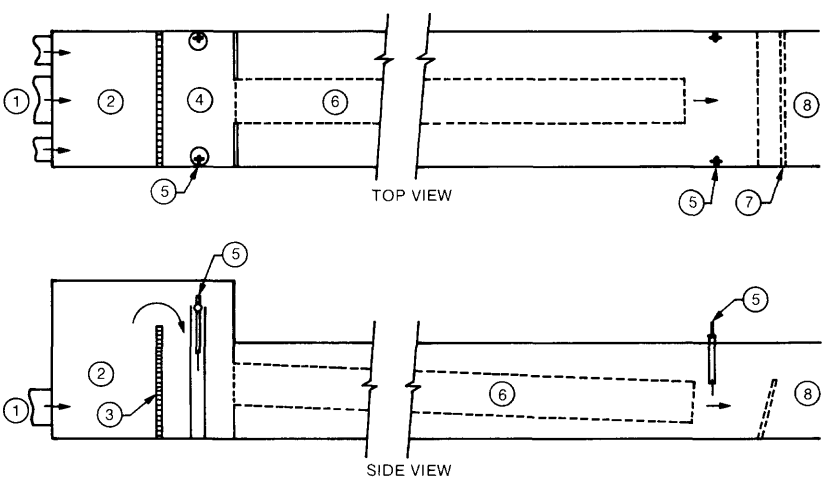

NOMENCLATURE

1 WATER SUPPLY, DISCHARGE MEASURED WITH ORIFICES OR "V"-NOTCH WEIR
2 HEADBOX
3 BAFFLE TO SIMULATE APPROACHING FLOW CONDITIONS
4 APPROACH SECTION
5 POINT GAGE, IN STILLING WELLS UPSTREAM
6 TEST PIPE
7 TAILGATE FOR BACKWATER CONTROL
8 WATER RETURNED TO CIRCULATING SUPPLY SYSTEM

Figure 3. General sketch of flume and test setup at GCHC Laboratory, NSTL, Mississippi

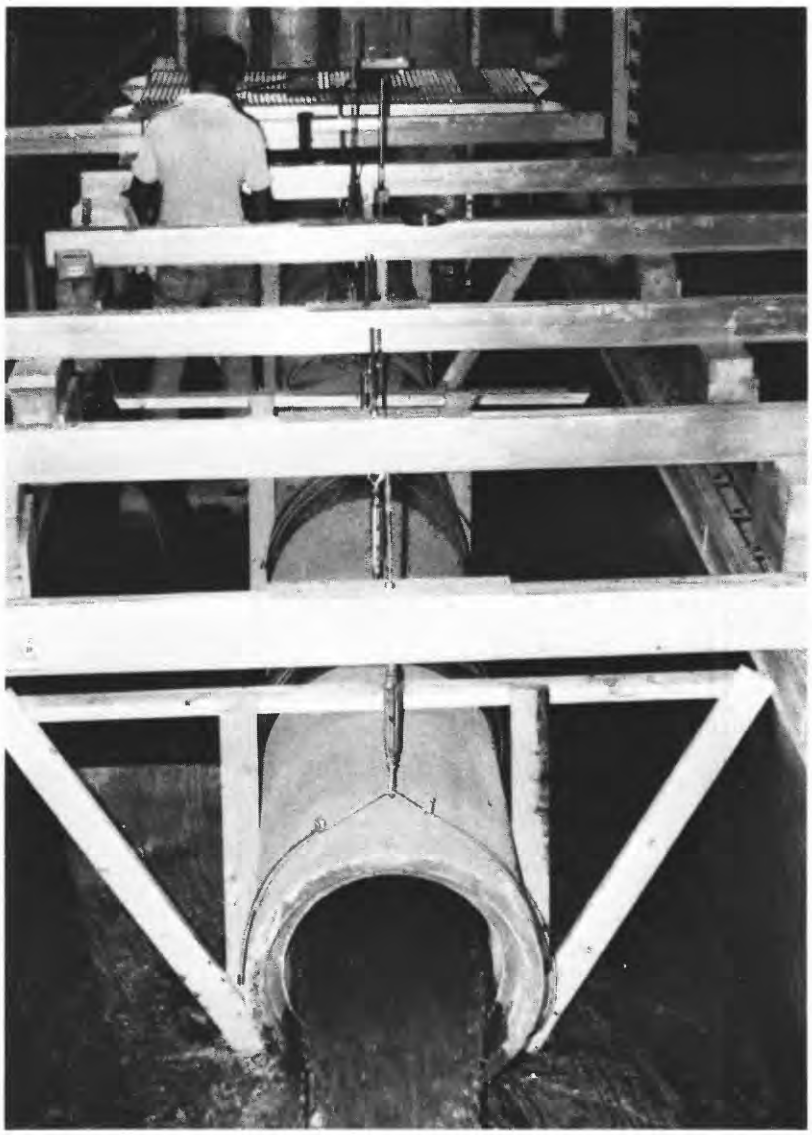

Figure 4. Test flume at USGS's GCHC Laboratory.

The water supply for the test flume is supplied via one or more pipes entering the head box. Discharge is measured by using orifices in the supply lines or by a 90° V-notch weir downstream. The upstream baffle is designed to simulate flows spilling from a street inlet into a catchment. Stilling wells with point gages were necessary for measuring heads in the approach section. The slope of the test pipe could be varied from 0 to 3 percent. The tailgate is used only when

backwater is desired. Downstream point gages are used to measure tailwater stages and are to the same datum as the upstream point gages. Pipe diameter, lengths, and configurations were varied to suit test purposes.

FIELD SITE

The field site to test the various instruments and techniques was located in Jackson, Mississippi. This site was chosen because it offered the opportunity to test all of the possible structures, instruments, and flow conditions and was typical of a modern highway storm drainage system. Figure 5 is a plan view of the highway intersection chosen, located immediately to the west of Interstate 220 in Jackson. Two curb inlets, 5 and 6 (see fig. 5) drain into a catchment and junction box, 3, and simple catchment, 7, respectively.

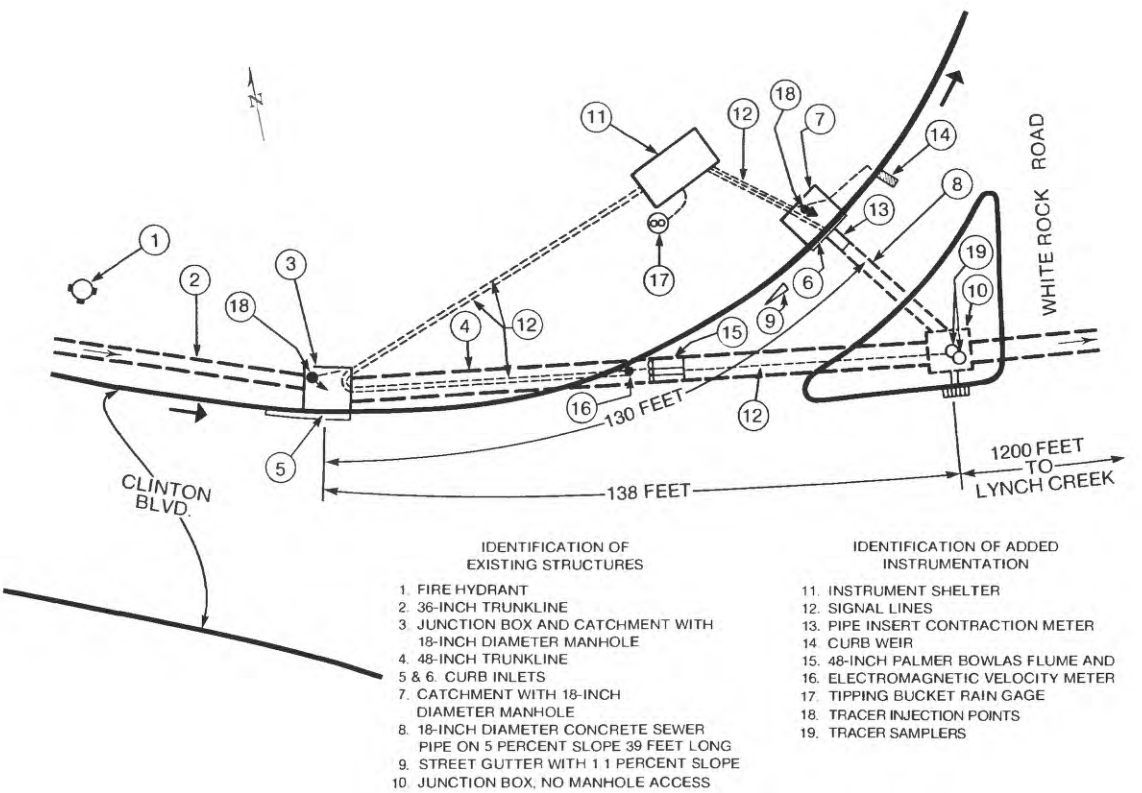

Figure 5. Plan view of instrument test site at Jackson, Mississippi.

A 48-inch trunkline receives the flow from these inlets as well as others not shown. This trunkline discharges into a nearby stream which may cause backwater in the trunkline during stream flooding. High-water marks found in the trunkline seemed to verify this possibility which, if it occurred, would test the validity of using an electromagnetic velocity meter in the trunkline. Figure 6 is a photograph of the test site. The instrument shelter is in the center rear of the photograph. All sensor lines are laid in pipes shallowly placed beneath the ground for protection. The only entrances to the storm-sewer system were via the two 18-in diameter manholes. Thus all measuring equipment would have to pass through these limiting openings--a typical and realistic situation.

Figure 6. Field test site at Jackson, Mississippi.

(The hydrologist is standing at upstream catchment number 3 (see fig. 5); the instrument shelter (11) is in the center; curb inlet (6) and catchment (7) are midway between shelter and car and dye sampling shelter (19) is at extreme right.)

FIELD CALIBRATIONS AND VERIFICATIONS

The objectives of constructing and operating the various measuring and recording instruments at a field site were fourfold: (1) to develop construction and fabrication techniques practical for operational use; (2) to test the performance and reliability of the instrumentation; (3) to verify instrument calibrations obtained in the

laboratory; and (4) to field rate certain of the measuring devices and installations in situ. The latter would be done using flow from a nearby fire hydrant (see fig. 5, item 1). The hydrant flows would be accurately measured using an acoustic flowmeter and tracer dilution techniques. Tracer dilution techniques would also be used to measure natural storm discharges through the measuring devices.

Field Calibration Techniques

As discussed earlier, the Jackson test site was chosen to test the proposed storm-water measurement system and in particular rate or verify the calibrations of the various measuring devices. As seen in figure 5, a fire hydrant located at the site allowed controlled flows to be established in the gutters, into the inlets and catchments, and through the 18-in and 48-in pipes and their respective measurement devices. The accurate, independent measurement of hydrant discharges was essential to verifying calibrations.

Acoustic Flowmeter Measurements

The discharge from the fire hydrant was collected from the various hydrant outlets via a manifold arrangement shown in figure 7. The collected hydrant flow was directed into the street gutter via the 20-ft long, 8-in diameter pipe shown in figure 8. The objective in collecting the hydrant flow into one pipe was so it could be accurately measured by an acoustic flowmeter clamped on the outside of the pipe as shown in figure 9. This flowmeter and pipe combination were carefully calibrated at the HIF laboratory prior to assembly at the Jackson site. It was essential that the pipe flow full for accurate measurements with this acoustic flowmeter. Flow data was read from the computer shown in figure 10.

Tracer Dilution Discharge Measurements

Concurrent with the acoustic meter measurements, tracer dilution discharge measurements were made of each hydrant flow. Numerous studies have investigated or advocated the use of the tracer dilution method for measuring flows in storm sewers.[31,32,33,34,35,36,37] The principle advantage of the technique is that measuring structures need not be installed in the pipes and catchments, and the normally turbulent conditions encountered are advantageous for rapid mixing of tracer and flow.

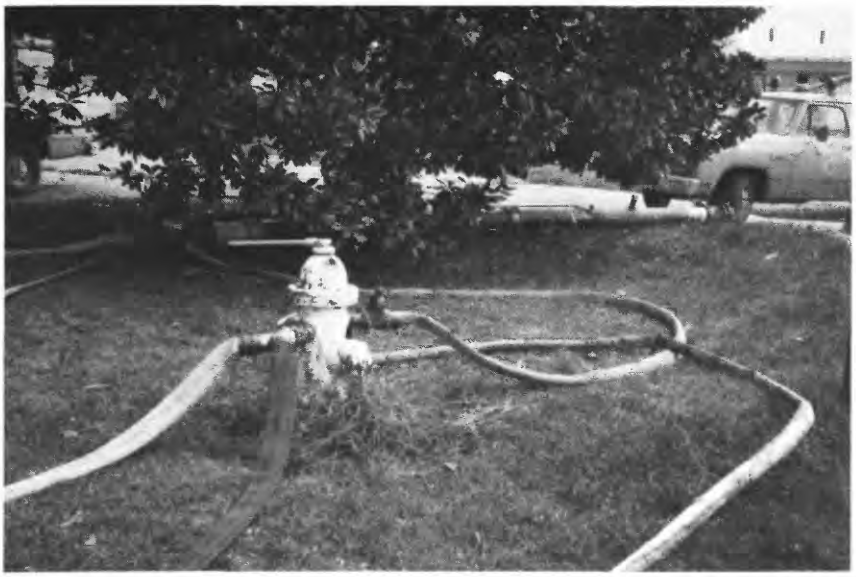

Figure 7. Hydrant hookup.

(Manifold pipe used to concentrate and measure flow is to rear.)

Figure 8. Manifold used to concentrate flows from fire hydrant.

(Acoustic flowmeter is attached to far end of pipe at upper left.)

Figure 9. Acoustic flowmeter transducers clamped to outside of hydrant manifold pipe.

(Two sensors are clamped on opposite sides of pipe a prescribed distance apart.)

Figure 10. Acoustic flowmeter computer and display.

For steady flow and using the constant injection method, the dilution discharge equation is

$$Q = q \frac{C}{\bar{c}} \tag{1}$$

where

Q is the discharge,

q is the rate of tracer injection and is assumed to be very small relative to Q,

C is the concentration of the tracer being injected, and

$\bar{c}$ is the resulting average plateau concentration after dilution by Q.

To perform these tests at the Jackson site, two tracer-injection systems were installed (items 18 in fig. 5): one to inject into the 48-in line at the upstream junction box (item 3 in fig. 5) and the other to inject into the catchment (item 7) and 18-in outflow pipe (see fig. 11). To measure the diluted concentrations after mixing in in the 48- and 18-in pipes, samples were withdrawn where these pipes enter the downstream junction box (item 10). To accomplish this, two water samplers were installed in a small shelter on the traffic island directly over this junction box (see fig. 6). Samples of the flow in the 48- and 18-in pipes were brought to the surface in separate hose lines via a 12-in concrete pipe which also discharged to this junction. These hose lines were led to the automatic samplers (item 19) which contain their own battery-driven pumps. The samplers could be signaled to collect samples on manual command or automatically by the micrologger upon sensing the occurrence of preselected stages in their respective pipes. As shown in figure 12, samples are withdrawn for shipment to the laboratory. The details of the sample analysis and computations will not be discussed here as it is well covered elsewhere.[38]

The tracer injection and sampling system just described and shown schematically in figure 13 was installed to measure each steady-state hydrant flow as well as natural flows which would occur during the field tests. Storm runoff flows might be expected to be very unsteady, especially if the surface drainage area was small and largely paved. If successful though, not only might the calibrations of the various measuring devices be checked at flows greater than could be obtained from the hydrant, but the possibilities of this approach to the measurement of storm-water flows in general could be investigated. Such an installation offered the possibility of calibrating measuring

Figure 11. Dye injection system.

(Calibrated mariotte vessel on left supplies constant rate pump on lower right which injects into flow. The pump is turned on upon command from micrologger when suffucicient flow occurs.)

devices or structures in situ, and might also provide directly all the storm runoff data desired as suggested by Wenzel.[39]

According to equation 1, if tracer was injected continuously at a constant rate into a flow varying as shown by the solid line in figure 14, the inverse tracer concentration graph shown as a dashed line would result. Thus, it would seem that any sample taken (assuming adequate mixing) during such an unsteady flow would be a measure of the discharge at that instant. Unfortunately, there are certain factors which limit the degree of unsteadiness that can be

Figure 12. Dye sampling system.

(Sampler with 24 bottles collects dicrete samples which are sent to the laboratory for analysis.)

practically measured by dilution techniques.[35] The occurrence of longitudinal dispersion is the primary reason errors will result in measuring unsteady flow by dilution.[37] For the theoretically correct measurement of unsteady flow using a continuous injection, it would be necessary for a given element of tracer to mix instantaneously in the flow element into which it was injected. Fortunately, field tests indicate that the method can be used and equation applied for rather high degrees of unsteady flow if certain precautions are employed.[36] Mixing lengths must be kept to a minimum. It has even been suggested that artifical means might be used to expedite mixing.[40] The presence of measuring flumes, weirs, and other conditions promoting turbulence will expedite mixing. Observations of mixing in storm-sewer catchments and at junctions indicates that for practical purposes "instantaneous mixing" may be nearly achieved. The long lengths required for complete mixing in pipes does not normally apply to storm-sewer pipe systems.[41]

The results of acoustic flowmeter and tracer dilution measurements of the hydrant flows and of dilution type discharge measurements of natural runoff will be discussed in turn subsequently.

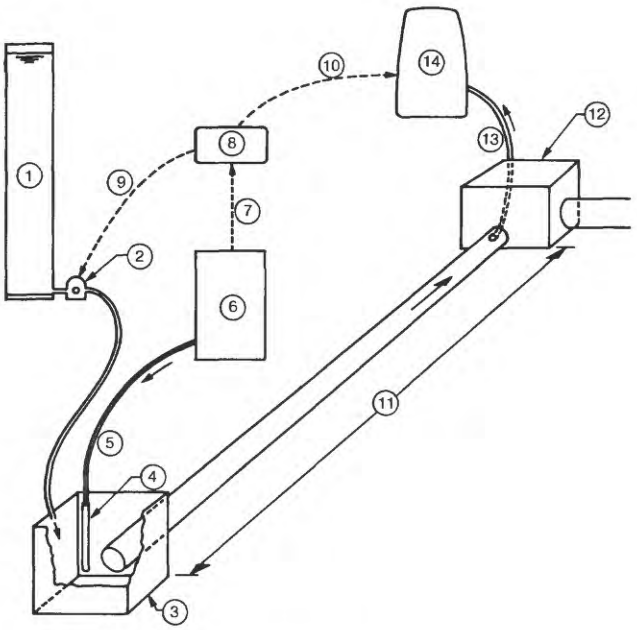

NOMENCLATURE

1. DYE RESERVOIR
2. CONSTANT RATE INJECTION PUMP
3. CATCHMENT
4. STILLING WELL CONTAINING BUBBLER ORIFICE
5. PNEUMATIC BUBBLER GAS LINE
6. PNEUMATIC BUBBLER TRANSDUCER SYSTEM
7. SIGNAL FROM PRESSURE TRANSDUCER
8. MICROLOGGER
9. SIGNAL TO PUMP
10. SIGNAL TO SAMPLER
11. MIXING LENGTH IN SEWER LINE
12. SEWER JUNCTION BOX
13. SAMPLING HOSE
14. AUTOMATIC SAMPLER

Figure 13. Sketch of automated dye-dilution discharge measurement apparatus.

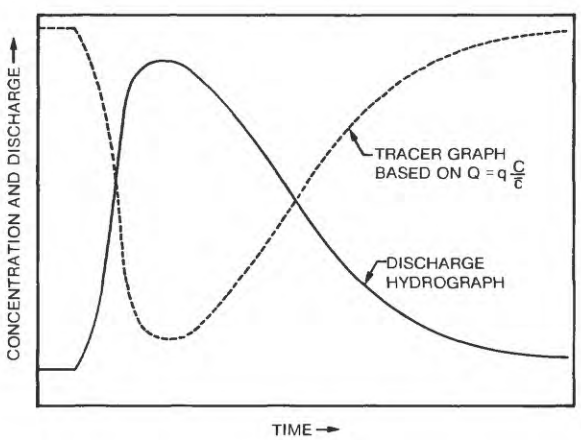

Figure 14. Tracer hydrograph produced by constant-rate injection into unsteady discharge.

HEAD MEASUREMENT SYSTEM

The pneumatic-bubbler transducer (PBT) system used in this study is shown in figure 15. The system consists of an individual sight feed regulator, pressure transducer, and orifice for each measuring point. The individual systems are connected in parallel to a single high-pressure nitrogen source and a calibration standpipe. Several identical sight feed units and their associated pressure transducers may be used to measure water-level changes at several locations. Only the individual pressure transducer (full-scale range) will vary depending on the amount of water-level change that is expected at each measurement location. Choice of transducer range is an important consideration if measurement precision and resolution are a critical concern.

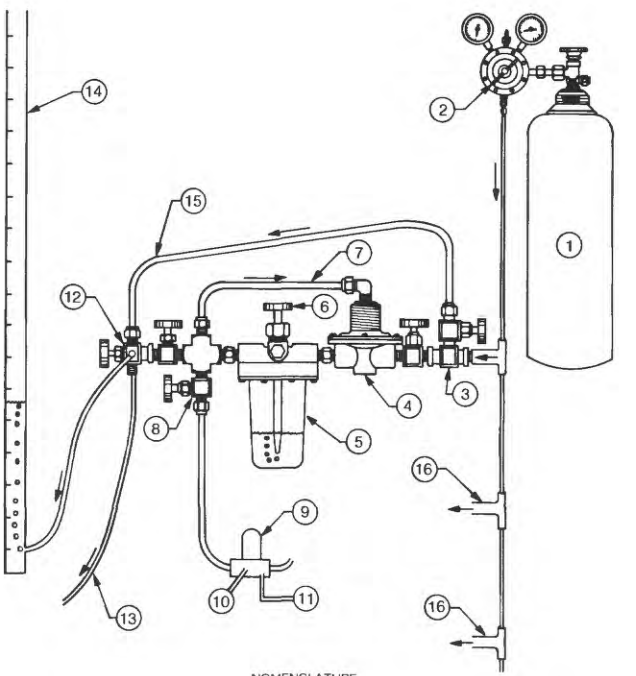

NOMENCLATURE

1. DRY NITROGEN GAS SUPPLY.
2. HIGH PRESSURE REGULATOR.
3. SYSTEM SHUTOFF VALVE.
4. CONSTANT FLOW DIFFERENTIAL REGULATOR.
5. SIGHT FEED INDICATOR.
6. BUBBLE RATE NEEDLE VALVE.
7. FLOW REGULATOR FEEDBACK LINE.
8. PRESSURE TRANSDUCER ISOLATION VALVE.
9. PRESSURE TRANSDUCER.
10. D.C. VOLTAGE EXCITATION, 8-20 VOLTS.
11. OUTPUT, 0-5 VOLTS, TO MICROLOGGER.
12. THREE-WAY BALL VALVE.
13. TO ORIFICE.
14. CALIBRATION TEST STANDPIPE.
15. HIGH FLOW GAS PURGE LINE.
16. GAS TO ADDITIONAL SYSTEMS.

Figure 15. Pneumatic-bubbler transducer head measurement system.

The overall system function is to provide a continuous dynamic gas flow in the form of a uniform bubble rate that escapes from the orifice. A precision needle valve on top of the glass sight feed indicator is used to set the bubble rate. The bubble rate should be slow enough to preclude pressure errors associated with friction losses along the orifice tube. Higher bubble rates are sometimes needed to smooth out the analog signals from very sensitive pressure transducers and to improve the response time of the system with rapidly changing water levels. The optimum bubble rate seems to be about 60 to 120 per minute; the higher rates are suggested for use where rapidly changing stage is expected. For installations requiring orifice tubes whose lengths are in excess of 300 feet, two tubes are often used; one to supply the gas flow to the orifice and a second tube connected to the orifice to transmit the true pressure back to the pressure sensor, thus eliminating the friction losses.

The instantaneous pressure on the output side of the sight feed indicator is fed directly back to a differential regulator to maintain constant flow rate and is also connected to a three-port selector valve. This valve can route the gas to the orifice line or to a calibration water column (standpipe) for transducer output verification.[42] This feature is quite useful to check pressure transducer calibration and long-term stability; this will be discussed more fully as part of the field tests.

Laboratory Tests

A critical component of the PBT system is the pressure transducer. It was, therefore, important to calibrate and determine the response characteristics of the transducers selected under different environmental conditions. The transducers chosen were the Schaeuitz Model P-3061. This is a diaphragm-type variable-reluctive-type transducer which produces an output voltage proportional to a pressure difference. This series has a 0 to 5 volt DC output and hence can be directly input to the micrologger with an appropriate voltage divider. Reluctive transducers use the ratio of the reluctance of the magnetic flux path of two coils and, therefore, are less subject to temperature effects than one-coil devices. This feature plus cost led to selection of this brand and series of pressure transducer.*

*Numerous manufacturers are producing transducers that should be considered depending on desired operation characteristics and costs; this is not an endorsement of this particular brand.

Three 100-in range, two 50-in range, and one 10-in range Schaevitz Model P-3061 series pressure transducers were tested in the laboratory. A dead-weight tester was used to apply a range of pressures to each transducer for three to four different temperatures. Each test consisted of increasing the pressure in increments from zero up to and in some instances slightly in excess of the rated range and then back down in increments to zero pressure to assess any hysteresis effects. Data obtained consisted of a voltage output for each applied pressure. For each transducer the pressure (converted to feet of water) and voltage output data for a given temperature were linearly regressed to obtain calibration equations for each transducer of the form

$$d = \frac{(V_o - b)}{s} \tag{2}$$

where

d is the computed depth of water in feet,

V_o is the voltage output from the transducer,

b is a constant, and

s is the slope of the regression.

Table 1 summarizes the calibration results for all six transducers; note in particular the consistancy of the regression slopes for a transducer of a given range and the small standard errors in most cases. To study the characteristics of each transducer as to possible temperature and hysteresis effects, the difference in computed depths using equation 2 and the actual depths were plotted versus actual depth as shown in figures 16, 17, and 18. The abscissas scale has been chosen to emphasize the differences or errors that might be expected using transducer-measured depths. Comparison of the three figures indicates that as would be expected, the greater the range of the transducer, the greater the potential error; the 100-in unit having about a ± 0.02-ft spread, while the 50-in and 10-in units are well within ± 0.01-ft spread. In fact, examination of figure 18 for the 10-in unit would indicate that if for the 0° and 50 °C tests the zero depth data were ignored in the regression computation, these two curves would have fallen very close to the 25° curve and the spread (except at zero depth) would have been at worst ± 0.005 ft. The regression computation of the form of equation 2 fits the best curve to the data and gives weight to the zero depth data which should logically be ignored. Examination of the curves in figures 16, 17, and 18 also indicates no recognizable trend with temperature and that hysteresis is not significant and is the least at colder temperatures.

Table 1. Summary of pressure transducer laboratory calibration results before and after field use.

$$\text{Computed depth} = \frac{[\text{Voltage output} - \text{constant (b)}]}{\text{Slope of regression, (s)}}$$

S_e = standard error of estimate in ± feet

Temperature °C	100-inch transducers								
	SN 5340*			SN 5343			SN 5344		
	(b)	(s)	(S_e)	(b)	(s)	(S_e)	(b)	(s)	(S_e)
	(1)	(2)	(3)	(4)	(5)	(6)	(7)	(8)	(9)
50	0.0785	0.606	0.01	0.0488	0.603	0.01	0.0134	0.602	0.10
25	0.0695	0.604	0.01	0.0548	0.603	0.01	0.0180	0.603	0.01
(25)**				(0.0256)	(0.6047)	(0.01)			
0	0.0578	0.602	0.01	0.0521	0.600	0.01	0.0310	0.593	0.02
-25	0.0889	0.601	0.01	0.0916	0.597	0.01	0.0308	0.595	0.01

Temperature °C	50-inch transducers								
	SN 4881			SN 4900			SN 4900***		
	(b)	(s)	(S_e)	(b)	(s)	(S_e)	(b)	(s)	(S_e)
	(10)	(11)	(12)	(13)	(14)	(15)	(16)	(17)	(18)
50	0.0773	1.202	0.00	0.0381	1.182	0.04	0.0003	1.219	0.00
25	0.0247	1.204	0.00	0.0541	1.176	0.08	0.1515	1.212	0.00
(25)**	(-0.4321)	(1.209)	(0.00)						
0	-0.0155	1.207	0.00	0.0770	1.180	0.07	0.0311	1.320	0.00
-10	-0.0088	1.203	0.01						
-25				0.0867	1.184	0.06	0.0702	1.200	0.03

Temperature °C	10-inch transducer		
	SN 4110		
	(b)	(s)	(S_e)
	(19)	(20)	(21)
50	0.1960	6.161	0.01
25	0.2447	6.072	0.01
(25)**	(0.2314)	(6.021)	(0.00)
0	0.1895	6.144	0.01

*Serial number.
**Bracketed data is post laboratory calibration results; regression equations excluded extreme data.
***Unlike other correlations, data for pressures above 48 inches of water were omitted.

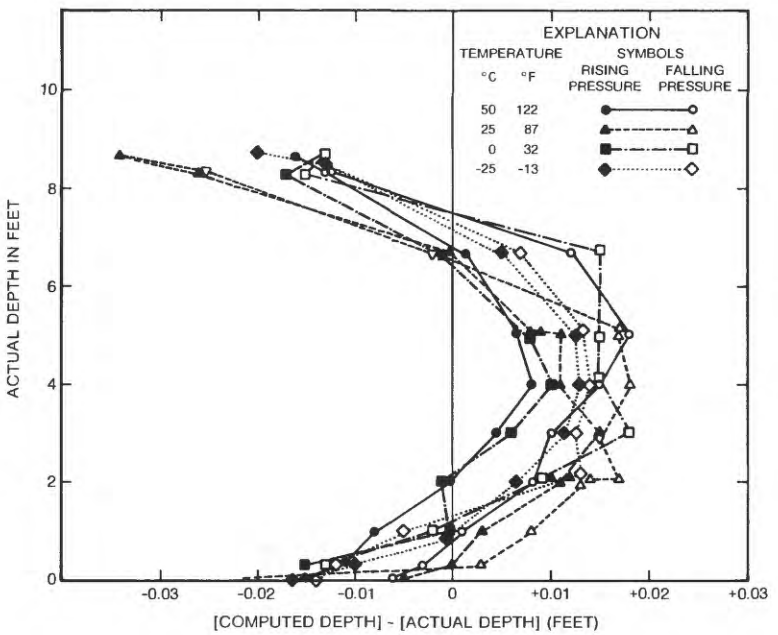

Figure 16. Laboratory test calibration of 100-inch pressure transducer.

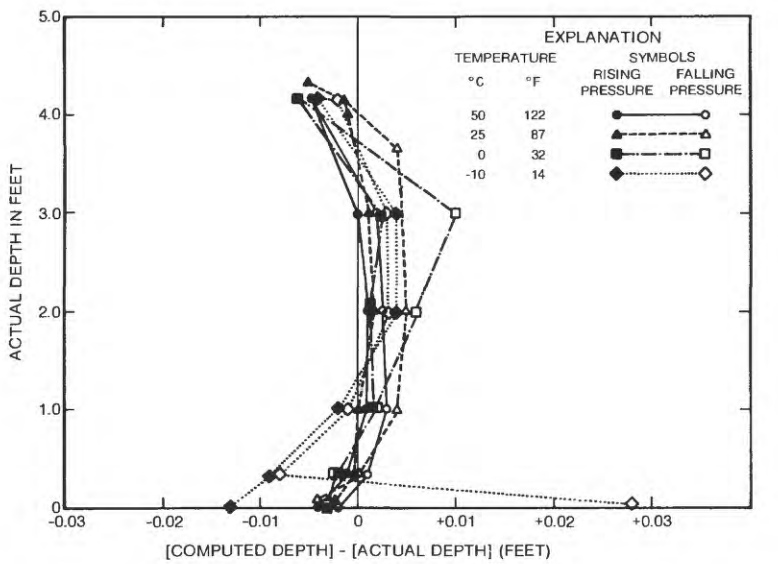

Figure 17. Laboratory test calibration of 50-inch pressure transducer, serial number 4881.

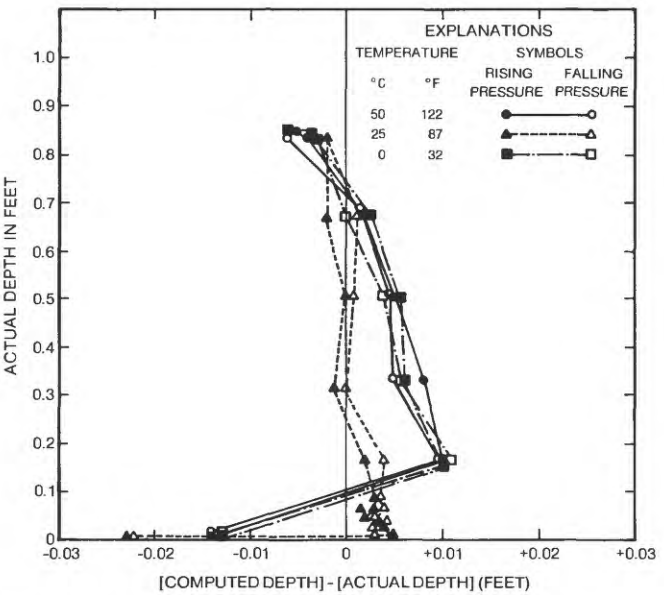

Figure 18. Laboratory test calibration of 10-inch pressure transducer, serial number 4110.

A second 50-in range transducer was tested with the results shown in figure 19. Note that the absissas scale is a factor of 10 less in order to plot this data, as the results are this order of magnitude worse. The curves in figure 19A are based on regressions using all the data. As can be observed, the four curves fall closely together but slope to compensate for the erratic data at the zero and maximum range depths. Recognizing that the correlations would be considerably improved by ignoring these data, new regressions were performed. The results were much improved as shown in figure 19B, and compare favorably with that of the other 50-in transducer shown in figure 17. Note the difference in standard errors in column 15 compared with column 18 in table 1. The comparisons shown in figures 19A and 19B are presented to emphasize the importance in any calibration analysis of examining the data at the extremes and, if advisable, omitting these data with the stipulation to the user to avoid the use of the transducer at its range extremes.

Data for all three 100-in transducers were plotted as for the one in figure 16 with the exception of transducer serial number 5344 for a temperature of 50 °C (see table 1). This transducer was the only one of the 100-in units found to be affected by high temperatures. Note in column 9 of table 1 the large standard error, S_e, for the 50 °C test. This and the tendency for hysteresis to be greatest at high temperatures suggests the desirability of insulating transducers from extremes in temperature.

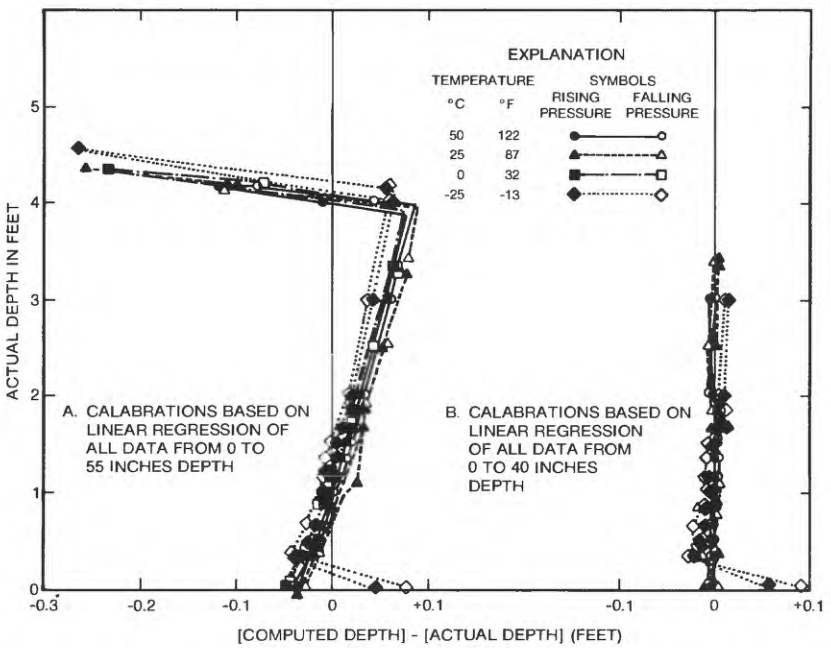

Figure 19. Laboratory test calibration of 50-inch pressure transducer, serial number 4900.

With the exception noted above, all data for the three 100-in transducers plotted very similar to that shown in figure 16. As a result, it was possible to present one curve that adequately characterized the 100-in transducers. Similarly the depth correction curve shown in figure 20 was feasible and provides a means of correcting transducer depths less than 1.3 ft and greater than 7.0 ft. Important is the fact that these three transducers appear to be reliable and accurate to ± 0.01 ft if their range extremes are avoided.

The following may be concluded from these transducer tests:

o Each transducer should be tested and calibrated in the laboratory over a range in depths and temperatures; experience may eventually indicate that calibration at one temperature is adequate.

o Temperature effects are not normally significant but high temperatures should be avoided or the transducer insulated from extremes.

o Hysteresis is not significant and is the least at colder temperatures.

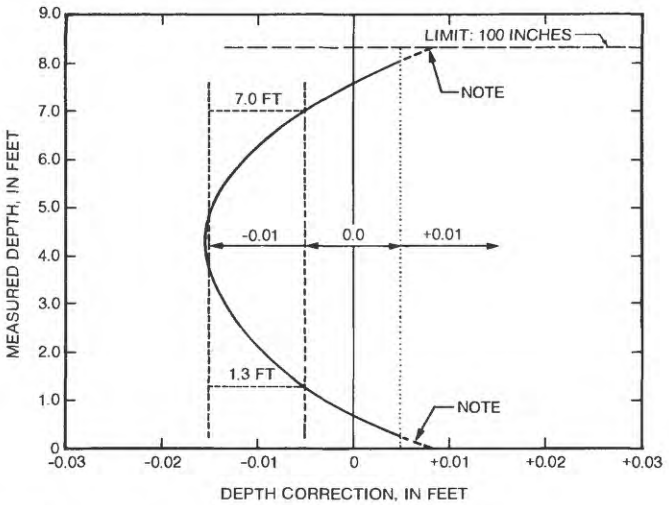

NOTE: USE WITH CAUTION ABOVE 8.0 FEET AND BELOW 0.2 FEET

Figure 20. Depth correction curves for 100-inch pressure transducers.

o Calibration regressions should exclude the use of data extremes.

o Transducers should not be used below about 5 percent and above about 95 percent of their stated ranges.

Field Tests

The system depicted in figure 2 was installed at the Jackson test site as shown in figure 5. The PBT system was located in the instrument shelter (see fig. 6) and consisted of five transducers, figure 21, connected to five pneumatic bubbler regulators as shown in figure 22. Figure 23 shows an individual regulator system which fits into the total system as shown in figure 15. Figures 15 and 22 show a test standpipe as part of this operational system. The test standpipe provided a column of water through which the gas flow could be diverted thus allowing for periodically checking the calibration of each transducer. This was done by diverting the pressure representative of any standpipe head of water to the appropriate transducer. The resulting voltage output was measured on the micrologger shown in figure 24 and allowed comparison of field values with the laboratory calibrations. Furthermore, it provided a means of zeroing the micrologger. As was seen from the laboratory tests, the transducers may be erratic at or near zero pressures. Therefore, field tests indicated the desirability of recording voltage outputs from the transducers, rather than their equivalent computed heads and later computing head of water using the individual transducer calibrations

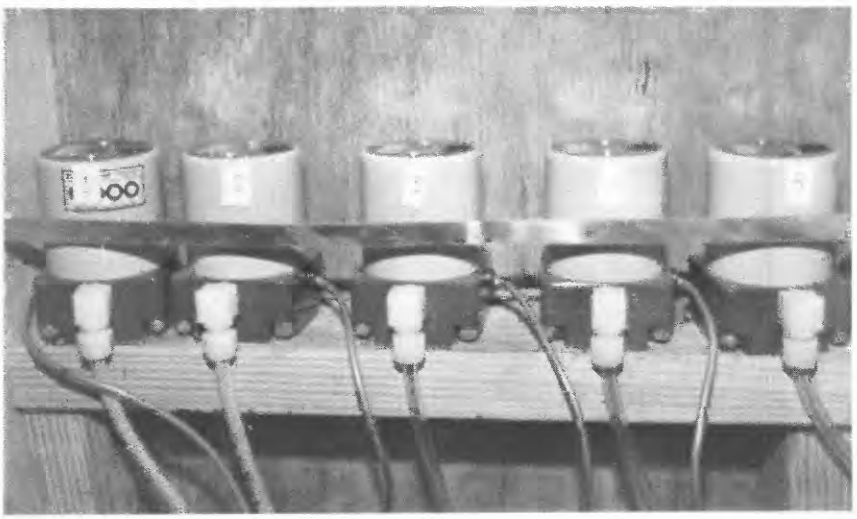

Figure 21. Five pressure transducers wall-mounted at field site.

(Tubing transmits pressure from five separate bubbler orifices. Tests indicated these should be insulated from high temperatures.)

(see table 1). After 6 months of use, three of the transducers in use at the field test site were removed for post calibration tests in the laboratory at the GCHC. Prior to doing so their calibrations were checked using the standpipe; air temperatures at the time were about 5 °C. Table 2, columns 2 and 4 show the test depths of water and corresponding voltages respectively read for depths established in the standpipe (all field data and results are bracketed in table 2). Column 5 indicates the depths computed by using the original laboratory calibrations obtained prior to their installation at the Jackson test site. As can be seen by column 6, the 100-in and 10-in transducers apparently have held their initial calibrations reasonably well whereas the 50-in one shows a consistent shift of about -0.37 ft.

Post Laboratory Transducer Tests

The three transducers were then retested in the laboratory at the GCHC in the manner previously described. The transducers were retested only at 25 °C. The test depths and corresponding transducer voltages obtained in the laboratory are presented in table 2, columns 1 and 3 respectively. The results duplicated the field data showing the same shift in the 50-in transducer as was observed in the field; column 6. New calibrations were derived for the three transducers

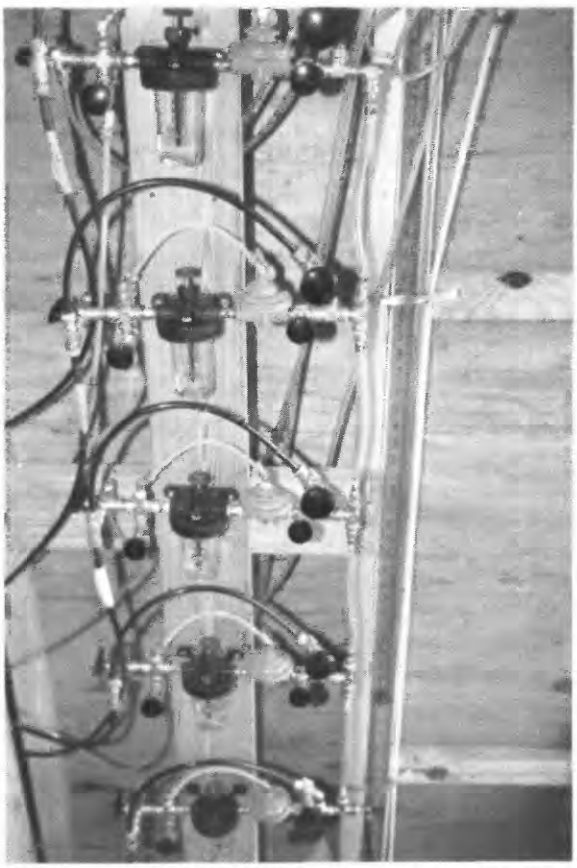

Figure 22. Five pneumtic bubbler regulator systems wall-mounted at test site.

(Calibration stand-pipe is to right and gas supply cylinder out of picture to left.)

from the laboratory data; these are the bracketed values in table 1. Based on the experience obtained from the original laboratory calibrations, the extreme data was not used in the regression analysis used to obtain new calibration equations. Furthermore, table 2 presents only the data obtained on the falling pressure portion of the laboratory tests, whereas all but the data extremes was used in the regressions. Based on these new calibrations, new depths were computed as shown in column 7 of table 2 with the small differences shown in column 8. Note that even though the zero depth data was not used in the regressions, computed depths for zero depth voltage readings are shown and in the case of the 100-in and 50-in transducers a significant difference exists. This is shown to emphasize the

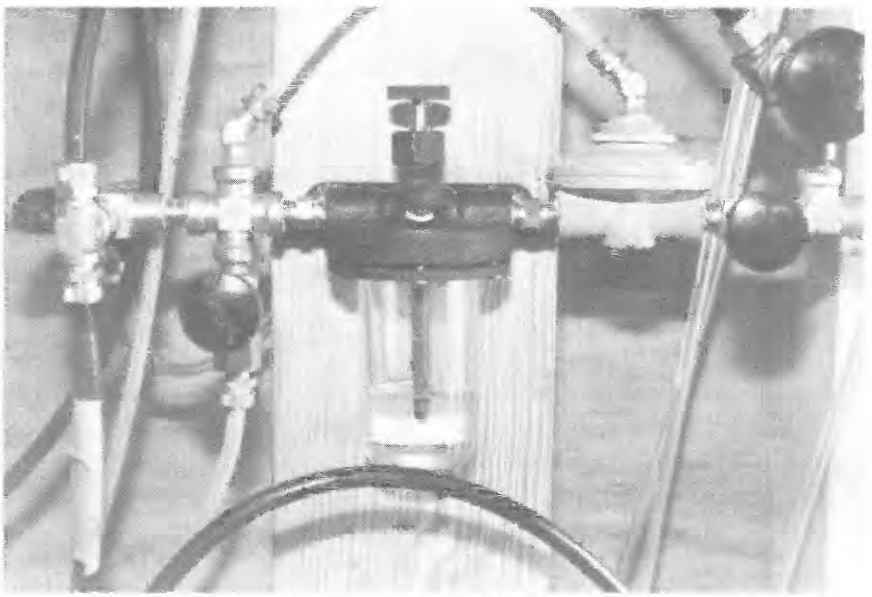

Figure 23. Pneumatic-bubbler gas regulator system.

Figure 24. Micrologger unit in center with relay board on left and data storage module at lower center.

Table 2. Results of field and post laboratory calibration of transducers

(All units in feet unless otherwise indicated)

Measured depths		Transducer output, volts		Computed depths and differences			
				Based on original calibration		Based on post laboratory calibration	
Laboratory	(Field)*	Laboratory	Field		Differences		Differences
(1)	(2)	(3)	(4)	(5)	(6)	(7)	(8)
			100-inch transducer; SN 5343				
8.33		5.0570		8.30	-0.03	8.32	-0.01
6.67		4.0580		6.64	-0.03	6.67	0.00
5.00		3.0560		4.98	-0.02	5.01	+0.01
	(4.48)		(2.75)	(4.48)	(0)	(4.51)	(+0.03)
4.00		2.4511		3.97	-0.03	4.01	+0.01
	(3.66)		(2.26)	(3.66)	(0)	(3.70)	(+.04)
3.00		1.8473		2.97	-0.03	3.01	+0.01
	(2.60)		(1.62)	(2.60)	(0)	(2.64)	(+0.04)
2.00		1.2396		1.97	-0.03	2.01	+0.01
	(2.00)		(1.26)	(2.00)	(0)	(2.04)	(+0.04)
1.00		0.6286		0.95	-0.05	1.00	+0.00
	(0.80)		(0.54)	(0.81)	(+0.01)	(0.85)	(+0.05)
	(0.40)		(0.31)	(0.43)	(+0.03)	(0.47)	(+0.07)
0.33		0.2215		0.28	-0.05	0.32	-0.01
0.00**		0.0864		0.05	+0.05	0.10	+0.10**
			50-inch transducer; SN 4881				
4.17		4.6000		3.80	-0.37	4.16	-0.01
	(3.66)		(3.97)	(3.30)	(-0.36)	(3.64)	(-0.02)
3.00		3.2010		2.64	-0.36	3.01	+0.01
	(2.60)		(2.71)	(2.26)	(-0.34)	(2.60)	(0.00)
2.00		1.9907		1.63	-0.37	2.00	0.00
	(2.00)		(1.99)	(1.66)	(-0.34)	(2.00)	(0.00)
1.00		0.7768		0.62	-0.38	1.00	0.00
	(0.80)		(0.55)	(0.47)	(-0.33)	(0.81)	(+0.01)
0.33		-0.0322		-0.05	-0.29	0.33	0.00
	(0.40)		(0.06)	(0.06)	(-0.34)	(0.41)	(+0.01)
0.00**		-0.3005		-0.27	-0.27	0.11	+0.11**
			10-inch transducer; SN 4110				
0.83		5.2490		0.82	-0.01	0.83	0
	(0.80)		(5.36)	(0.84)	(+0.04)	(0.85)	(+0.05)
0.67		4.2600		0.66	-0.01	0.67	0
0.50		3.2480		0.50	0	0.50	0
	(0.40)		(2.94)	(0.45)	(+0.05)	(0.45)	(+0.05)
0.33		2.2405		0.33	0	0.34	+0.01
0.00**		0.2216		0	0	0.00	0**

*Using standpipe - see figure 15, item 14, and figure 22.

**Zero depth data not used in post-laboratory regression analysis.

importance of not operating these transducers at very shallow depths or at least to be aware of their limitations.

These field and laboratory tests on these three transducers re- the need for periodic checking and recalibration of transducers in the field. Thus the calibration standpipe is virtually a mandatory requirement. On the positive side, it is believed the transducers go through an aging process and continued use will result in a stablization of the calibration. The constancy of the shifts, the -0.37 ft for the 50-in unit and -0.03 ft for the 100-in one, seem to indicate the probability of a consistant aging process. It might be desirable to age transducers artificially, before field use. An assessment of this aging process and of the ultimate stability of transducers needs further laboratory and field testing.

CATCHMENT TESTS

Most catchments have either 12-in or 18-in diameter sewer drainpipes, usually of concrete. Two PIC meter sizes were designed to fit these two pipe sizes. The PIC meter is fabricated of plastic and consists of a rounded entrance section* which fits against the entrance to the drainpipe and is sealed to the catchment wall around this pipe (see fig. 25) This entrance is fastened to a pipe section which extends down into the drainpipe. To fit the 12- and 18-in drainpipes, a 10- and 15-in diameter plastic pipe and entrance opening were chosen to yield the desired contraction. Figure 25 and table 3 show the dimensions of the two PIC meters. Figures 26 and 27 show the PIC meter before and after assembly. The design required that each piece fit through an 18-in diameter manhole as shown in figure 26, the catchment, and eventually into the drainpipe.

Laboratory Rating of Unaltered Catchment and 12-inch Outflow Pipe

For both sizes of PIC meters, testing consisted of initially rating the unaltered catchment-outflow pipes. This was done on the premise that if head readings could be obtained in the catchment in the approach to the outflow pipe, it might prove feasible in many instances to rate existing catchments without adding metering devices of any sort. Furthermore, it was desirable to determine the loss of capacity, if any, with the installation of a PIC meter.

The pipe slope for all laboratory PIC meter tests was zero. The flush, square entrance 12-in outflow pipe was calibrated for cases 1, 2, and 3 (see fig. 1).

---

*Adapted from a plastic liftgate irrigation valve assembly manufactured by Plastics, Inc., of Rayne, Louisiana.

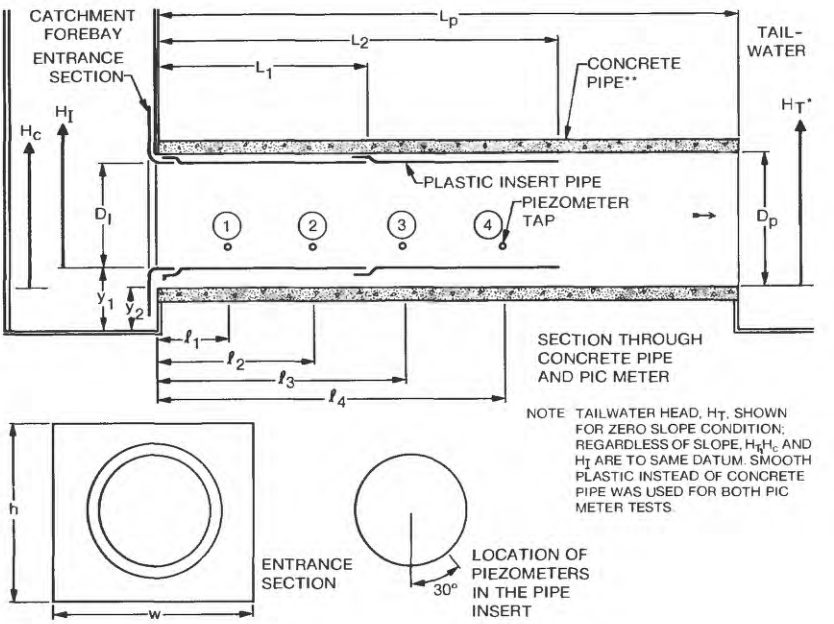

Figure 25. Sketch of pipe insert contraction meter laboratory setup.

Table 3. Dimensions of PIC meter laboratory setups.

(All dimensions are in feet except as noted; see figure 25 for explanation.)

Test meter	Diameters		Entrance section				Lengths						
	Plastic pipe, D_p	Insert pipe D_I	Width, w	Height, h	Radius of rounding, r	Invert heights above catchment floor, y_1/y_2	One insert tube, L_1	Two insert tubes, L_2	Concrete sewer pipe L_p	Piezometer Taps l_1	l_2	l_3	l_4
	(1)	(2)	(3)	(4)	(5)	(6)	(7)	(8)	(9)	(10)	(11)	(12)	(13)
12 inch	1.00	0.833	1.50	1.50	0.032	0.33/0.08	1.67	3.00	10.0	0.67	1.33	2.00	2.67
18 inch	1.50	1.250	1.88	1.75	0.083	0.86/0.70	3.00	5.67	10.0		2.17		4.46

Figure 26. Components making up Pipe Insert Contraction meter.

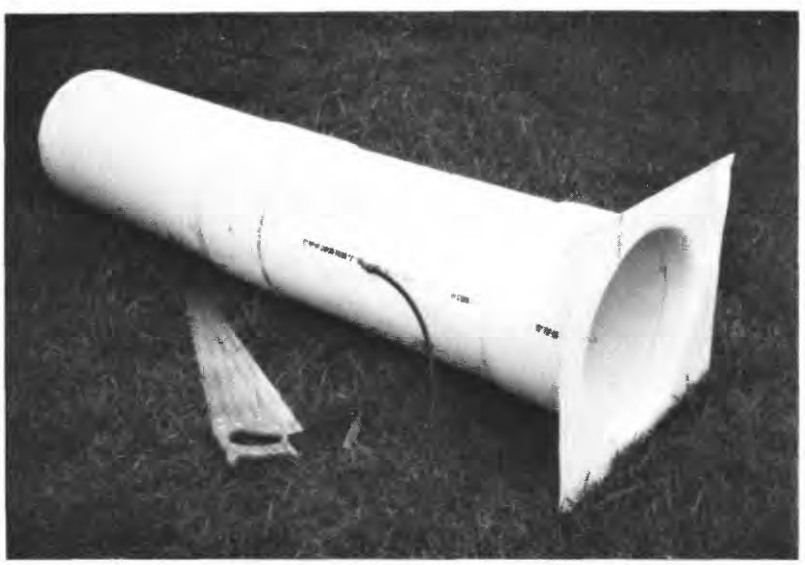

Figure 27. Preassembled Pipe Insert Contraction meter.

From the reduced data H_C and Q (the head difference, ΔH_{CT} and Q for backwater conditions), a set of rating curves for each set of flow conditions for the flush entrance outflow pipe were obtained and are shown in figure 28. As can be seen, the 12-in pipe has a capacity of about 2.2 ft^3/s when the head reaches the elevation of the crown of the pipe. Above this, separation takes place (case 2) with the pipe still flowing partially full at the maximum head tested, even with the pipe on zero slope. The pipe could be forced to flow full only by increasing tailwater stages downstream. The rating with the pipe forced to flow full (curve 3 in fig. 28) requires the measurement of the head difference between the catchment and the tailwater.

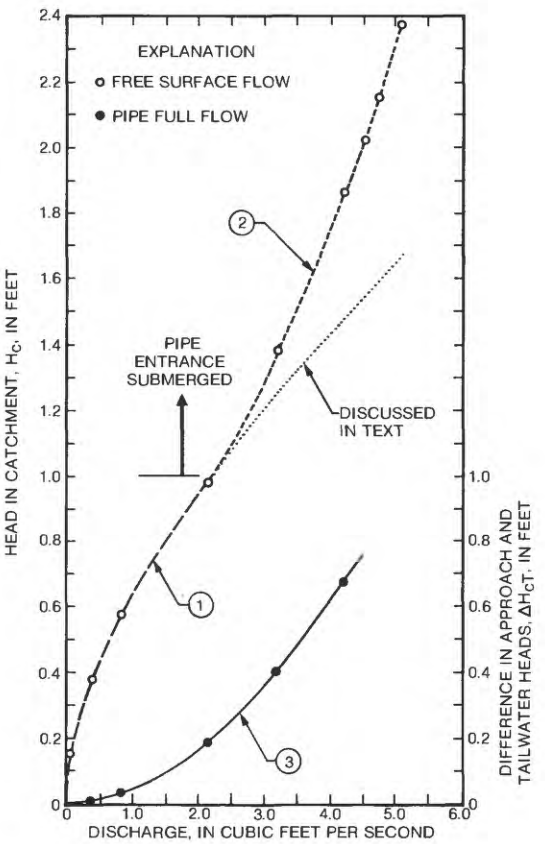

Figure 28. Ratings for unaltered catchment and 12-inch outflow pipe.

All ratings are well defined and indicate the viability of rating such structures in their unaltered state. Every installation would probably have a slightly different rating. Approximate equations for the curves in the form of $Q = aH^b$ ($Q = a\Delta H^b{}_{c_I}$ for backwater conditions) were obtained by using a power curve fitting program on an HP-97 desk calculator.* Table 4 lists these equations with their range, pipe flow conditions, and coefficient of determination (r^2) for each equation. All data points obtained with nonbackwater conditions fell within 5 percent of one of the two calibration curves derived from testing.

Ten-Inch PIC Meter Laboratory Calibrations

The 10-inch PIC meter was tested in the laboratory for one and two 20-in pipe lengths (see fig. 25 and table 3). The meter was tested at zero slope through four flow conditions as follows:

1. Flow from zero up to the crown elevation of the meter insert.

2. Flow and stages in the catchment above the crown but with the insert barrel flowing only partially full.

3. Pipe insert flowing full and limited submergence due to tailwater or backwater conditions.

4. Pipe insert flowing full and backwater conditions sufficient to affect upstream catchment stages; unit acts as a venturi meter.

Figure 29 presents the calibration curves for the 10-inch PIC meter for the first three cases. Curve 1 is the calibration for heads up to the crown of the insert indicating it has a capacity of approximately 1.5 ft^3/s before the entrance becomes submerged. Note in figure 28 that the unaltered 12-in plastic pipe has a discharge capacity of about 2.2 ft^3/s when the head reaches the crown.

---

*The curve fitting program supplied by Hewlett-Packard for their HP-97 calculator uses the least-squares method for the determination of coefficients of the generated curve. The curve can be forced through only the first data point (the data point set to be the zero point). More exact equations could be obtained by forcing curves through all of the data points; to do so, a cubic spline interpolation would be needed. Depending on the number of data points, this would yield one or more cubic equations of the form of $y = a + bx + cx^2 + dx_3$. The simpler form of equation is used here as it generally fit the data sufficiently well.

Table 4. Summary of discharge rating curve equations for 12-inch outflow pipe.

Curve number	Equation	Flow conditions	Head range of equation*	r^2
1	$Q = 2.319H_c^{1.948}$	Water level below top of entrance of pipe	0.0 - 0.95	0.9992
2	$Q = 2.292(H_c-0.979)^{0.820} + 2.125$	Water level above top of entrance of pipe	0.96 - 2.40	0.9991
3	$Q = 5.312(\Delta H_{cT} - 0.004)^{0.683} + 0.350$	Backwater	0.004 - 0.70	0.9978

*ΔH_{cT} head difference for backwater conditions.

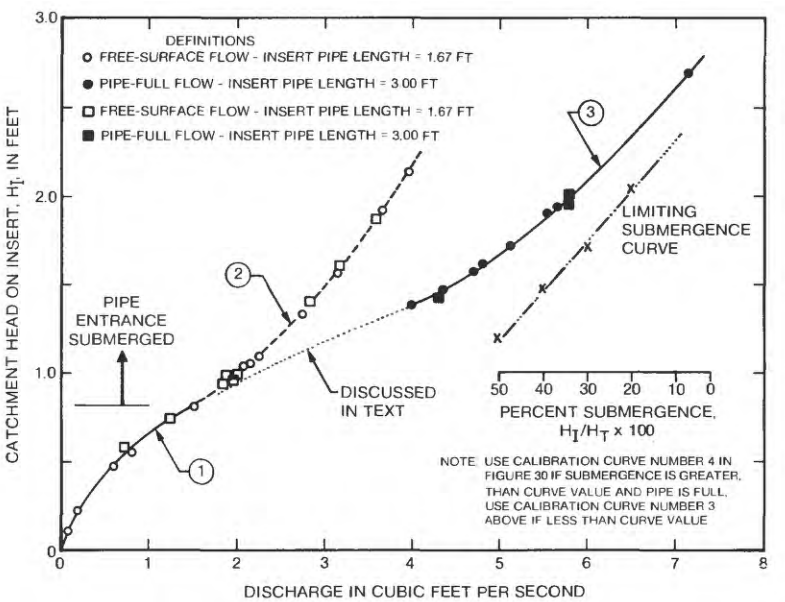

Figure 29. Ten-inch PIC meter calibrations for free-surface and pipe-full flow with limited submergence.

Curve 2 resulted with a continued increase in flow up to about 4 ft^3/s. For this range in head, 0.833 ft to about 2.15 ft, separation takes place, and the insert barrel flows only partially full. Calibrations 1 and 2 were found to hold for both the long and short insert barrel lengths which indicates clearly that control is at the entrance of the insert, the barrel length having no affect.

At H_I = 2.15 ft and the discharge = 4 ft^3/s, the insert barrel fills. Note from figure 28 that the unaltered 12-in plastic pipe has a capacity of about 4.75 ft^3/s at this head; hence the capacity has not been greatly reduced. Curve 3 is the calibration for when the insert barrel is flowing full and submergence conditions downstream are limited. Control for curve 3 is the insert barrel. Note that the same rating holds for the short- or long-length insert; probably because the smooth plastic insert pipe has insignificant friction loss.

Submergence tests indicated that ratings 1, 2, and 3 held if tailwater heads and, hence, submergence did not exceed certain levels. These levels varied with headwater; the limiting submergences are shown to the right in figure 29. Thus when submergence, defined as H_I/H_T x 100 (see fig. 25), exceeded the values defined by this limiting curve, catchment heads would increase with any increase in tailwater heads; in effect, increases in tailwater were being transmitted upstream and reflected in the headwater stages.

For pipe-full flow where submergence was above the limit, the PIC meter was treated as a venturi meter. Figure 30 presents the calibration curve for full venturi pipe flow where, in terms of relative head, the equation takes the form

$$Q/D_I^{5/2} = a\left[\frac{\Delta H_{IT}}{D_I}\right]^b \qquad (3)$$

in which ΔH_{IT} is the pressure drop in terms of feet of water from the catchment to the tailwater and D_I is the diameter of the insert pipe; a and b are constants for a particular rating.

To use the PIC meter and the calibration curves in figures 29 and 30 requires knowing what flow condition exists. Referring to figure 25, catchment head, H_I, and tailwater head, H_T, are needed and can be recorded by having pneumatic bubbler orifices located accordingly. In the laboratory tests, heads at the end of the insert barrel were measured by observing piezometer number 4. In the laboratory, these data indicated what flow condition existed. A pneumatic bubbler orifice located just downstream of the PIC meter but in the barrel of the 12-in concrete pipe should provide head data equivalent to the H_T as well as to indicate the flow conditions. That is, if

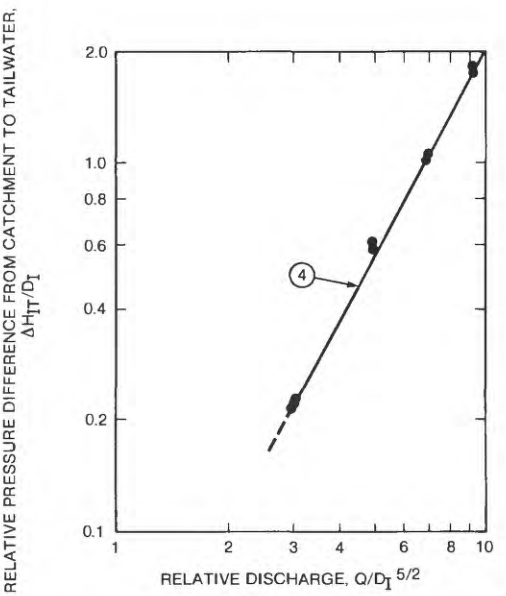

Figure 30. Ten-inch PIC meter calibration for pipe-full flow above limited submergence conditions.

the 12-in pipe is full, then the 10-in insert pipe would normally be full. One exception was noted and that was at very high discharges, the velocities in the insert barrel were very high and the pipe did not flow completely full even though very high submergences existed. This condition will rarely be reached as the catchment inlets rarely have this capacity.

Table 5 summarizes the discharge calibration curve equations for the 10-inch PIC meter.

It can be speculated what the calibrations would be for different pipe slopes. Curves 1 and 2 should not change, but curve 2 might be extended to slightly greater heads and discharges before the insert filled up and jumped to curve 3. Still the flow condition should be observable by measuring tailwater conditions in the 12-in pipe.

It is of interest to note in figures 28 and 29 the calibration curves which might have occurred if the separation producing curve 2 could have been avoided by more effective entrance rounding. The dotted curve extrapolations have been added to show what head-discharge relation would likely occur if both the unaltered 12-in pipe and 10-in insert pipe could be made to flow full when catchment stages just passed the crown elevations. In effect the greater hydraulic efficiency of pipe-full flow would be realized immediately,

Table 5. Summary of discharge calibration curve equations for 10-inch PIC meter.

Curve number	Equation	Pipe-flow conditions	Head range of equation*	r^2
1	$Q = 2.231H_I^{1.875}$	Water level below top of entrance	0.0 - 0.825	0.9998
2	$Q = 2.026(H_I-0.815)^{0.774} + 1.496$	Water level above top of entrance; drain pipe not flowing full	0.825 - 2.25	0.9983
3	$Q = 2.740(H_I - 1.379)^{0.873} + 4.030$	Water level above top of entrance; drain pipe flowing full	1.379 - 2.0	0.9995
4	$Q/D^{5/2} = 6.781(\Delta H_{IT}/D)^{0.534}$	Backwater conditions	0.2 - 1.8	0.9983

*ΔH_{IT} for backwater conditions.

and overall sewer capacities would be nearly doubled. Obviously a better PIC meter design would have featured a much larger radius entrance rounding, especially near the crown.

Laboratory Rating of Unaltered Catchment and 18-inch Outflow Pipe

Figure 31 shows the rating for the unaltered catchment with an 18-in diameter plastic outflow pipe at zero slope. As with the 12-in pipe tested previously, the control is the entrance to the pipe. The pipe has a capacity of nearly 19 ft^3/s at a head, H_C, of 5.0 ft. As before, even at this head, which is 3.5 ft above the crown of the pipe, it does not flow full when discharging freely. Table 6 summarizes the rating curve equations for the three segments of the rating shown in figure 31. There are two curves for case 1 flow instead of one. This reflects the contracting affect on the flow as the pipe area decreases rapidly toward the crown.

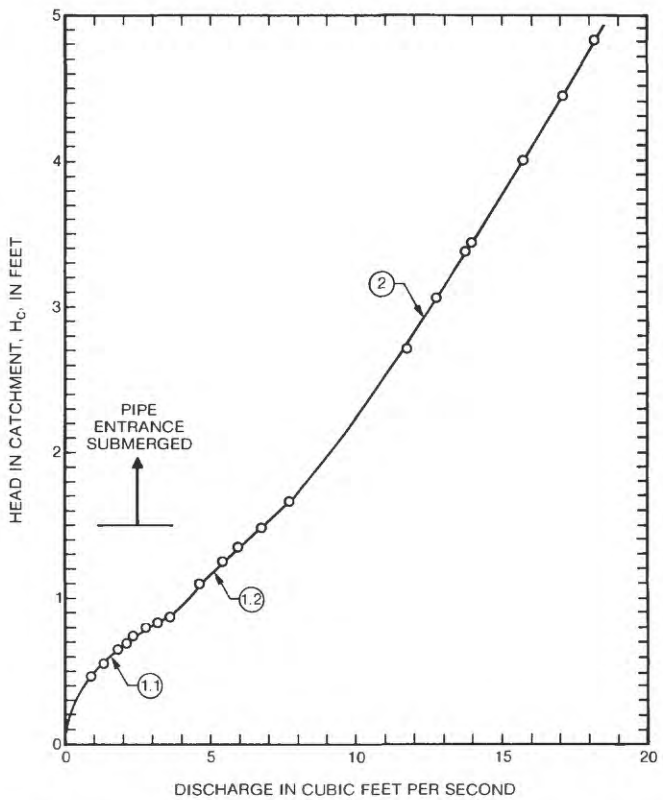

Figure 31. Rating for unaltered catchment and 18-inch outflow pipe.

Table 6. Summary of discharge rating curve equations for 18-inch outflow pipe.

Curve number	Equation	Flow conditions	Head range of equation	r^2
1.1	$Q = 4.646\ H_c^{2.127}$	Water level below crown	0 to 0.9 ft	0.9948
1.2	$Q = 5.294(H_c-0.876)^{1.078} + 3.585$	Water level slightly above crown	0.9 to 1.62 ft	1.0000
2	$Q = 4.393(H_c-1.346)^{0.828} + 5.927$	Water level above crown, open channel	1.62 to 5.0 ft	0.9992

Fifteen-inch PIC Meter Laboratory Calibrations

Figure 32 presents the calibration curves for the 15-inch PIC meter for both one and two insert barrel lengths. While there is a slight scatter in the data for the different barrel lengths, it is not considered significant. It should be noted that two data points for the short insert barrel plot to the right as the short barrel approaches full condition. The flow conditions in the long barrel configuration appeared more stable; therefore, it is the one recommended.

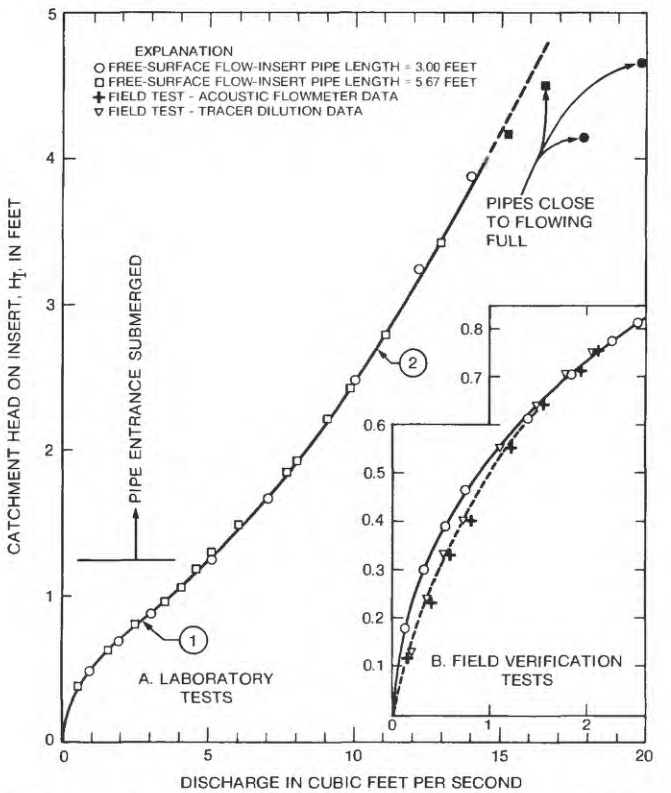

Figure 32. Fifteen-inch PIC meter calibration for free-surface flow.

Since the PIC meter with the long barrel configuration never flowed full and a case 3 flow condition did not occur, submergence limits were not determined. It is suggested that unless tailwater levels as measured downstream from the meter in the 18-in pipe indicate pipe full flow, the curves in figure 32 be used. When backwater conditions force the meter to flow full, the calibration curve shown in figure 33 should be used. Despite the agreement of the data at low values of $\Delta H_I/D_I$, the calibration should probably not be used

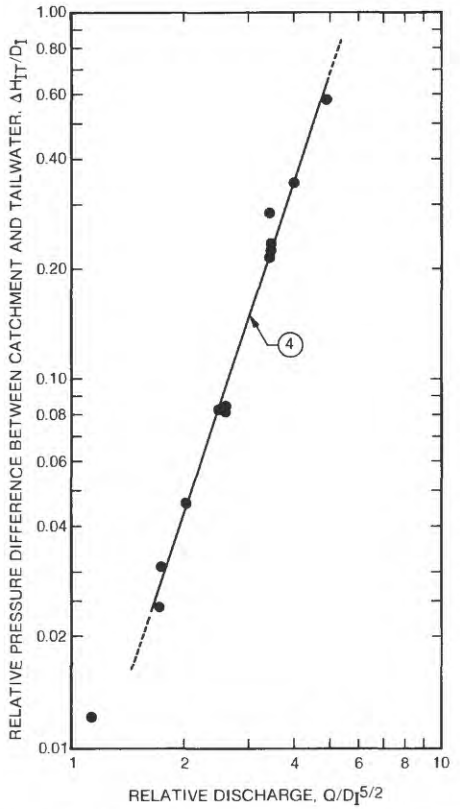

Figure 33. Fifteen-inch PIC meter calibration for pipe-full flow.

at relative heads less than 0.05 as sizeable errors are likely with such small head differences (0.062 ft). Table 7 summarizes the discharge calibration curve equations for the 15-inch PIC meter.

Inspection of figures 31 and 32 indicate very little loss in capacity by installing the 15-inch PIC meter compared with the 18-in unaltered pipe.

PIC Meter Field Tests

Placement

Figure 34 shows passing the 15-in insert pipe through the 18-in manhole entry to the catchment (item 7 in fig. 5). This plastic pipe section is turned 90° and inserted into the 18-in concrete pipe. This is repeated with a second pipe length which is meshed with the first one. The rounded entrance section (see figs. 26 and 27) is then added and fastened flush with the vertical catchment walls as shown in figure 35.

Table 7. Summary of discharge calibration curve equations for 15-inch outflow pipe.

Curve number	Equation	Flow conditions	Head range of equation	r^2
1	$Q = 4.042H_I^{2.073}$	Water level below crown	0 to 0.9	0.9948
2	$Q = 4.286(H_I-0.900)^{0.981} + 3.249$	Pipe flowing partially full	9.0 to 4.0	1.0000
4	$Q/D^{5/2} = 5.638\left[\frac{\Delta H_{IT}}{D}\right]^{0.331}$	Pipe full	0.2 to 0.8	0.9992

Figure 34. Placement of 15-inch insert pipe through 18-inch manhole into catchment.

(The 20-inch long pipe is subsequently turned 90° and inserted into 18-inch sewer line. The black plastic bubbler piezometric line is attached prior to inserting pipe.)

Figure 35. Installed Pipe Insert Contraction meter as viewed through 18-inch manhole into catchment.

For the field tests, pneumatic bubbler orifices were located in the second pipe section 1.21 ft from the exit end and in the catchment (see fig. 25). For the latter, a stilling well was fastened to the wall of the catchment as shown in figure 36. Note this stilling well and its bubbler orifice have been recessed below the floor of the catchment so this PBT unit would always operate with a minimum positive pressure head of several tenths of feet of water. The bubbler lines are both led back to the instrument shelter through a shallow underground pipe and to their respective PBT units.

Results

To verify the calibration of the 15-inch PIC meter installed at the test site, eight hydrant discharges were diverted into the inlet (item 6 in fig. 5) containing this meter. In each case the discharge was measured independently by the acoustic meter and by tracer dilution methods. The tracer used in all tests was rhodamine WT. This dye tracer in dilute solutions will be quenched by chlorine; fortunately the quenching reaction is not rapid. To neutralize the chlorine in the hydrant water, 1 mL of 27.5 g/L sodium thiosulfate solution was added in advance to each 250 mL sample bottle; see figure 12. This concentration was based on the assumption the chlorine in the hydrant water would not exceed 2 ppm.

Figure 36. Stilling-well pipe in corner of catchment.

(Bubbler tube enters top of pipe and is secured near bottom which is recessed into hole in floor to cause 0.4 ft of water to exist over bubbler at the inception of flow.)

Figure 32 compares the field rating with the laboratory calibration (curve 1). As can be seen, there is very close agreement between the tracer dilution and acoustic measurements; a curve fitted to both is to the right of the laboratory calibration at lower heads, but both converge at higher heads. Percentage wise, the discrepancy is considerable at the lower heads but this is probably not surprising considering the violent and skewed flow conditions in the catchment, especially when the catchment volume is small. As heads increase, the flow conditions in the catchment might be expected to smooth out. While it would be desirable to measure any and all flows

into and out of a catchment, it is the higher discharges which would be of most concern and for which the limited data seems to indicate reasonable agreement.

As previously discussed, an automatic tracer injection and sampling system was installed to obtain dilution discharge measurements in the 15-inch PIC meter with the occurrence of natural runoffs. This unit was set to turn on at flows in excess of that obtained with the hydrant, 2.1 ft^3/s. While numerous runoffs occurred, none were sufficiently large to trigger this system. Much of the gutter flow greater than 2 ft^3/s tended to bypass the inlet.

TRUNKLINE MEASUREMENT SYSTEM

Design of Palmer-Bowlus Flume

Palmer-Bowlus (P-B) flumes take many configurations, but most are trapezoidal in cross section with a flat horizontal throat about one-third pipe diameter wide and one diameter long with sloping side walls at anywhere from 1:6 to 1:1 slopes.[8] Entrance and exit slopes at about 1:3 are common. As indicated by the originators, what is important is that the constriction produce critical velocities in the throat; size and dimensions are important only as far as they meet the problem at hand in a practical manner.[6] The problem at hand was to develop a flume of such design that it could be used in up to 48-in trunklines or larger and yet passed through an 18-in diameter manhole. The decision was to fabricate the skeleton of the flume of structural aluminum or steel that could be assembled in place in the pipe and its final shape made of concrete, if possible, without using forms. Previous experience in constructing trapezoidal supercritical flumes in natural streams influenced the design and construction of the flumes tested in this study.[43] Hence, the principle modification from the typical P-B flume was making the side walls 1:1 slope instead of 1:3 to permit construction of concrete. A stiff mix of concrete can be readily placed on a 45° slope without forms to contain it. Furthermore, the height of the flume floor was made D/6 instead of about D/10 which is more typical. This greater height was selected to compensate for the lesser constricting affect of the flatter side walls. This configuration, shown in figure 37, results in an area ratio of flume throat area to pipe area of 0.782. This is also slightly greater contraction than typical as it was the intention to operate the flume as a venturi meter when pipe-full flow occurred. For the same reason, the throat length was made 1.5 D long rather than 1.0 D in the belief that this would improve venturi performance as well as performance as a supercritical flow flume if free-surface flow heads were also measured in the flume throat. It was also the intention, by using this high-contraction ratio, to force subcritical flow in the approach even if supercritical flow occurred

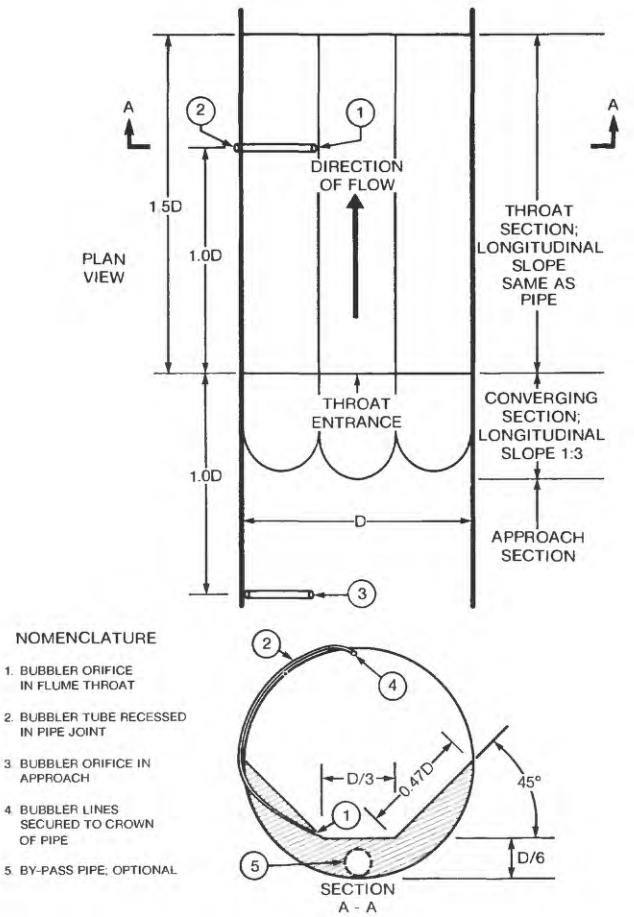

Figure 37. Design of Palmer-Bowlus flume.

upstream. Furthermore, it was desirable to force pipe-full flow in the approach where it was the intention to operate an electromagnetic point velocity meter at transition and pipe-full flows.

As shown in figure 37, bubbler orifices are located 1 D upstream and downstream from the throat entrance; the one in the throat located at the intersection of the floor and side wall. It was felt that piezometer readings 1 D distance down the throat (instead of D/2) would be in a region of more nearly parallel flow. The dual piezometers would provide the needed differential head when the P-B flume operated as a venturi meter.[13]

Three sizes of P-B flumes conforming to the dimensional ratios shown in figure 37 were tested: an 18-inch flume in the laboratory test pipe shown in figure 4; 30-inch and 48-inch units in storm drains at the GCHC and Jackson, Mississippi, test sites, respectively (see fig. 5, item 15).

Laboratory Tests of 18-inch Palmer-Bowlus Flume

The 18-inch P-B flume shown in figure 38 was calibrated for four slopes, 0, 1, 2, and 3 percent for both the approach and throat. It was the intention that the calibration in the approach would probably be for subcritical flow for most slopes. The calibrations for the throat were expected to be for supercritical flow except that for zero slope the depth-discharge relationship might be very close to critical. All calibrations are generalized in terms of relative head with the equations taking the form

$$Q/D^{5/2} = a(H/D)^b \qquad (4)$$

in which H is the head on or in the flume and D the diameter of the pipe or other physical parameter descriptive of depth; a and b are constants for a particular calibration.[13]

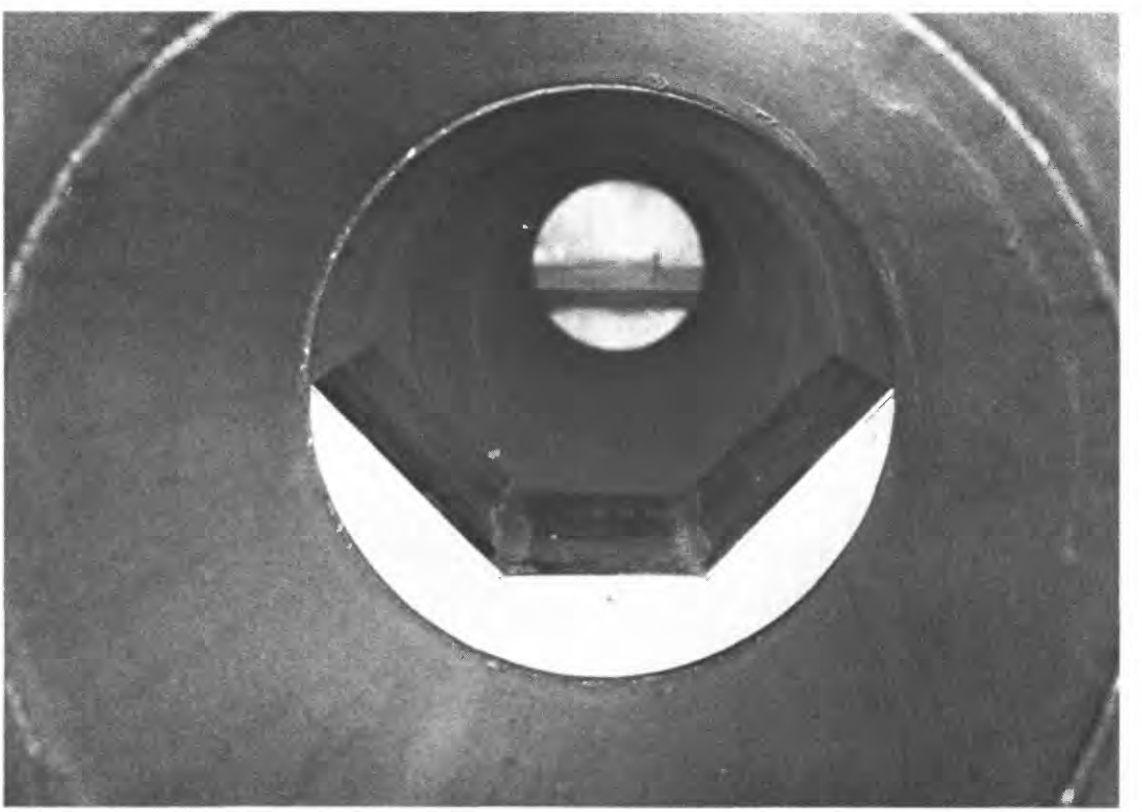

Figure 38. Palmer-Bowlus flume in test section in 18-inch concrete pipe.

Figure 39 shows the data for each of the four slopes for the approach; that is at D distance upstream from the leading edge of the flume throat. The flume throat in each case is parallel to the pipe invert and each is on the same slope. The zero datum for the approach. calibration is the upstream lip of the P-B flume throat floor.

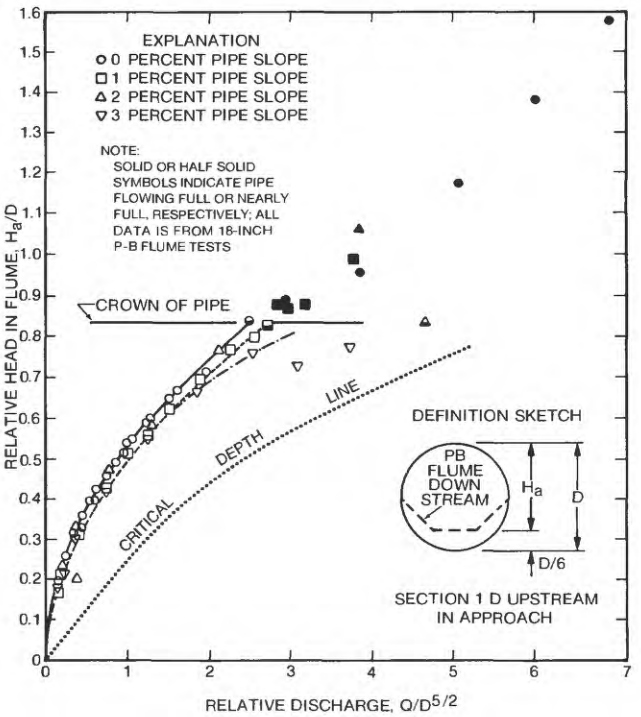

Figure 39. Generalized laboratory determined calibration curves for Palmer-Bowlus flume; head measured in approach.

Three separate calibration curves have been drawn through the zero, 1, 2, and 3 percent slope data respectively. As can be seen, all calibration when compared with the critical depth curve at this location indicate the existence of subcritical flow at even the steepest slope of 3 percent up until flow approaches pipe full. For practical purposes there appears to be a very well defined rating for the zero slope flume even extending up to pipe full; $H_a/D = 0.833$ or $H_a = 1.25$ ft.

The data for 1 and 2 percent slopes shows no significant difference nearly up to pipe full. Hence one composite calibration curve is shown for P-B flumes of this configuration for between 1 and 2 percent slope (see table 8). This calibration will probably apply for most field installations as most trunklines are between 1/2 and 2 percent slopes. It will be noted that in table 8, two sets of equations have been presented: one based on a visual best fit to the

Table 8. Summary of generalized equations for Palmer-Bowlus flume calibrations.

A. In approach to flume: $\frac{Q}{D^{5/2}} = a\left[\frac{H_a}{D}\right]^b$

D = full-pipe diameter

H_a = head on flume, zero datum the flume floor at the entrance

	"Visual" best fit equations		Linear regression equations		
Slope	a	b	a	b	r^2
0%	3.536	2.055	3.533	2.059	.9981
1&2%	3.685	1.868	3.349	1.718	.9814
3%	3.969	1.922	4.176	1.988	.9984

B. In flume throat: $\frac{Q}{d_t^{5/2}} = a\left[\frac{H_t}{d_t}\right]^b$

d_t = height between flume floor and crown of pipe at 1 D downstream from flume entrance

H_t = head in flume measured 1 D downstream from flume entrance

	"Visual" best fit equations		Linear regression equations		
Slope	a	b	a	b	r^2
0%	7.157	1.988	7.338	1.979	.9938
1&2%	-----	-----	6.557	1.730	.9997
3%	-----	-----	6.603	1.667	.9979
1,2,&3%	6.916	1.746	6.537	1.694	.9977

C. Venturi calibration equation based on visual curve fit:

$$Q/D^{5/2} = 8.335\left[\frac{\Delta H_{at}}{D}\right]^{0.512}$$

data and a second based on a linear regression. The first is provided because the latter gives equal weight to all data and does not weigh what may be questionable data such as that in the vicinity of the transition zone.

The calibration curve for the P-B flume on a 3 percent slope appears to be the same as that for one on a 1 to 2 percent slope up to a relative discharge of about 1.5 (4 ft^3/s in the 18-inch flume). This calibration breaks to the right at greater discharges when the pipe is close to filling and when velocities and, hence, depths in the approach are approaching critical values. Any further increase in slopes would probably cause flow in the pipe to become supercritical throughout. Fortunately, such slopes are seldom encountered in trunkline sewers. It appears that by using a fairly high contraction ratio, flow in the approach to the flume was forced to become and remain subcritical even at fairly high slopes. With the exception of the 3 percent rating, the ratings between 0 and 2 percent should be reliable up to nearly pipe full. The rating for the P-B flume at 3 percent slope should probably not be used at relative heads in excess of $H_a/D = 0.7$.

It may be recalled that this P-B flume design featured a throat length of 1 1/2 D instead of the customary 1 D length. It was the intent to calibrate this P-B flume as a supercritical flow flume whereby head measurements would be made at a distance 1 D down the throat. The flume floor at this point is zero datum for these calibrations. Figure 40 shows the data for the four slopes tested. Two well-defined calibration curves were obtained: one for zero slope at which depths in the throat were close to critical and a second for any slope between 1 and 3 percent. Unlike the calibrations for subcritical flows in the approach, those in the throat for 1, 2, and 3 percent are in very close agreement since all these flows are already supercritical; that is the flow at 3 percent is not approaching critical, it has already passed through critical and is supercritical. This supercritical flow calibration (see table 8) would probably hold also for greater slopes than 3 percent as supercritical flow is insensitive to depth changes at the greater slopes, the increased energy becoming primarily velocity head. It should be noted that at relative discharges in excess of 4.5, some scatter in the data occurs. As can be seen in figure 39, the pipe is flowing full upstream at this relative discharge (depths are subcritical) even though it is not full in the throat (depths are supercritical). Thus, between relative discharges of about 4.5 and 6.0, pipe-full flow occurs upstream and "breaks" into open channel flow in the throat of the flume. There is a "pulsing" action in which as flow increases, the throat section periodically "fills" and "opens." It appears that flow may actually be pulsating in this transition region even if flow entering the system is relatively steady.

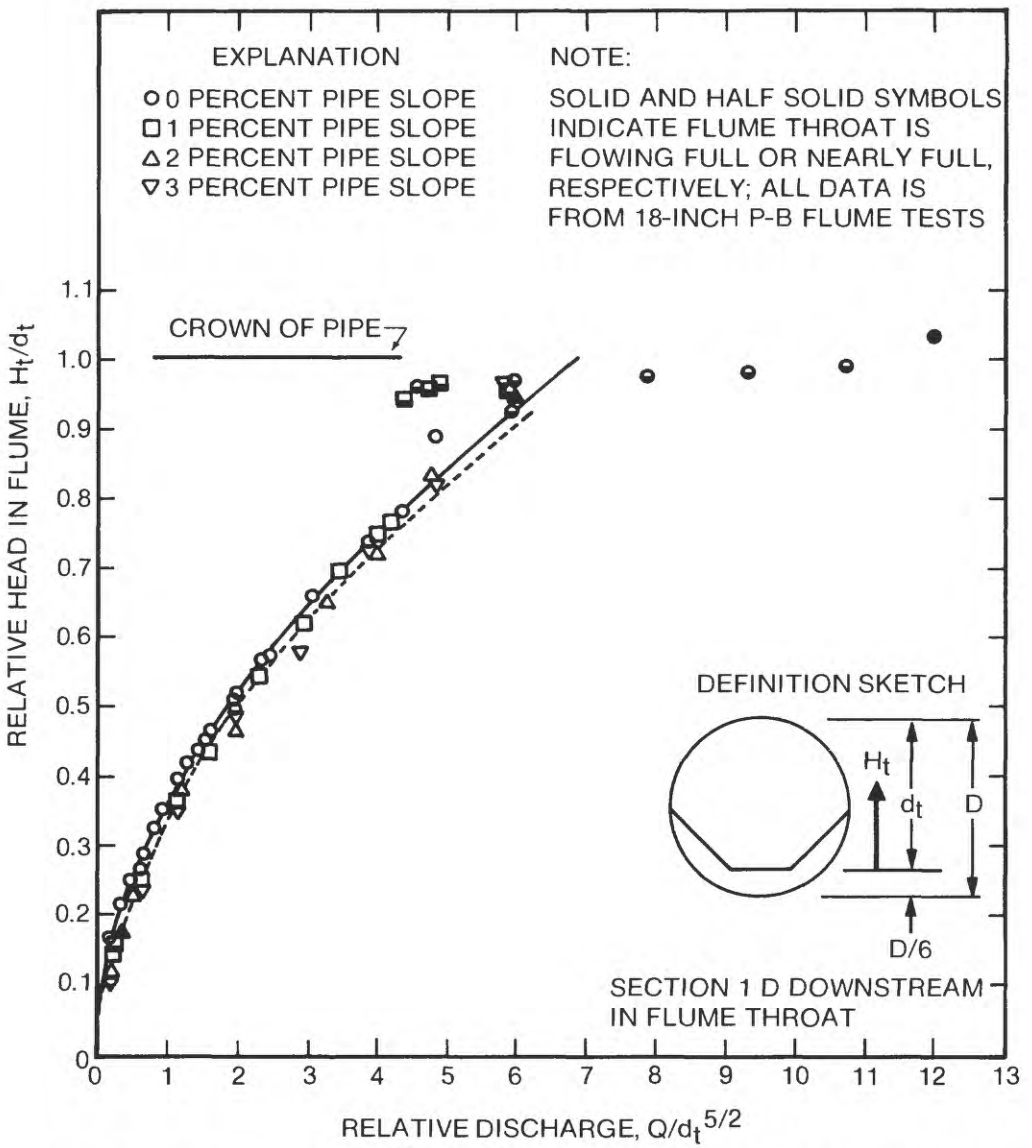

Figure 40. Generalized calibration curves for Palmer-Bowlus flume; head measured in throat.

As soon as pipe-full flow exists throughout the P-B flume, pressurized flow exists, and it can be treated as a venturi meter. Considerable difficulty was experienced in getting the 18-inch P-B flume to flow completely full without raising the tailwater and creating backwater. Discharges on the order of 20 ft^3/s would just barely cause the pipe and flume to fill. Most of the data in figure 41 are based on tests in which tailwater was increased to force the system

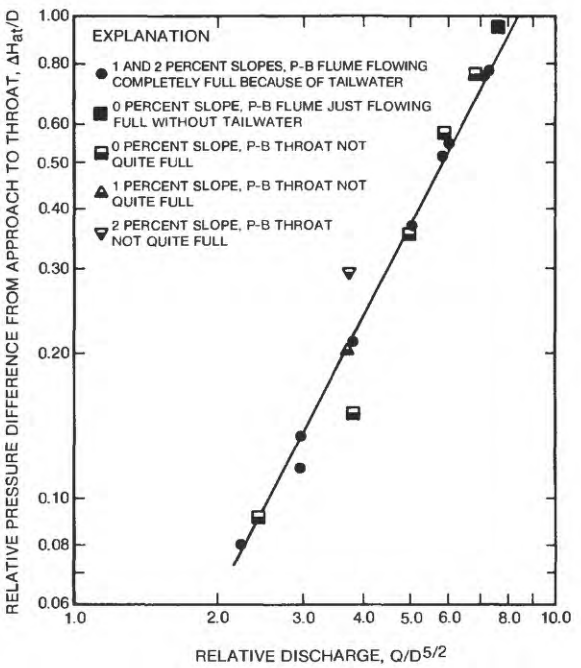

Figure 41. Venturi calibration for 18-inch Palmer-Bowlus flume.

to flow full. Data are also shown for those tests where pipe-full flow occurred or almost occurred without tailwater. As can be seen, most of the scatter is for those measurements where full-pipe flow was not definitely established throughout. These data are purposely shown to emphasize that fully pressurized flow must exist through the P-B flume for this calibration to apply. Nevertheless, this calibration seems to be good if piezometric heads are as little as 0.1 ft greater than that corresponding to the crown of the pipe in the flume throat.

From a practical standpoint, it is suggested that the throat calibrations using the P-B as a supercritical flow flume in conjunction with the venturi calibration when the flume is flowing full will yield good results with a limited transition zone in between. Care must be taken to determine which flow condition exists. The advantage of using the P-B flume as a supercritical flow flume are the improved self-cleaning characteristics and the greater range in discharge available (about 10.5 ft^3/s compared to 7.5 ft^3/s for the 18-inch P-B flume) before the pipe nears flow-full conditions. Furthermore, sediment deposition cannot occur in the throat as it might in the approach, possibly affecting head readings. The chief disadvantage is the lesser sensitivity of the throat calibration.

Table 8 summarizes the two sets of calibration curve equations for the P-B flume for approach, throat, and venturi calibrations. Tables 9 and 10 compare measured discharges and computed discharges for the laboratory data as a means of assessing the accuracy of these calibrations.

Theoretical Calibrations

Theoretical discharge calibrations can be derived for the P-B flume for both approach and throat by use of the total energy equation. Advantage is taken of the fact that flow passes through critical depth at some point just below the entrance to the flume and can be used as a starting point for energy computations. The location of critical depth may vary slightly with flow, being nearly at the entrance at lower discharges and as much as D distance downstream from the entrance at higher flows. For this P-B flume, it was assumed that critical depth is at D/2 distance downstream from the entrance as shown in the definition sketch in figure 42.

Equating total energy at the critical-depth cross section at the head of the throat reach to total energy at the stage-measurement cross sections in the approach and in the throat results in

$$\frac{V_a^2}{2g} + h_a + y_a = \frac{V_c^2}{2g} + d_c + t + y_c = \frac{V_t^2}{2g} + H_t + t + y_t \qquad (5)$$

where

V is mean velocity,

g is acceleration of gravity,

h_a, d_c, and H_t are vertical depths,

t, thickness of flume floor; D/6, and

y is the elevation of flume floor or pipe above any arbitrary datum plane.

Friction losses have been ignored; in such short reaches they would not be significant. The computation of the theoretical calibrations starts with the assumption of a critical depth at the critical section and the computation of the corresponding critical discharge. The critical discharge Q_c is defined as

$$Q_c = Z\sqrt{g/\alpha} \qquad (6)$$

Table 9. Comparison of measured and computed discharges for 18-inch Palmer-Bowlus flume for approach and throat calibrations.

(All discharges are in cubic feet per second.)

			Visually fitted curves				Regression curves			
			In approach		In throat		In approach		In throat	
H_a/D	H_t/d_t	Measured discharge	Computed discharge	Percent difference	Computed discharge	Percent difference	Computed discharge	Percent difference	Computed discharge	Percent difference
					Slope = 0 percent					
.182	.165	0.32	0.29	-9.4	0.35	+9.4	0.29	-9.4	.36	+12.5
.254	.215	0.56	0.58	+3.6	0.59	+5.4	0.58	+3.6	0.61	+8.9
.313	.249	0.86	0.90	+4.7	0.79	-8.1	0.89	+3.5	0.82	-4.7
.360	.285	1.13	1.19	+2.7	1.03	-8.8	1.19	+2.7	1.07	-5.3
.395	.323	1.40	1.44	+2.9	1.32	-5.7	1.44	+2.9	1.37	-2.1
.426	.350	1.61	1.69	+5.0	1.55	-3.7	1.68	+4.3	1.61	-0.0
.456	.391	1.97	1.94	-1.5	1.93	-2.0	1.93	-2.0	2.00	+1.5
.490	.419	2.26	2.25	-0.4	2.22	-1.8	2.24	-0.9	2.29	+1.3
.515	.432	2.57	2.49	-3.1	2.36	-8.2	2.48	-3.5	2.43	-5.4
.537	.450	2.65	2.72	+2.6	2.56	-3.4	2.71	+2.3	2.64	-0.4
.549	.465	2.81	2.84	+1.1	2.73	-2.8	2.83	+0.7	2.82	+0.4
.591	.514	3.38	3.31	-2.1	3.33	-1.5	3.30	-2.4	3.43	+1.5
.597	.509	3.39	3.38	-0.3	3.27	-3.5	3.37	-0.6	3.37	-0.6
.649	.563	4.08	4.01	-1.7	3.99	-2.2	4.00	-2.0	4.11	+0.7
.667	.570	4.30	4.24	-1.4	4.09	-4.9	4.23	-1.6	4.21	-2.1
.715	.658	5.30	4.89	-7.7	5.44	+2.6	4.88	-7.9	5.60	+5.7
(a)	.778	7.57	(a)	(a)	7.59	+0.3	(a)	(a)	7.80	+3.0
.836	.733	6.75	6.74	-0.1	6.74	-0.1	6.73	-0.3	6.93	+2.5

(a) In transition in approach; crown reached at $H_a/D = 0.833$.

Table 9. Comparison of measured and computed discharges for 18-inch Palmer-Bowlus flume for approach and throat calibrations--Continued.

(All discharges are in cubic feet per second.)

H_a/D	H_t/d_t	Measured discharge	Visually fitted curve		Regression curves			
			In approach		In approach		In throat	
			Computed discharge	Percent difference	Computed discharge	Percent difference	Computed discharge	Percent difference
			Slope = 1 and 2 percent					
0.167	.135	0.36	0.36	0	.43	+19.4	0.36	0
.203	.154	0.45	.34	-24.4	.41	-8.9	.45	0
.307	.247	1.02	1.12	+9.8	1.21	+18.6	1.02	0
.421	.366	1.95	2.02	+3.6	2.09	+7.2	2.01	+3.1
.509	.437	2.68	2.88	+7.5	2.89	+7.8	2.74	+2.2
.556	.494	3.41	3.39	-0.6	3.37	-1.2	3.38	-0.9
.621	.543	4.04	4.17	+3.2	4.07	+0.7	3.98	-1.5
.693	.617	5.11	5.12	+0.2	4.92	-3.7	4.97	-2.7
.766	.691	6.06	6.17	+1.8	5.84	-3.6	6.04	-0.3
.830	.769	7.32	7.17	-2.0	6.70	-8.5	7.27	-0.7
(b)	.955	10.25	(b)	----	(b)	----	10.60	+3.4
			Slope = 3 percent					
.165	.117	.34	.34	0	.32	-5.9	.32	-5.9
.204	.149	.47	.52	+10.6	.49	+4.3	.48	+2.1
.292	.229	.93	1.03	+10.7	1.00	+7.5	.99	+6.5
.414	.362	1.98	2.01	+1.5	1.99	+0.5	2.12	+7.1
.547	.478	3.40	3.43	+0.9	3.47	+2.1	3.37	-0.9
.662	.577	5.07	4.95	-2.4	5.07	0	4.61	-9.1
.757	.723	6.91	6.41	-7.2	6.62	-4.2	6.72	-2.7
(b)	.822	8.44	(b)	---	(b)	---	8.32	-1.4
(b)	.963	10.26	(b)	---	(b)	---	10.83	+5.6

(b) Flowing full in approach but not in throat.

Table 9. Comparison of measured and computed discharges for 18-inch Palmer-Bowlus flume for approach and throat calibrations--Continued.

(All discharges are in cubic feet per second.)

H_t/d_t	Measured discharge	Visually fitted curve		Regression curve	
		In throat		In throat	
		Computed discharge	Percent difference	Computed discharge	Percent difference
		Slope = 1, 2, and 3 percent			
.117	0.34	0.28	-17.6	.30	-11.8
.149	0.47	0.44	-6.4	.45	-4.2
.135	0.36	0.37	+2.8	.38	+5.6
.154	0.45	0.46	+2.2	.48	+6.7
.229	0.93	0.92	-1.1	.94	+1.1
.247	1.02	1.05	+2.9	1.07	+4.9
.362	1.98	2.05	+3.5	2.04	+3.0
.366	1.95	2.09	+7.2	2.08	+6.7
.437	2.68	2.85	+6.3	2.81	+4.9
.478	3.40	3.33	-2.1	3.27	-3.8
.494	3.41	3.53	+3.5	3.46	+1.5
.543	4.04	4.16	+3.0	4.06	+0.5
.577	5.07	4.63	-6.7	4.50	-11.3
.617	5.11	5.20	+1.8	5.04	-1.4
.691	6.06	6.34	+4.6	6.11	+0.8
.723	6.91	6.86	-0.7	6.59	-4.6
.742	6.94	7.18	+3.5	6.89	-0.7
.769	7.32	7.64	+4.4	7.32	0
.822	8.44	8.58	+1.7	8.19	-3.0
.955	10.25	11.15	+8.8	10.56	+3.0
.963	10.26	11.31	+10.1	10.70	+4.3

Table 10. Comparison of measured and computed discharges for 18-inch Palmer-Bowlus flume functioning as a venturi meter.

(All discharges are in cubic feet per second.)

$\Delta H_{at}/D$	Measured discharge	Computed discharge	Percent difference
0.080	6.14	6.303	+2.7
0.135	8.13	8.239	+1.3
0.116	8.17	7.623	-6.7
0.203	10.16	10.15	0.0
0.359	13.62	13.59	-0.2
0.522	16.16	16.47	+1.9
0.550	16.56	16.91	+2.1
0.755	19.78	19.89	+0.6
0.773	20.11	20.13	+0.1
0.957	20.96	22.46	+7.2

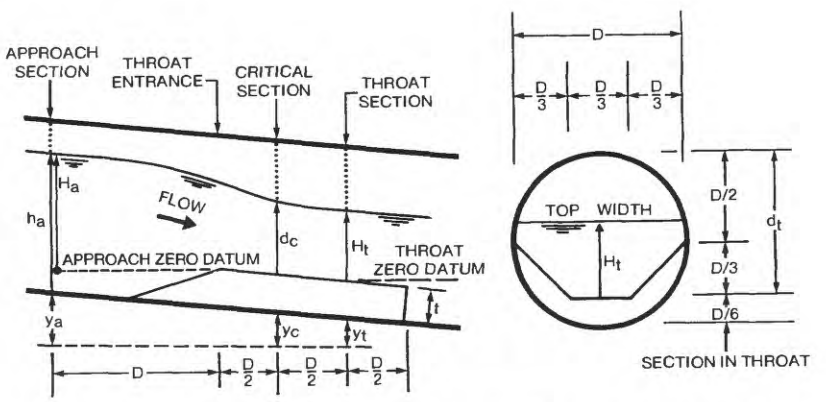

Figure 42. Definition sketch for Palmer-Bowlus flume.

where from the properties of critical flow, the critical-section factor (Z) is computed by the formula

$$Z = A_c\sqrt{\frac{A_c}{T_c}} \qquad (7)$$

where T_c and A_c are the top width and area at the critical-depth cross section respectively and α is an energy coefficient.[44] As can be seen, Z is unique to any flow section and a function only of its physical geometry. The critical depth curve shown in figure 39 is

computed using the Z factors and the continuity equation for the approach for a range in depths. The energy coefficient is assumed to equal unity.

Using the continuity equation for the critical depth section, $Q_c = A_c V_c$ allows the solution for V_c and the evaluation of the total energy at this section. For a range of critical discharges, the energy equations in the approach and throat are solved by repeated trials until the total energy at both locations equals that at the critical section.

The resulting depths, h_a and H_t for the various critical discharges that were selected provides the theoretical calibration. Note that for the approach calibration, the head on the P-B flume, $H_a = h_a - t$ + a datum correction which depends on the pipe slope; t being the thickness of the flume floor above the pipe invert in feet. The head, H_t, in the throat may be used directly. The results of these theoretical calibration curve computations are shown in figures 43 and 44 and are compared with the calibrations determined in the laboratory. The data have been generalized to apply to any size P-B flume of the same design. The theoretical calibrations are for 0 and 2 percent sloping flumes and are tabulated in table 11. As can be seen in figure 43 for the approach, the laboratory calibrations are in very close agreement with the theoretical calibrations and lend credulousness to the tests. The curves for zero slope are almost indistinguishable they are in such close agreement. While the 2 percent slope theoretical calibration is slightly to the left of the single laboratory calibration for 1 through 3 percent pipe slopes, the agreement is good considering the scatter in the original data; figure 39. Additional computations reveal that if the critical depth section is assumed to be farther down the throat than D/2, the theoretical calibration is shifted to the right, more nearly coinciding with the laboratory calibration. The actual laboratory calibrations are nevertheless to be recommended over the theoretical calibrations. The theoretical calibrations do indicate that pipe slope must be considered in selecting or in computing a calibration. Furthermore, that reasonable confidence may be placed on theoretical calibrations of flumes of other design configurations.

The theoretical and laboratory calibrations for the P-B flume throat, shown in figure 44, do not compare as favorably, especially at higher heads. By coincidence the zero slope laboratory and 2 percent slope theoretical calibrations virtually coincide up to $H_t/d_t = 0.75$. The sharp deviation of the theoretical calibration curves to the right at the higher relative heads is because Z becomes quite large as the top width approaches zero (see fig. 42 and equation 7). For these reasons, theoretical values above H_t/d_t values of 0.75 should be suspect. The laboratory calibrations should be used in preference to the theoretical calibrations.

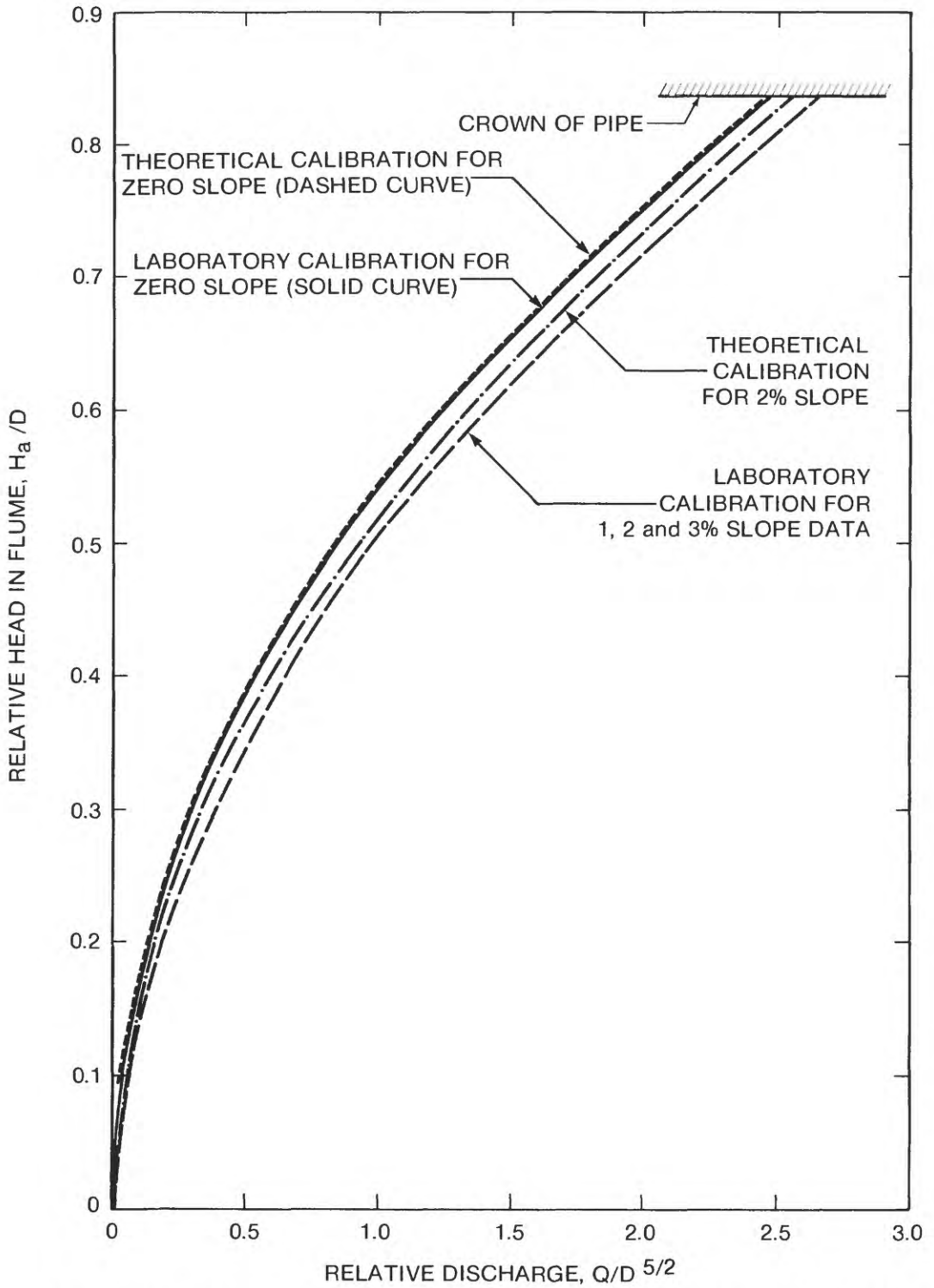

Figure 43. Comparison of laboratory and theoretical calibration curves for Palmer-Bowlus flume; head measured in approach.

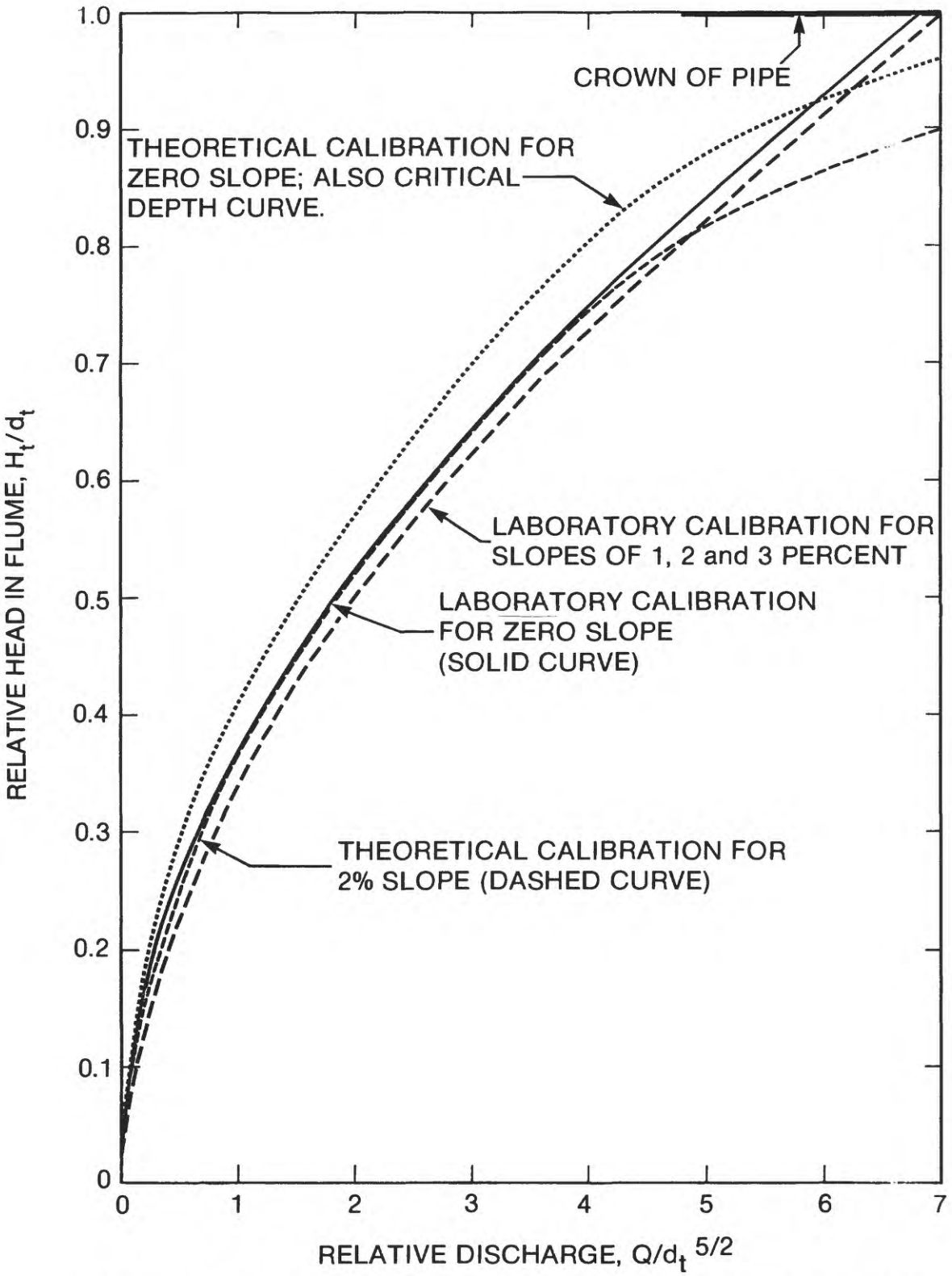

Figure 44. Comparison of laboratory and theoretical calibrations for Palmer-Bowlus flume; head measured in throat.

Table 11. Theoretical calibrations for Palmer-Bowlus flume

(All units are in feet unless otherwise shown)

Critical depth section				Approach section**							Throat section**				
					Zero slope			2 percent slope				Zero slope		2 percent slope	
d_c*	A_c	Z	Q_c	$\frac{Q}{D^{2.5}}$	h_a	H_a	H_a/D	h_a	H_a	H_a/D	$\frac{Q}{d_t^{5/2}}$	H_t***	H_t/d_t	H_t	H_t/d_t
	ft^2	$ft^{1.5}$	ft^3/s	$ft^{0.5}$							$ft^{0.5}$				
(1)	(2)	(3)	(4)	(5)	(6)	(7)	(8)	(9)	(10)	(11)	(12)	(13)	(14)	(15)	(16)
0.10	0.06	0.018	0.100	0.036	0.393	0.143	0.095	0.345	0.125	0.083	0.060	0.10	0.08	0.079	0.063
0.20	0.14	0.055	0.313	0.114	0.525	0.275	0.183	0.476	0.256	0.170	0.179	0.20	0.16	0.161	0.129
0.30	0.24	0.112	0.636	0.231	0.645	0.395	0.263	0.598	0.378	0.252	0.364	0.30	0.24	0.252	0.202
0.50	0.50	0.289	1.64	0.594	0.885	0.635	0.423	0.831	0.611	0.407	0.934	0.50	0.40	0.440	0.352
0.75	0.87	0.682	3.87	1.40	1.215	0.965	0.638	1.152	0.932	0.621	2.22	0.75	0.60	0.690	0.552
1.00	1.19	1.23	6.97	2.53	1.53	1.28	0.853	1.49	1.27	0.847	3.99	1.00	0.80	0.920	0.736
1.10	1.29	1.55	8.80	5.04	-----	-----	-----	-----	-----	-----	5.04	1.10	0.88	1.025	0.820
1.20	1.37	2.17	12.29	7.04	-----	-----	-----	-----	-----	-----	7.04	1.20	0.96	1.125	0.90
1.23	1.38	2.75	15.62	8.94	-----	-----	-----	-----	-----	-----	8.94	1.23	0.98	1.175	0.94

*Values selected to cover full range in head for open-channel flow.

**Values shown are final trial values causing total energy to agree with total energy at critical depth section.

***Same as d_c in critical depth section at zero slope.

Field Tests of Palmer-Bowlus Flumes

Placement

As mentioned previously, the P-B flume design considered the requirement that it be passed through an 18-in manhole. The preassembled P-B flume for use in the 48-in trunkline at Jackson, Mississippi, is shown in figure 45. This one used sections of aluminum plate to form the throat. The components of this flume are shown disassembled in figure 46 just prior to passing them through the manhole, figure 47, which allows access to the 48-in trunkline. The skeletonal P-B flume is shown assembled in the 48-in pipe in figure 48. The space within the skeleton form was filled with a lean concrete mix and then the floor and wall plates secured in place

Figure 45. Pre-assembled Palmer-Bowlus flume.

(Pipe bypasses flow during construction.)

Figure 46. Components of Palmer-Bowlus flume.

Figure 47. Passage of part of Palmer-Bowlus flume form through 18-inch manhole.

Figure 48. Framework for forming Palmer-Bowlus flume of concrete.

(fig. 49). The lean mix of concrete was used with the objective of making eventual removal easier. The concrete was mixed above ground and lowered in buckets through the manhole and placed on a low cart and transported 50 ft down into the pipe for placement. The cart also had to be taken apart and reassembled in the junction box. The concrete used in the approach was made stiff and allowed to harden slightly before placement. The 30-inch P-B flume installed at GCHC was constructed in an identical manner as for the 48-inch flume except that the aluminum floor and wall plates were omitted and the skeleton form was used to screed a stiff mix of concrete to the desired shape and slopes. It should be noted that the bubbler orifice line was conveniently recessed into a pipe joint and brought up to the crown of the trunkline then up to the junction box and eventually to the instrument shelter and the PBT system. This pipe joint also served as a means of keying the flume into the walls of the pipe. The massiveness and sealing features of this type of P-B flume construction avoided any problems with leakage or buoyance and pressure forces. In each case the flumes were constructed completely in less than a day. The use of a drainpipe is highly recommended as there is often some seepage flow in storm drain systems.

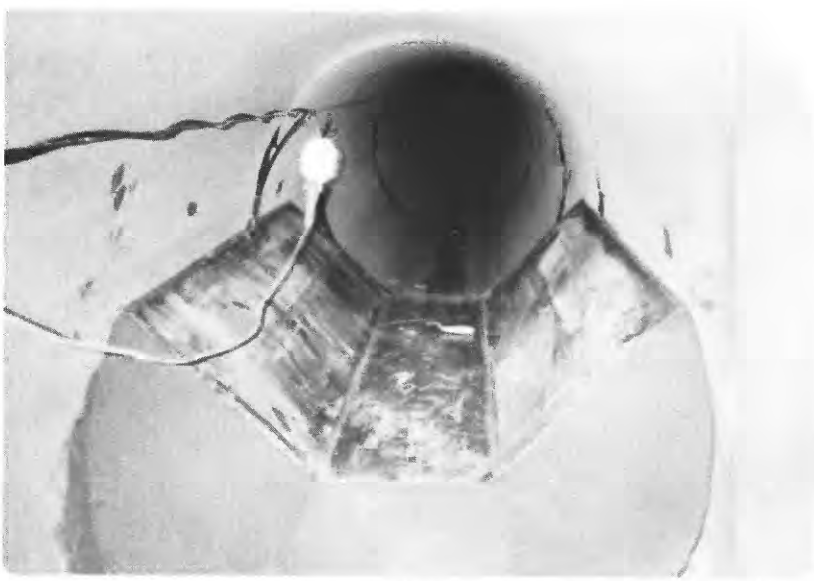

Figure 49. Photograph looking downstream at completed Palmer-Bowlus flume.

(Bubbler piezometric opening is in side wall at trowel.)

The pneumatic bubbler line in the approach to the P-B flume was secured below the elevation of the crest of the flume and off to one side of the invert (see fig. 50). This placed an initial head of water on this orifice to purposely avoid operating the transducer serving this orifice at low heads where most errors were known to occur. Unfortunately, this could not be done with the throat bubbler orifice. The transducer for this type of orifice needs to be selected carefully, based on laboratory screening, to function accurately at low pressure heads.

Figure 50. Plastic bubbler piezometric line secured near invert of concrete pipe.

Results of Field Tests

Five hydrant discharges were directed into the most upstream inlet (number 5 in fig. 5) into the 48-in trunkline and through the 48-inch P-B flume. Once each flow had stablized, it was measured by both tracer dilution and acoustic meter as previously described. The dilution and acoustic discharge measurements are so close in agreement that only their averages are plotted. These measurements are plotted in figure 51 with the respective approach and throat calibtations as

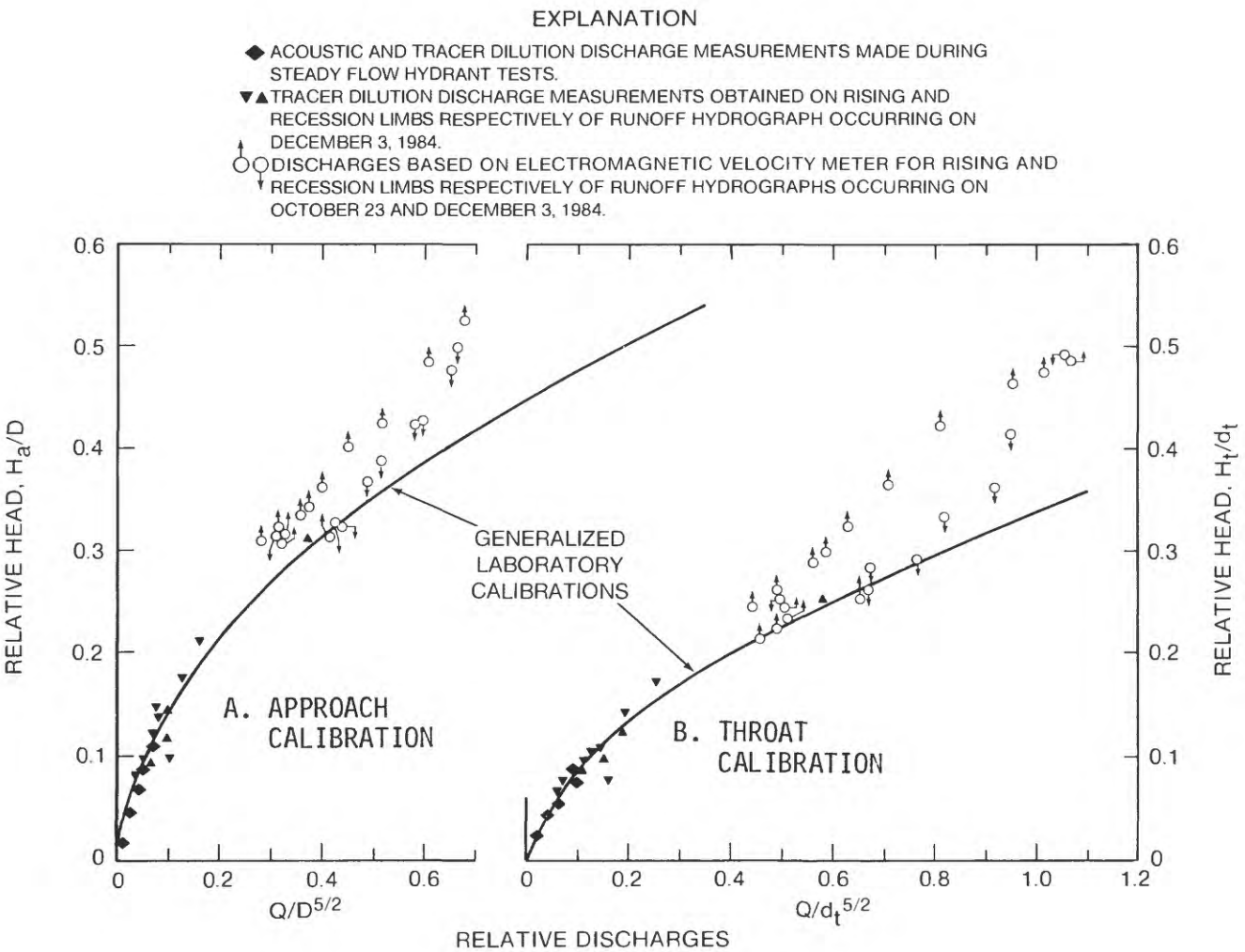

Figure 51. Comparison of field discharge measurements with generalized calibrations of Palmer-Bowlus flume.

obtained in the laboratory. Agreement is excellent but it can be seen that only a very limited range was evaluated due to the limited flow available from the fire hydrant; 2.2 ft^3/s. Based on the generalized calibration in figure 39, the maximum discharge in the 48-in trunkline with the 48-inch P-B flume would be about 85 ft^3/s at pipe-full flow, using the approach calibrations.

While several storm runoffs were experienced during the field test period, dilution type discharge measurements were obtained only during several rapidly occurring runoffs on December 3, 1984.* Light,

---

*Equipment malfunctions prevented earlier runoff events from being measured using the tracer dilution techn ue.

scattered rainfall produced four distinct runoffs having durations varying from 15 minutes up to 1 hour. The largest went from a head at the P-B flume of 0.5 ft to 1.5 ft in 6 minutes and back down in 16 minutes. This corresponds to an increase in discharge in the 48-in trunkline of approximately 2 to 14 ft^3/s in 6 minutes!

All together, 12 dilution measurements were obtained automatically, some on the rapidly rising limbs of the hydrographs and others on the slower recessions. These data are shown in figure 51 for comparison with both the approach and throat laboratory derived calibrations. As might be expected, these measurements scatter more than the dilution measurements made during the steady flow hydrant tests. Nevertheless, agreement is good and seems to verify the laboratory calibrations. Normally the dilution measurements made on the slower changing recessions would be expected to give the most accurate results. In this case no distinction can be made, probably because mixing is so nearly instantaneous. Factors causing such good mixing are the turbulence in the junction (item 3, fig. 5) at the point of injection and the hydraulic jumps above and possibly below the P-B flume.

Electromagnetic Velocity Meter

The electromagnetic point velocity meter chosen for testing in the laboratory was a Marsh-McBirney model number 523; the unit installed at the Jackson test site was a Montedoro-Whitney model number PVM-2. The first is a smaller unit more suited to use in the 18-in laboratory test pipe and the latter a larger and more rugged unit that was considered best for use in the field.

These velocity meters utilize the electromagnetic effect principle described by M. Faraday in 1831.[45] The Faraday law states that a conductor in the presence of magnetic lines of flux will have an emf (electro-motive force or voltage) generated in that conductor proportional to the change in flux. As applied in these meters, a signal is generated and sent to an electromagnet within the probe which creates the magnetic lines of flux. The conductor is the water into which the probe is immersed. As the water (the conductor) flows through the magnetic field, a voltage is generated in the water in the vicinity of the electrodes which sense the voltage. The PVM-2 has an output of 0 to 2 volts and hence is compatible with the micrologger recorder. The polarity and magnitude of this signal is directly proportional to the direction and velocity of the water. According to the manufacturer (Product literature, 1984), "Unlike techniques which generate a magnetic field entirely around the probe,

the PVM-2 probe utilizes a "folded field" principle which confines the magnetic lines of flux in the area immediately around the electrode surfaces. This feature allows the user to measure velocities very close to pipe or channel walls without disturbing the magnetic field and, consequently, the calibration, as with other types of electromagnetic velocity meters." The streamlined shape of the probe is designed to minimize shape-induced turbulence and the effects of viscous drag, thereby allowing a very accurate and linear measurement of velocity.

Laboratory Tests

In the laboratory, the EVM was located to measure point velocities along a vertical traverse as shown in the definition sketch of figure 52. The velocity probe was located D/4 to the left of the center of the pipe, 1 D upstream of the entrance to the throat of the P-B flume. This is the same distance upstream that flume approach heads are measured so that pipe-flow area can be calculated. The EVM point velocity probe was lowered vertically through a hole drilled at the quarter point in the 18-in concrete pipe (see fig. 4). For pipe-full flow, a sleeve was placed around the EVM support and sealed over the hole in the concrete pipe.

The EVM tests were performed concurrently with the rating of the P-B flume. Point velocities were measured along the vertical traverse at 0.1 ft increments. These velocities were plotted for each flow condition and for all three pipe slopes tested. From these vertical velocity curves, point velocities for selected depths of 0.3D, up to 0.7D were plotted as a ratio of the mean velocity in the pipe versus relative depth as shown in figures 52A through E. The data scattered badly, so badly that the data for a 3 percent slope is not plotted. It was subsequently realized that much of the scatter was probably the result of probe vibration since it was not supported at the bottom but cantelivered from the top as it was traversed vertically. Vibration was particularly bad when the pipe was placed on a 3 percent slope; probably as a result of velocities nearing critical (note the upper rating for the flume approach in fig. 39) at this slope. This may have also resulted from the plunging effect of supercritical flow in the approaching pipe as the hydraulic jump moves closer to the P-B flume and EVM with increasing slope.

It was further noted that the vertical velocity curves for open-channel flow were different than those at pipe-full flow. The first tended to be almost vertical, whereas the latter were generally more convex. Those made when the approach was nearly full and in transition were the most convex in shape and the data the most erratic. This probably indicates the effect of the unsteady pulsating flow action as mentioned previously. Unfortunately, it appears that where

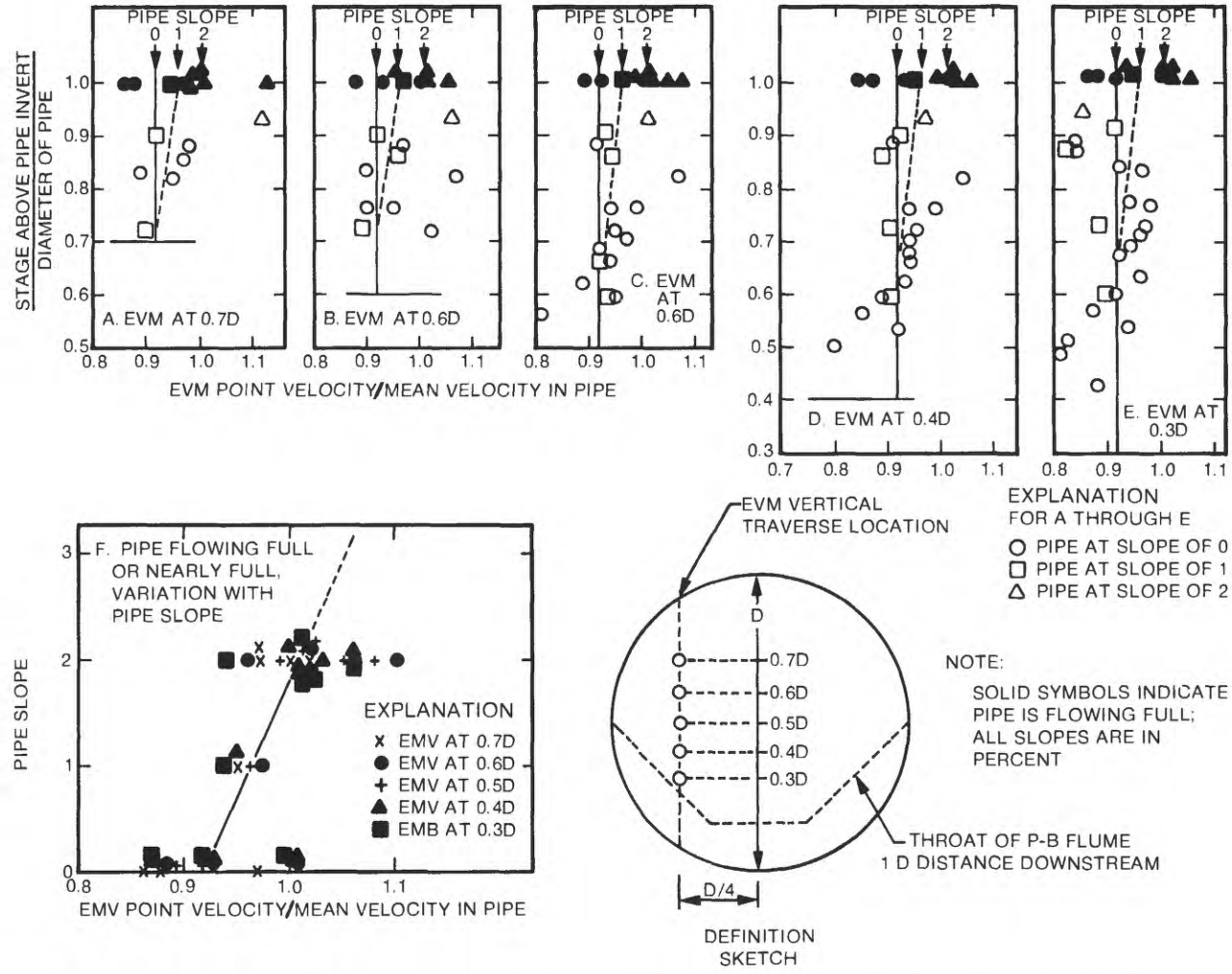

Figure 52. Variation of electromagnetic velocity meter coefficient with vertical location in pipe, pipe slope, and flow condition; all tests in 18-inch concrete pipe.

the EVM is needed the most, in the transition range, it is the least reliable due to the unsteady flow conditions that may exist at such times.

The EVM coefficient for pipe-full flow was noted to vary slightly with pipe slope as shown in figure 52F. It is suggested that until more conclusive tests can be performed, the coefficients shown in table 12 should be used. The EVM would seem to hold the most promise if used to measure flows under backwater conditions. Fortunately, for such conditions the vertical velocity profiles appear quite stable and a coefficient of 1.00 is recommended regardless of pipe slope; for pipe full-backwater conditions this coefficient should yield results with ± 5 percent accuracy.

Table 12. Recommended electromagnetic velocity meter coefficients for selected meter locations and flow conditions.

EVM location above pipe invert*	Flow condition							
	Free-surface, any stage pipe slope in percent			In transition, pipe slope in percent				Pipe full due to back-water, all slopes
	0	1	2	0	1	2	3	
0.3D	0.92	0.92	1.00	0.92	0.96	1.01	1.05	1.00
0.4D	0.92	0.92	1.00	0.92	0.96	1.01	1.05	1.00
0.5D	0.92	0.93	1.00	0.92	0.96	1.01	1.05	1.00
0.6D	0.92	0.93	1.00	0.92	0.96	1.01	1.05	1.00
0.7D	0.92	0.94	1.00	0.92	0.96	1.01	1.05	1.00

*At D/4 from centerline and 1 D upstream of Palmer-Bowlus flume throat entrance.

Field Tests of the EVM

The EVM was installed on a vertical support rod in the approach to the P-B flume 0.4D above the invert as shown in figure 53. This is 1 D distance upstream of the entrance to the P-B flume at the same location as H_a was measured. The unit was mounted on a current meter wading rod with current meter vanes added to provide stability, laboratory tests having indicated that vibration could be a problem at high velocities without the vanes. The signal line for the EVM

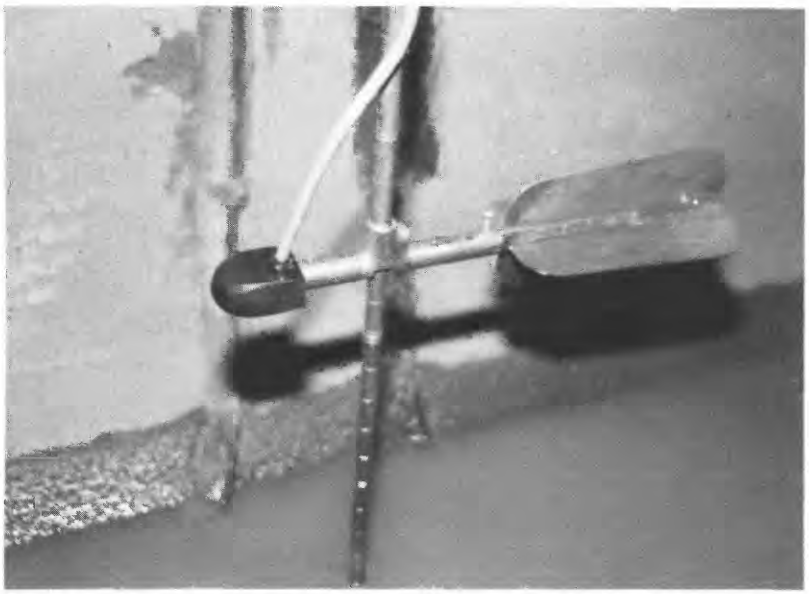

Figure 53. Electromagnetic velocity meter installed in approach to Palmer-Bowlus flume in 48-inch trunkline.

(Current meter fins were found to prevent vibrations.)

was led up the crown of the trunkline and to the instrument shelter. The EVM was activated only when the micrologger sensed sufficient stage existed during a given flow event. The voltage output was then recorded on the micrologger.

The system worked without flaw during all field tests. For comparison purposes, discharges were computed using the EVM measured velocities in the 48-in pipe as recorded every 2 minutes and the flow areas based on concurrent measurements of H_a. An EVM coefficient of 1.00 was assumed. No pipe-full flows occurred during the field tests so all data are for free-surface flow.

The EVM was adequately submerged only at H_a values at and above 1.2 ft ($H_a/D=0.3$). For this reason data were obtained only during two runoff events: October 23 and December 3, 1984. Most of the EVM data, 21 velocity readings at 2-minute intervals, were obtained for the runoff of October 23. These computed discharges are plotted in figure 51 for comparison with the laboratory determined P-B flume calibrations. As can be seen, the data plots to the left of the calibration curves initially, then forming a loop rating, back down and eventually merging with the calibration curve on the recession of

the hydrograph. Two factors could account for this failure of the EVM data to plot on the calibration curves: the coefficients for the EVM are much greater than 1.00 or backwater in the trunkline is partially submerging the P-B flume. Very large EVM coefficients would have to be used to shift the data to the right to the calibration curve and would also have to be different for rising and recession limbs of the hydrograph. While the applicable EVM coefficients may not be exactly 1.00, very large values are ruled out as being unrealistic.

Instead it is believed that backwater in the trunkline is causing this loop rating to the left of the calibration curve. A plot of head in the approach, H_a, versus that in the throat, H_t, did show a break at about $H_a/D = 0.3$, suggesting that H_t was being affected by backwater. A similar plot of laboratory data for open-channel flow without tailwater showed no such break. The loop is the result of the recession of the tailwater in the trunkline as the hydrograph enters the recession period; with the recession, the P-B flume once again becomes effective. Unfortunately, the EVM was not activated until $H_a/D = 0.3$ or greater. Unfortunately, too, the highest dilution discharge measurements thus far obtained is at approximately the same head as when the EVM is activated, thus the validity of the EVM based discharges cannot be confirmed at this time. Field tests are continuing in hopes that higher dilution discharge measurements will confirm this backwater effect. If so, the validity of using the EVM to measure flows under backwater conditions would be confirmed.

BYPASS FLOWS

Inlet In-situ Rating

By sealing off the entrance to the upstream inlet, number 5 in figure 5 (see fig. 54), all the hydrant flow was directed to the next inlet (number 6) downstream. The total hydrant discharge for each of eight tests was measured with the acoustic flowmeter as described earlier; for each, the catchment outflow was measured using the 15-inch PIC field rating shown in figure 32. At a discharge of 1.4 ft^3/s, flow began to bypass this inlet as shown in figure 55. With increasing total discharge, much of the increase became bypass flow with the remainder an increase in the outlet flow from the catchment. Conceptually it was viewed that for each inlet design and configuration a unique relationship existed between the flow into and out of the catchment and that bypassing the inlet. The unique relationship for this inlet is shown in figure 56 where the bypass discharge is plotted versus the catchment outlet discharge. The results are good, although it was not possible to extend the rating as high as might have been desired due to the limiting hydrant discharges available.

Figure 54. Sealing of curb inlet.

(This forces hydrant flows to bypass to next curb inlet.)

Figure 55. Bypass flow at point of flow separation at curb inlet.

(Manhole opening to catchment box is at upper left.)

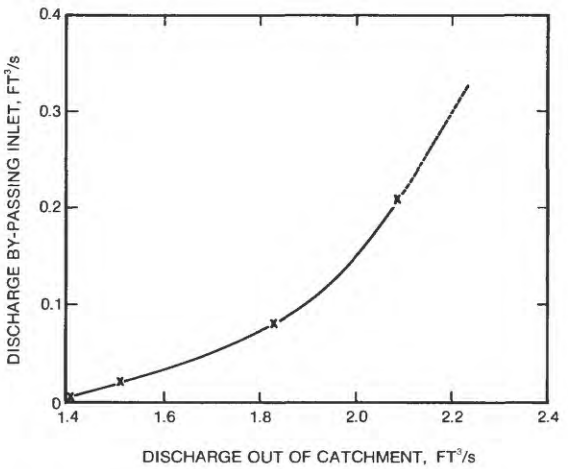

Figure 56. In-situ bypass discharge rating for inlet at field test site.

While this method requires considerable effort to accomplish, it would be the ultimate in assessing the hydraulics of a given storm-drainage system. There can be little question that in practice every inlet will have different physical and hydraulic characteristics regardless of similarity in design. The in-situ rating of each would resolve this problem, though with considerable effort.

Curb Weir

The difficulties of measuring bypass flow in the gutters is primarily due to the hostile conditions which exist, such as vehicular traffic and debris. The placement of sophisticated measuring instruments in the gutter or curb adjacent to inlets was judged to have very limited chance of success. Nevertheless, an alternative to the in-situ rating technique was desirable.

It was decided to try a broad-crested weir structure located in the street gutter to intercept bypass flows. The structure would have to have a low profile and be sturdy, capable of withstanding vehicular traffic and preferably be self-cleaning. Figure 57 is a diagram of the curb dual weir field tested at the Jackson site; item 14 in figure 5. Figure 58 is a photograph of the installation looking upstream. The structure is fabricated of an 8-in wide, 1-in thick by 2-ft long section of aluminum channel secured and sealed to the street gutter. Cold mix asphalt was used to form a 45-degree abutment on the right and the existing curb acted as an abutment on the left. A pneumatic bubbler tube was placed in a hole drilled through the concrete curb and buried in a shallow trench back to the

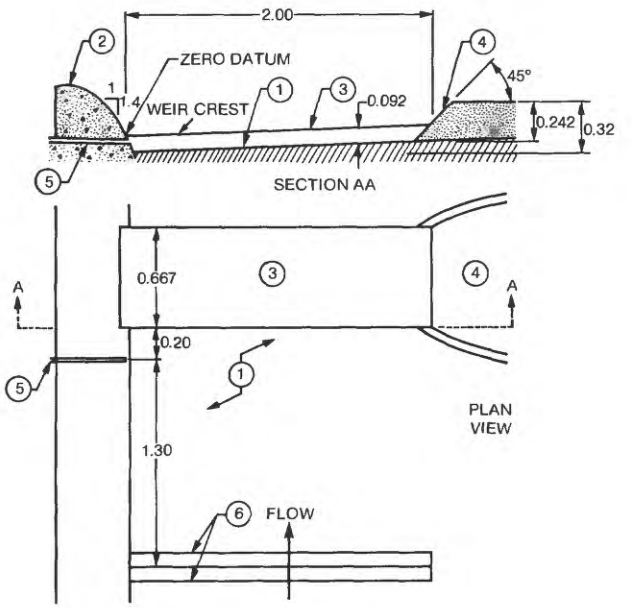

NOMENCLATURE

1 STREET GUTTER
2 CURB
3 RECTANGULAR BROAD-CRESTED WEIR; SLOPES IN DIRECTION OF FLOW AT 1:50
4 WEIR ABUTMENT, SHAPED OF ASPHALT
5 PNEUMATIC BUBBLER TUBE; ORIFICE SET AT -0.05 FEET ZERO DATUM
6 UPSTREAM TRIANGULAR WEIR OF 1 1/2" x 1 1/2" ANGLE IRON

NOTE: ALL DIMENSIONS ARE IN FEET UNLESS OTHERWISE INDICATED

Figure 57. Diagram of curb dual weir installation.

instrument shelter (see fig. 59). The bubbler orifice was made flush with the curb face, 0.05 ft below the low point of the weir crest so that some initial head would exist on the 10-in transducer serving this PBT system.

To rate this broad-crested weir in the field, the hydrant flows were forced past the two inlets lying between the hydrant and the curb weir by temporarily sealing the inlets with canvas; this can be seen in the upper part of the photograph in figure 58. The initial flow tests indicated that supercritical flow was occurring in the gutter with a hydraulic jump forming just upstream of the weir due to its presence. To produce subcritical flow in the approach to the measuring weir, a second weir was placed 2.0 ft upstream, hence the name, dual weir. This caused the hydraulic jump to form upstream of this second weir with subcritical flow between the two weirs, providing reasonably good head measuring conditions in the approach to the broad-crested measuring weir. In figure 58, head is being measured at the curb, 0.2 ft upstream from the weir.

Figure 58. Curb weir looking upstream.

(Note that supercritical flow approaching upstream weir becomes subcritical in approach to broad-crested weir. The bubbler orifice is in curb face where ruler is being held.)

Figure 59. Placement of bubbler line in shallow trench leading to curb weir.

(Tubing is cut flush with curb surface.)

Hydrant discharges were measured with an acoustic flowmeter as described previously. The field rating for this curb dual weir is shown by the solid curve in figure 60.

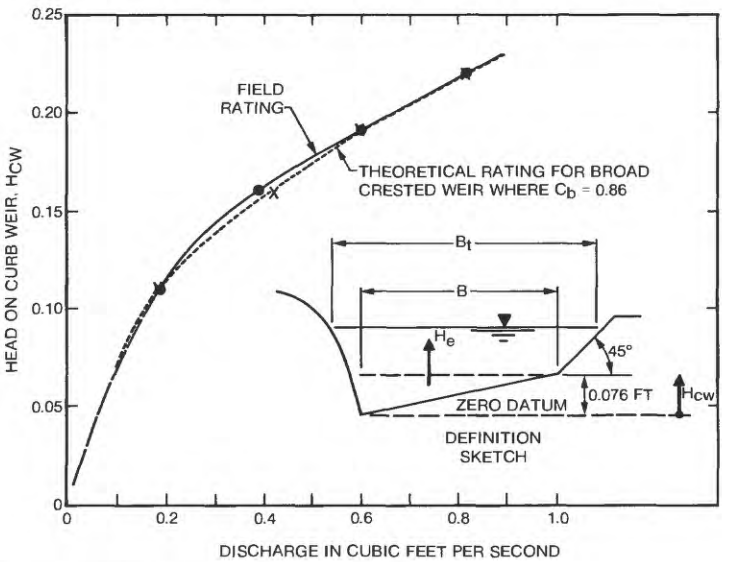

NOTE: $H_e = H_{cw}$ - 0.038 FT. AT AND ABOVE H_{cw} = 0.076 FT

Figure 60. Discharge ratings for curb dual weir.

The equation for a broad-crested weir is

$$Q = C_b \times 2/3\ B\ \sqrt{2g}\ H_b^{3/2} \qquad (8)$$

where

C_b is a discharge coefficient,

B is the width of the weir crest at right angles to the flow, and

H_b is the head on the weir.[46]

As noted in figures 54 and 55, the curb dual weir is not horizontal and the abutment, 4, and curb, 2, are not vertical, resulting in the top width, B_t, increasing with head. For the same reason, the effective head, H_e, is not the same as the head, H_{cw}, measured from zero datum at the low point next to the curb. If the effective width, B_e, is determined for each flow as the mean width for that head and the effective head made the mean head, equation 8 becomes

$$Q = C_b \times 2/3\ B_e \sqrt{2g}\ H_e. \quad (9)$$

This rating for $C_b = 0.86$ is also shown in figure 57 and shows very close agreement with the field rating. The coefficient, C_b, for the normally higher broad-crested weir is on the order of 0.50 to 0.57. As pointed out by Vennard, C_b will be larger for a low profile weir with a high velocity of approach; obviously this is the case for this broad-crested weir.[46]

These tests, while limited, lend some credibility to using this kind of curb dual weir installation and the theorectical rating to measure bypass flows. More extensive tests would be needed to evaluate C_b for different velocities of approach; it is that expected they would seldom be higher than the 0.86 obtained here. Where subcritical flow naturally exists (that is where the addition of the upstream weir was unneccessary), it is likely C_d would be on the order of 0.60.

PRECIPITATION MEASUREMENT

The rapidity of runoff in response to rainfall in highly paved areas such as highways makes it vital that the rain gages being used have very flat (immediate) responses.[47] Schaake studied the characteristics of rainfall-runoff data and instrument response and emphasized the use of tipping-bucket type rain gages where immediate response is necessary.[48] Numerous other investigators have indicated a preference for tipping-bucket type rain gages where fast response is required.[2,19,49,50,51] The tipping feature, in contrast to weighing type rain gages is also the most suitable for digital type recording of rainfall volumes and intensities.

Several manufacturers produce tipping-bucket type rain gages. The USGS has used the Weathertronics model 6010 tipping-bucket rain gage to measure rain, at increments of 0.01 in (0.25 mm), in dozens of small modeling basins nationwide as well as at a number of lake evaporation and evapotranspiration study sites throughout the country.[30*]

Rainfall is collected by an 8-in diameter orifice and directed by the orifice funnel to a calibrated bucket which tips when 0.01 in of rain has been collected (see fig. 61). The tip causes a mercury switch to close and electrically mark or count the event, and position the second bucket below the funnel orifice ready to fill and repeat the cycle. Bounce is prevented by shock-absorbing pads which,

---

*This is not an endorsement of this particular product by the USGS.

Figure 61. Tipping-bucket rain gage.

along with the mercury switch instead of a reed switch, prevent spurious signals through the electronic circuitry.

All internal parts of the gage are made of chrome-plated brass with screens installed on all openings to exclude insects and debris. The gage, to work properly, must be leveled; a spirit level is mounted on the three-legged base to aid in installation and operation maintenance of the gage. The outer cylinder is attached to the cast aluminum base with nonconductive screws.

This gage has proven to be a reliable and accurate sensor in studies where comparisons have been made between weighing recording rain and snow gages that are positioned on an approximate side-by-side configuration at study areas. Results at sites in Mississippi and Illinois indicate differences of 0.02 in on weekly and 0.01 in on single event samples. These results are attributed to first class construction, the more dependable mercury switches versus the reed type, and the overall maintenance-free record of the gage. It should be pointed out, however, that tipping-bucket rain gages demonstrate errors that are rate dependent. The higher the rainfall rate, the greater the error. The error is positive for higher rates but is insignificant until rates exceed 3 in/hr.

While the Weathertronics rain gage has proven accurate and relatively trouble free, the market is continuously changing and final selection should depend on the quality of construction and on laboratory tests of accuracy, responsiveness, and compatibility with

the data recording system. For example, the Meterological Research Incorporated (MRI) Model 302 tipping bucket rain gage has been extensively used by the city of Portland and features a plastic tipping bucket supported by knife edges on teflon cradles. Accuracy and maintenance of these units have been superior to a brand constructed of chrome and brass; corrosion being a problem with the latter. A reed-type switch is used on this model; therefore, its suitability may depend on the method of recording data.

DATA RECORDING, STORAGE, AND DISPLAY

The standard Campbell CR-21 micrologger has a small capacity internal storage chip designed to unload its contents onto a cassette storage unit or solid-state recording unit as the chip approaches capacity. The Campbell SM 64 solid-state storage module was chosen for this study for its compatibility with the system, storage capacity, and environmental adaptability. The SM 64 has a memory capacity of 32,768 data points where a data point is defined as a single data entry. The solid-state unit also has the advantage of being more reliable at very low temperatures than the cassette units.

The solid-state recorder interfaces with a computer terminal and (or) modem by means of the RS 232, made by Campbell Scientific, which splices into the data transmission line with a standard 25 pin plug. The RS 232 requires an external power source and may be left in place in the transparent mode during normal computer terminal operations. A short Basic or Fortran program is used to query the storage module and output the data as desired.

The typical format of the recorded data in output form is covered in detail in the CR-21 micrologger manual. Each record has a code which indicates what triggered the following record and thus, what format it will have. The code is followed by certain variables such as date, time of event, and user-designated input channel readings. Figure 62 illustrates a typical printout for a portion of data collected for the runoff occurring on October 23, 1984. The printout indicates that rainfall started 7:15 a.m. with 17 bucket tips in the first 5 minutes and 25 in the next 5 minutes. The other columns show the heads in the P-B flume approach and throat, in the catchment to the 15-inch PIC meter, in its barrel, and EVM velocity measurements every 2 minutes. This rainfall hydrograph and the four responding hydrographs mentioned above are printed out directly as shown in figure 63. Also obtained but not shown here due to space is head on the curb weir and the timing of sample collection when the tracer dilution system was turned on.

Explanations of Printout Codes
(First 2 digits refer to channel)

Code	Time in minutes	Precipitation (P) x 1/100 inches OR head on P-B flume, H_a, ft	Head in PIC meter barrel, ft	Head in catchment, H_I, in feet	Head in throat of P-B flume, H_t, ft	EVM velocity, ft/s
01+0248.	02+0715.	03+17.00(P)				
01+0054.	02+0718.	03+1.313	04+0.023	05+0.531	06+0.435	07+1.128
01+0248.	02+0720.	03+25.00(P)				
01+0044.	02+0720.	03+1.527	04+0.023	05+0.580	06+0.576	07+1.212
01+0054.	02+0722.	03+1.644	04+0.023	05+0.608	06+0.681	07+1.340
01+0044.	02+0724.	03+1.572	04+0.023	05+0.616	06+0.617	07+1.344
01+0248.	02+0725.	03+19.00(P)				
01+0054.	02+0726.	03+1.519	04+0.027	05+0.661	06+0.576	07+1.312
01+0044.	02+0728.	03+1.624	04+0.023	05+0.735	06+0.637	07+1.280
01+0248.	02+0730.	03+54.00(P)				
01+0054.	02+0730.	03+1.855	04+0.023	05+0.816	06+0.834	07+1.504
01+0044.	02+0732.	03+1.907	04+0.023	05+0.735	06+0.887	07+1.620
01+0054.	02+0734.	03+1.863	04+0.023	05+0.702	06+0.858	07+1.684
01+0248.	02+0735.	03+25.00(P)				
01+0044.	02+0736.	03+1.871	04+0.023	05+0.674	06+0.794	07+1.712
01+0054.	02+0738.	03+1.806	04+0.027	05+0.649	06+0.762	07+1.720
01+0248.	02+0740.	03+31.00(P)				
01+0044.	02+0740.	03+1.713	04+0.027	05+0.665	06+0.713	07+1.724
01+0054.	02+0742.	03+1.834	04+0.027	05+0.792	06+0.826	07+1.744
01+0044.	02+0744.	03+1.948	04+0.027	05+0.731	06+0.975	07+1.792
01+0248.	02+0745.	03+49.00(P)				
01+0054.	02+0746.	03+1.972	04+0.027	05+0.735	06+1.007	07+1.844
01+0044.	02+0748.	03+2.049	04+0.027	05+0.820	06+1.096	07+1.884
01+0248.	02+0750.	03+083.0(P)				
01+0054.	02+0750.	03+2.198	04+0.027	05+0.939	06+1.241	07+1.948
01+0044.	02+0752.	03+2.308	04+0.047	05+0.849	06+1.418	07+2.104
01+0054.	02+0754.	03+2.546	04+0.027	05+0.947	06+1.551	07+2.216
01+0248.	02+0755.	03+089.0(P)				
01+0044.	02+0756.	03+2.700	04+0.403	05+1.347	06+1.636	07+2.312
01+0054.	02+0758.	03+2.595	04+0.304	05+1.302	06+1.652	07+2.396
01+0248.	02+0800.	03+60.00(P)				
01+0044.	02+0800.	03+2.506	04+0.320	05+1.126	06+1.584	07+2.428
01+0054.	02+0802.	03+2.303	04+0.027	05+0.857	06+1.390	07+2.464
01+0044.	02+0804.	03+2.295	04+0.027	05+0.743	06+1.225	07+2.400
01+0248.	02+0805.	03+38.00(P)				
01+0054.	02+0806.	03+2.150	04+0.027	05+0.694	06+1.128	07+2.308
01+0044.	02+0808.	03+2.073	04+0.027	05+0.621	06+0.991	07+2.268
01+0248.	02+0810.	03+2.000(P)				

NOTE: Heads not to datum; (P) is not printed out by program.

Figure 62. Computer printout of data collected at Jackson, Mississippi, test site for runoff of October 23, 1984.

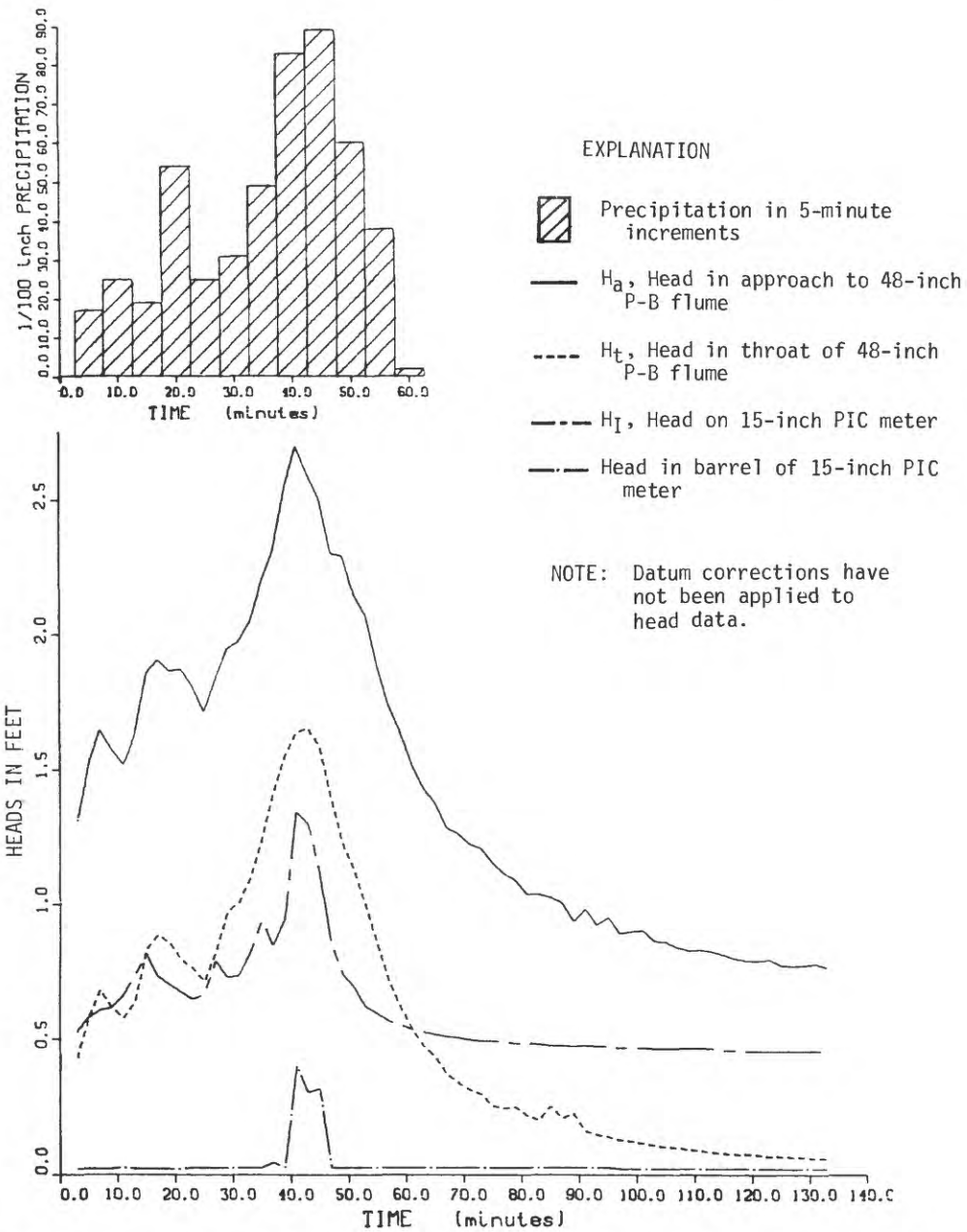

Figure 63. Precipitation and stage hydrographs as measured at Jackson, Mississippi, test site, runoff of October 23, 1984.

DISCUSSION OF RESEARCH RESULTS

As with most studies as diverse as this one, some approaches succeed, some show possibilities, and others point to better ways of accomplishing the desired measurement objectives.

It is concluded that the P-B flume open channel and venturi calibrations were very successful, particularly since the design yielded, in the former case, stable and predictable calibrations that remained subcritical in the approach even up to slopes of 3 percent. Important too, the laboratory calibrations for the P-B flume were determined to be in close agreement with the theoretical calibrations based on total energy computations. Furthermore, that the P-B flume tests indicated it could be operated as a supercritical flow flume with a range in discharge significantly greater than if operated in the conventional manner as a subcritical flow flume. For example, for a 48-inch P-B, the maximum flow just reaching the crown is about 85 ft^3/s as compared with about 142 ft^3/s for the throat calibration (supercritical) at pipe full. While neither can quite be reached before transition conditions exist, the comparison is valid. Similarly, the use of the throat calibration extends the range of the P-B flume reducing the range of transition flows.

A satisfactory pipe full (venturi) calibration was obtained which appears to be valid if both P-B flume approach and throat sections are known to be flowing full. The reliability of the pneumatic bubbler stage sensing system seems to offer a clear means of identifying what flow condition exists and hence what calibrations to use with the P-B flume.

For transition flows, neither open-channel nor venturi calibrations fully cover the region in question. It is suggested that in operational use the transition zone need not be a problem. The solution offered is to measure flows up to as close to the transition as possible with the P-B flume serving as a supercritical flow flume and then as a venturi when full. This narrows the transition range during which discharge is uncertain. It should be entirely practical and adequate to interpolate the discharge hydrograph in between for the questionable data in the transition range.

The electromagnetic velocity meter tests were less than satisfactory except when fully developed pipe flow existed. The unsteady flow existing in the transition zone may be reflected in the EVM velocity data, and thus it cannot be counted on to resolve the transition flow measurement problem. The EVM is suggested for use only where backwater conditions invalidate P-B flume calibrations.

Less satisfactory was the PIC meter design and calibrations for measuring catchment outflows. There can be little doubt that approach conditions are so adverse and unpredictable in catchments that any attempt to use calibrations of such a meter under such circumstances will be subject to lower accuracy unless rated in place. Nevertheless, the PIC meter is a relatively inexpensive device and may be an acceptable compromise in many instances. The use of a plastic pipe insert did prove feasible and offers possibilities as to a means of placing a meter out of the area of influence of the catchment.

While neither the in-situ rating or curb weir approaches to measuring bypass flows are entirely practical, no better solutions can be offered at this time. The in-situ rating of inlets and catchments provides the ultimate means of measuring bypass flows. Admittedly, the method is difficult and depends critically on the availability of an outside water supply.

The curb weir tests were surprisingly successful. While the situations where such a weir can be utilized will be limited, it should not be completely discounted. The successful use of the pneumatic bubbler orifice in the curb as part of the curb dual weir offers encouragement to use this device in any measurement scheme attempted.

The selection of a pneumatic bubbler transducer head measurement system was successful but laboratory and field transducer calibration tests indicated the need to periodically check transducer calibrations. Futhermore, transducers were found to be less reliable if operated at the extremes of their stated ranges. In general the five transducers were found to be reasonably temperature stable but results did suggest the desirability of insulating transducers from extremes in operating temperatures. The PBT system tested shows definite promise as a means of measuring pressure heads in a variety of flow measuring devices if suitable precautions are exercised.

The selection of a micrologger to sense and record data from five separate measuring devices was very successful. Furthermore, it proved capable of activating an electromagnetic velocity meter and two tracer dilution systems with the occurrence of selected flows. The unit tested is probably only a forerunner of the microcomputer systems forthcoming for handling the multiplicity of measuring tasks in a storm-drainage system.

While not a part of the instrumentation development package, dilution discharge measurements proved successful in measuring both steady flows as obtained from a fire hydrant but also unsteady flows occurring with natural runoffs. The use of an automated dilution discharge measurement system was successful and pointed the way to

possible widespread use of this approach to the in-situ rating of measuring devices or of existing storm-drainage structures.

SUGGESTED MEASUREMENT AND RECORDING SYSTEM

This study has been successful in identifying certain measuring devices and techniques which can be suggested for inclusion in any storm-drainage measurement system. A P-B flume of the prescribed design can be relied upon for measuring flows in trunklines whether open channel or pipe full. A pipe insert meter was developed and calibrated with variable results; nevertheless, it is suggested for measuring catchment outflows until a better device or method is available. The electromagnetic velocity meter can be used for measuring pipe-full flow caused by backwater conditions. The in-situ rating of catchment inlets, while difficult, can be used to evaluate gutter bypass flows. Quality tipping-bucket rain gages are available commercially which will yield quick response and accurate measurement of rainfall. The pneumatic bubbler-transducer system is a reliable means of measuring the various heads in the measuring devices as long as the transducers are kept calibrated and the micrologger can serve all of the instruments, both recording data and activating instruments as needed.

Table 13 summarizes these various measuring and recording instruments or techniques evaluated in this study and their expected accuracies and costs. The instruments and techniques most suitable for a given storm-drainage measurement study must be tailored to each situation as well as be governed by desired accuracies and funds available.

The use of a micrologger capable of storing a wide range of data inputs and having programmable and command capabilities is highly recommended. The wedding of the micrologger to a transducer-pneumatic bubbler system provides the design flexibility needed in any storm-drainage measuring system. Furthermore, the accurate timing characteristics of these microloggers avoids the necessity of intergrating all measuring devices into one network. For a highway system, this can eliminate miles of circuitry or other sophisticated and probably expensive approaches. It is suggested that a highway system under consideration for study be divided into small units in each of which one or more catchments and inlets, trunkline gages, and rain gages are served by one transducer-pneumatic network which in turn interfaces with its own micrologger. For example, using the preferred instrumentation, column 2 in table 13, for a segment of highway requiring two trunkline P-B flumes with one EVM; three catchments with PIC meters, for which it is assumed two inlets require rating in situ; and one rain gage; all to be served by one Campbell CR-21 would cost approximately $21,000 to instrument. The ability of one

Table 13. Summary of instrumentation and techniques tested, those suggested for use, and approximate costs.

(Preferred instrumentation or technique shown by *.)

Desired measurement	Measuring instrument or technique	Expected accuracy (percent)	Limits of application	Approximate costs ($)			
				Instrument(s)	Materials	Installation	Total unit cost
(1)	(2)	(3)	(4)	(5)	(6)	(7)	(8)
I. Precipitation	Tipping-bucket rain gage*	± 1	0-3 in/hr	400	100	200	700
II. Catchment outflows	1. PIC meter*	± 10	none	100	100	200	400
	2. In-situ rating using automatic tracer dilution apparatus	± 5	Good mixing conditions	3,000 (1)	200	200	3,400
III. Inlet bypass flows	1. In-situ rating using outside water supply* and		Water supply capacity				
	a. Acoustic flowmeter	± 5		5,000	100	200	5,300
	b. Tracer dilution method* (2)	± 5		500	100	100	700
	2. Curb weir	± 10	Highway traffic		50	100	150
IV. Trunklines							
a. For base flows	Palmer-Bowlus flume*	± 10	None		1,000	1,000	2,000
b. For open and pipe-full flows	Palmer-Bowlus flume*	± 5	None		1,000	1,000	2,000
c. With backwater or reverse flows	Electromagnetic velocity meter*	± 5	None	2,400	100	200	2,700
V. Head sensing system	Pneumatic-bubbler transducer system*		None, range of transducer				
	a. Per orifice	± 5		400	100	100	600
	b. Add per multiple installation			200 (3)	100	200	500
VI. Data recording and reduction system	Data logger*	NA	9 input channels 4 output ports	2,900	100	2,000 (4)	5,000

(1) Includes injection pump, tank, and commercial water sampler.
(2) Performed manually; excludes commercial water sampler.
(3) Calibration standpipe and gas supply.
(4) Instrumentation shelter.

datalogger to serve this number of measuring instruments depends on the number of head measurements needed which depends on the kind of flow anticipated in the segment of storm sewer to be studied. If pipe-full flow and backwater conditions are not expected to occur in the trunkline, head need be measured in only one location in each P-B flume. Similarly, only one head measurement in each PIC meter-catchment installation is likely to be needed.

It is recommended that the dilution gaging approach be considered in any study if mixing conditions appear favorable. This approach could be used to rate in situ existing catchments without any modifications except the addition of pneumatic bubblers and stilling wells. Consideration should also be given to using dilution gaging to measure entire runoff events in catchments. This data could be used without resorting to adding measurement devices, rating existing catchments, or making any changes in the existing storm-sewer system except to sample the tracer.

There is a danger in trying to develop fixed or "canned" approaches to storm-drainage measurement. It is recommended that each drainage system be assessed on its own as to the best measurement approaches and that the selection of test sites be chosen with care and due regard for the probability of success.

SUGGESTED FUTURE RESEARCH

Additional work needs to be performed on developing instrumentation to measure flows out of catchments. The PIC meter developed as part of this study was only partially successful as it depends on the measurement of heads in the catchment. The use of a plastic pipe insert did prove feasible and offers possibilities as to a means of placing a meter out of the region of influence of the catchment. For example, a viable approach to measuring catchment outflows might be to locate a P-B flume at the most distant end of the pipe insert and incorporate pneumatic bubbler orifices into approach and throat as was done with the PIC meter. By placing the P-B flume well away from the catchment, calibration should be possible and be independent of the complex flow conditions that can be experienced in catchments. The contraction for this P-B flume might be greater than utilized for the design presented here with the objective that a subcritical approach rating could be kept for pipe slopes in excess of 3 or 4 percent. A P-B insert meter, such as is being suggested here, should have a large radius, well-rounded entrance to produce pipe-full flow at or close to when crown stage is reached and thus avoiding flow separation. It is unlikely that overall outflow capacities would be greatly reduced since the rounding would produce pipe-full flow. Such a meter should handle all flow conditions except backwater; when

this is suspected as likely to occur, an electromagnetic velocity meter could be incorporated into the pipe insert.

The P-B flume design tested in this study was particularly successful. Nevertheless, the transition zone problem still exists, even though less extensive if the P-B flume is operated as a supercritical flow measuring device and then as a venturi meter with pipe-full flow. Additional design modifications to the P-B flume might narrow the transition range even further. One of the design features of the Parshall flume is a raised exit section to cause submergence ratings to be more predictable since tailwater levels are controlled in part by the flume design.[43] A somewhat analogous approach is offered as a means of improving the P-B flume calibrations in the transition zone. It is suggested that two design additions to the P-B flume discussed in this report be considered. One would be to add a low sill to the crown of the pipe near the exit of the P-B flume. This might cause pipe-full flow to occur more positively with less pulsating action. A vent pipe incorporated into this crown sill might be advisable. The efficiency of the pipe should not be affected as pipe-full flow is more efficient. The other approach, with the same objective, is to add a low sill to the invert several pipe diameters downstream of the P-B flume to cause subcritical flow to exist at all times in the tailwater region regardless of pipe slope. By experience, the authors believe the crown sill to be the most viable, as premature tailwater submergence might adversely affect the throat calibration.

The pneumatic-bubbler transducer system used in this study was satisfactory with the exception of the erratic behavior of the transducers at the low and high portions of their operational ranges; especially at near zero heads. A means of surcharging transducers to impose an initial head of about 0.5 ft needs to be investigated. The P-B flume when used as a supercritical flume as well as other measuring devices require reliable and accurate zero or near zero head measurements. Passing the bubbler gas through an enclosed fluid-filled reservoir prior to its release through the gaging orifice may be the answer to this problem.

The laboratory tests of the electromagnetic velocity meter were less than satisfactory due probably to vibration problems and erratic flow conditions at the location in the approach to the P-B flume. Further laboratory and field tests need to be performed with the EVM to provide a better understanding of where it can be used and as to what velocity coefficients apply.

GLOSSARY

Calibration - The empirical relationship between a sensor or measuring apparatus and the true magnitude of the parameter being investigated; for example, discharge as a function of head. Normally the implication is that such a rating is reproducible and transferable for a given device.

Catchment - The drop structure or box receiving the flow from the street or roadway inlets and discharging it from the area via outlet sewers.

Head - Fluid height above a datum referenced to the zero flow of a measuring device such as a weir or flume.

Inlet - Intake openings in street and roadway gutters or channels collecting storm runoff.

Junction - A box or other structure receiving and joining flows via connecting pipes or other flow inlets.

Rating - The relationship defining discharge as a function of head or stage for a stream or a hydraulic structure.

Stage - A general term for the elevation of water as in a river or canal and, unlike head, not necessarily referenced to an exact zero datum.

Tailwater - The stage or head downstream of a measuring device or other structure.

REFERENCES

1. American Society of Civil Engineers, 1965, Report - Engineering Foundation Research Conference - Urban Hydrology Research: Proctor Academy, Andover, New Hampshire, Cosponsored by the Urban Hydrology Research Council.

2. McPherson, M. B., and Zuidema, F. C., 1977, Urban hydrological modeling and catchment research: International summary, Technical Memorandum IHP-13, American Society of Civil Engineers, Urban Water Resources Research Program, New York.

3. U.S. Department of Transportation, 1979, Design of urban highway drainage - The State of the Art: FHWA-TS-79-225.

4. Wood, D. J., 1980, The analysis of flow in surcharged storm sewer systems: International Symposium on Urban Storm Runoff, July 28-31, 1980, University of Kentucky, Lexington, Kentucky,

5. Shelley, P. E., and Kirkpatrick, G. A., 1975, Sewer flow measurement, a state-of-the-art assessment: Environmental Protection Technology Series EPA-600/2-75-027, 424 p.

6. Palmer, H. K., and Bowlus, F. D., 1936, Adaptation of venturi flumes to flow measurement in conduits: American Society of Civil Engineers Transactions, v. 101, p. 1195-1216.

7. Ludwig, J. H., and Ludwig, R. G., 1951, Design of Palmer-Bowlus Flumes: Sewage and Industrial Wastes, v. 23, no. 9, p. 1096-1107.

8. Wells, E. A., Jr., and Gataas, H. B., 1958, Design of venturi flumes in circular conduits: American Society of Civil Engineers Transactions, v. 123, p. 749-775.

9. Diskin, M. H., 1963, Temporary Flow Measurement in Sewers and Drains: Journal of the Hydraulics Division, American Society of Civil Engineers, v. 89, no. HY4, proceedings paper 3574, p. 141-159.

10. Stevens, J. C., 1964, Temporary flow measurements in sewers and drains: American Society of Civil Engineers, Proceedings of the Hydraulics Division, 4146, vol., p. 241-247.

11. Replogle, J. A., 1970, Flow meters for water resource management: Water Resources Bulletin, p. 345-374.

12. Ludwig, R. G., and Parkhurst, J. D., 1974, Simplified application of Palmer-Bowlus flow meters: Journal, Water Pollution Control Federation, v. 46, no. 12, p. 2764-2769.

13. Schneider, V. R., Barnes, H. H., Jr., and Davidian, J., 1972, A control for gaging runoff in storm sewers: American Society of Civil Engineers, Cornell Hydraulics Division Specialty Conference, August 1972.

14. Wenzel, H. G., 1975, Meter for sewer flow measurement: Journal of the Hydraulics Division, American Society of Civil Engineers, v. 101, no. HY1, p. 15-133.

15. Smoot, G. F., 1974, A rainfall-runoff quantity-quality data collection system, in Proceedings of A Research Conference, Urban Runoff, Quantity and Quality, August 1974: American Society of Civil Engineers, p. 178-183.

16. Herschy, R. W., and Newman, J. D., 1982, The measurement of open channel flow by the electromagnetic gauge in Advances in Hydrometry, Proceedings of the Exeter Symposium, July 1982: International Association of Hydrological Sciences Publication Number 134.

17. World Meteorological Organization, 1980, Manual on Stream Gauging - Volume 1 - Fieldwork: World Meteorological Organization Number 519.

18. Albertson, M. L., Tucker, L. S., and Taylor, D. C., 1971, eds., Treatise on urban water systems: Fort Collins, Colorado State University.

19. Arnell, V., Falk, J., and Malmquist, P., 1976, Urban storm water research in Sweden: Report number 19 presented at the Engineering Foundation Conference, Instrumentation and Analysis of Urban Storm Water Data--Quantity and Quality, in Easton, Maryland.

20. City of Los Angeles, 1982, Calibration of flumes and weirs for the Los Angeles County Sanitation Districts: Bureau of Engineering, HRL 20-82.

21. Blyth, K., and Kidd, C. H. R., 1976, The development of a meter for the measurement of discharge through a road gully: Institute of Hydrology, Wallingford, England.

22. Craig, J. D., 1983, Installation and Service Manual for U.S. Geological Survey Manometers: Techniques of Water-Resources Investigations of the U.S. Geological Survey, Book 8, Chapter A2, 57 p.

23. Buzay, K., 1974, Pneumatic level and open channel flow measuring systems, in Proceedings of the International Seminar and Exposition on Water Resources Instrumentation: Water Resources Instrumentation, v. 1, measuring and sensing methods, Chicago, Illinois.

24. Wires, H. O., 1975, Modern developments in hydrometry, in Proceedings of the International Seminar convened by the World Meteorological Organization, Padua, Italy, September 1975: World Meteorological Organization no. 427, v. 2, p. 24-33.

25. Zaye, R., 1973, Water level gauging by pressure measuring, in Symposium on Hydrology, Koblenz, September 1970: International Association of Hydrological Sciences, v. 1, no. 99.

26. Sherlock, D. J., and others, 1973, Water-level transducers, in Symposium on Hydrology, Koblenz, September 1970: International Association of Hydrological Sciences, v. 1, no. 99.

27. Walker, S. T., 1982, Hydrometric data capture using intelligent solid state logging systems in Advances in Hydrometry, Proceedings of the Exeter Symposium, July 1982: International Association of Hydrological Sciences Publication Number 134.

28. Paulson, R. W., Billings, R. H., and Cherdak, A. S., 1982, Advanced hydrologic instrumentation activities within the Water Resources Division of the U.S. Geological Survey: Proceedings of the Exeter Symposium, International Association of Hydological Sciences Publication Number 134.

29. Van Haveren, B. P., and Leavesley, G. H., 1979, Hydrologic modeling of coal lands: Report of joint workshop held by U.S. Geological Survey and Bureau of Land Management, December 12-14, 1978, Billings, Montana.

30. Kilpatrick, F. A., and others, 1985, in press, Coal basin modeling for hydrologic impact assessments, part A - General description of hydrology, geology, and data collection: U.S. Geological Survey Open-File Report.

31. Anderson, J. J., 1960, Determining rates of flow in sewers using calcozine red BX dye method: 33rd Annual Meeting of Central States Sewage and Industrial Wastes Association and Conference of Wisconsin Sewage Works Operators, Madison, Wisconsin.

32. Gizzard, T. J., and Harms, L. L., 1974, Measuring flow with chemical gaging: Water and Sewage Works, v. 121, no. 11, p. 82-83.

33. Marsalek, J., 1974, A technique for flow measurements in urban runoff studies, in Proceedings of the International Seminar and Exposition on Water Resources Instrumentation, June 4-6, 1974, Chicago, Illinois: Water Resources Instrumentation, v. 1, Measuring and Sensing Methods.

34. Katz, B. G., and Fisher, G. T., 1983, A comparison of selected methods for measuring flow rate in a circular storm sewer: International Symposium on Urban Hydrology, Hydraulics and Sediment Control, University of Kentucky, Lexington, Kentucky, July 26-28, 1983.

35. Harvey, R. A., Kidd, C. H. R., and Lowing, M. J., 1980, Automatic dilution gauging in storm sewers: in Institute of Hydrology report no. 75.

36. Duerk, M. D., 1983, Automatic dilution gaging of rapidly varied flow: U.S. Geological Survey Water-Resources Investigations Report 83-4088.

37. Kilpatrick, F. A., and Cobb, E. D., 1984, Measurement of dis charge using tracers: U.S. Geological Survey Open-File Report 84-136.

38. Wilson, J. F., Jr., Cobb, E. D., and Kilpatrick, F. A., 1985, Fluorometric procedures for dye tracing: U.S. Geological Survey Techniques of Water-Resources Investigations, Book 3, Chapter A12.

39. Wenzel, H. G., Jr., 1968, A critical review of methods of measuring discharge within a sewer pipe: American Society of Civil Engineers Urban Water Resources Research Program, Technical Memorandum 4, 20 p.

40. Johnstone, D. E., 1982, An automatic constant-rate injection dilution gauging system: Water and Soil Science Centre, Christchurch, report no. WS 608.

41. Filmer, R. W., and Yevjevich, V. M., 1961, The use of tracers in making accurate discharge measurement in pipelines: Report to the Bureau of Reclamation, U.S. Department of the Interior by the Engineering Research Center, Colorado State University, Fort Collins, Colorado.

42. Hardee, Jack, 1979, Instrumentation of urban hydrology monitoring sites in southeast Florida: U.S. Geological Survey Water-Resources Investigations 79-37.

43. Kilpatrick, F. A., and Schneider, V. R., 1983, Use of flumes in measuring discharge: Surface Water Techniques, Book 3, Chapter A-14.

44. Chow, V. T., 1959, Open-channel hydraulics: New York, McGraw-Hill, 680 p.

45. Faraday, Michael, 1832, Experimental Researches in Electricity, Parts I and II: Phil. Trans. Royal Society, p. 125-193.

46. Vennard, J. K., 1961, Elementary Fluid Mechanics: New York, John Wiley & Sons, Inc.

47. Eagleson, P. S., Shack, W. J., 1966, Some criteria for measurement of rainfall and runoff: Water Resources Research, v. 2, no. 3, p. 427-436.

48. Schaake, J. C., Jr., 1968, Response characteristics of urban water resource data system: American Society of Civil Engineers, Urban Water Resources Research Program, Technical Memorandum 3, 57 p.

49. Knapp, J. W., Schaake, J. C., and Viessman, Warren, 1963, Measuring rainfall and run-off at storm-water inlets: American Society of Civil Engineers Proceedings, Paper 3644, Journal Hydraulics Division, v. 89, no. HY5, pt. 1, p. 99-115.

50. Smoot, G. F., 1971, Data collection for real-time systems, in Treatise on urban water systems, Albertson, M. L., Tucker, L. S., and Taylor, D. C., eds.: Fort Collins, Colorado State University, p. 499-508.

51. Tucker, L. S., 1968, Oakdale Avenue gaging installation, Chicago, instrumentation and data: American Society of Civil Engineers, Urban Water Resources Research Program, Technical Memorandum 2, 76 p.